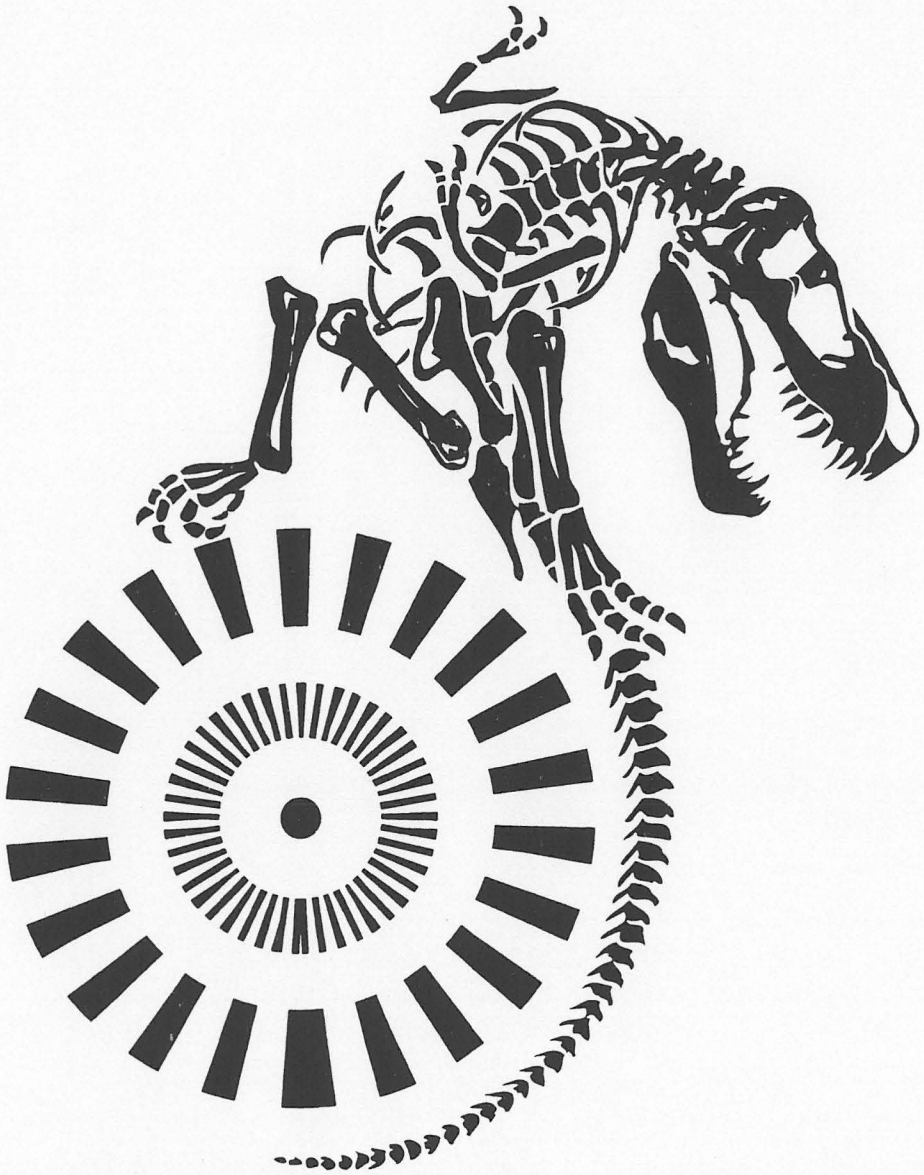

FIELD GUIDE TO

CRETACEOUS-TERTIARY BOUNDARY SECTIONS IN NORTHEASTERN MEXICO

LPI

UNIVERSITY OF HOUSTON
Clear Lake

FIELD GUIDE TO CRETACEOUS-TERTIARY BOUNDARY SECTIONS IN NORTHEASTERN MEXICO

Prepared by

Gerta Keller
Wolfgang Stinnesbeck
Thierry Adatte
Norman MacLeod
Donald R. Lowe

FIELD TRIP ASSOCIATED WITH THE CONFERENCE ON NEW DEVELOPMENTS REGARDING THE KT EVENT AND OTHER CATASTROPHES IN EARTH HISTORY

February 5–8, 1994

Conference Sponsors
Lunar and Planetary Institute
University of Houston–Clear Lake

Field Guide/Field Trip Sponsors
Lunar and Planetary Institute
University of Houston–Clear Lake
Facultad de Ciencias de la Tierra de Universidad Autónoma de Nuevo León at Linares
Gobierno de Tamaulipas: Consejo Estatal para la Cultura y las Artes
Instituto Nacional de Antropología y Historia

LPI Contribution No. 827

Compiled in 1994 by
Lunar and Planetary Institute

The Institute is operated by the University of Houston Space Research Association under contract No. NASW-4574 with the National Aeronautics and Space Administration.

This contribution may be cited as

Keller G. et al. (1994) *Field Guide to Cretaceous-Tertiary Boundary Sections in Northeastern Mexico.* LPI Contribution No. 827, Lunar and Planetary Institute, Houston 110 pp.

This contribution is distributed by

ORDER DEPARTMENT
Lunar and Planetary Institute
3600 Bay Area Boulevard
Houston TX 77058-1113

Mail order requestors will be invoiced for the cost of shipping and handling.

PREFACE

This guide was prepared for the field trip to the KT clastic sequence of northeastern Mexico, February 5–8, 1994, in conjunction with the Conference on New Developments Regarding the KT Event and Other Catastrophes in Earth History, held in Houston, Texas. The four-day excursion offers an invaluable opportunity to visit three key outcrops: Arroyo El Mimbral, La Lajilla, and El Piñon. These and other outcrops of this sequence have recently been interpreted as tsunami deposits produced by the meteorite impact event that produced the 200–300-km Chicxulub basin in Yucatan, and distributed ejecta around the world approximately 65 m.y. ago that today is recorded as a thin clay layer found at the K/T boundary.

The impact tsunami interpretation for these rocks has not gone unchallenged, and others examining the outcrops arrive at quite different conclusions: *not* tsunami deposits but turbidites; not KT at all but "upper Cretaceous". Indeed, it is in hopes of resolving this debate through field discussion, outcrop evaluation, and sampling that led the organizers of the conference to sanction this field trip.

This field guide provides participants with background information on the KT clastic sequence outcrops and is divided into two sections. The first section provides regional and logistical context for the outcrops and a description of the clastic sequence written by Keller et al. The second section presents three representative interpretations of the outcrops by their advocates. There is clearly no way that these models can be reconciled and so two, if not all three, must be fundamentally wrong. Readers of this guide should keep in mind that many basic outcrop observations that these models are based upon remain unresolved. While great measures were taken to ensure that the information in the description section was as objective as possible, many observations are rooted in interpretations and the emphasis placed on certain observations depends to some degree upon the perspective of the author. It would not be surprising, therefore, if this field guide requires extensive revision as a consequence of the investigations initiated by this field trip. When it comes to these outcrops, nothing should be considered "written in stone."

This publication benefited greatly from the efforts of all the contributors listed elsewhere in this publication. In particular, Gerta Keller and Wolfgang Stennisbeck, the field trip leaders, were instrumental, as was the staff of Publications and Program Services Services Department at the Lunar and Planetary Institute.

Virgil L. Sharpton
Graham Ryder

LIST OF CONTRIBUTORS

Thierry Adatte
Institut de Géologie
University of Neuchâtel
2001 Neuchâtel
Switzerland

Walter Alvarez
Department of Geology and Geophysics
University of California
Berkeley CA 94720

Bruce F. Bohor
Mail Stop 972
U.S. Geological Survey
Box 25046
Denver CO 80225

Gerta Keller
Department of Geological and
Geophysical Sciences
Princeton University
Princeton NJ 08544

J. G. Lopez-Oliva
Department of Geological and
Geophysical Sciences
Princeton University
Princeton NJ 08544

Donald R. Lowe
Department of Geological and
Environmental Sciences
Stanford University
Stanford CA 94305

Norman MacLeod
Department of Geological and
Geophysical Sciences
Princeton University
Princeton NJ 08544
Present Address:
Department of Paleontology
The Natural History Museum
Cromwell Road
London SW7 5BD
United Kingdom

Alessandro Montanari
Osservatorio Geologica di Coldigoco
Frontale di Apero (MC)
Italy

Eric Robin
Centre des Faibles Radioactivités
CEA/CNRS
91190 Gif-sur-Yvette
France

Robert Rocchia
Centre des Faibles Radioactivités
CEA/CNRS
91190 Gif-sur-Yvette
France

Virgil L. Sharpton
Lunar and Planetary Institute
3600 Bay Area Boulevard
Houston TX 77058-1113

Jan Smit
Institut of Earth Sciences
Vrije Universiteit
de Boelelaan 1085
1081 HV Amsterdam
The Netherlands

Wolfgang Stinnesbeck
Facultad de Ciencias de la Tierra
Universidad Autónoma de Nuevo León
67700 Linares, N. L.
Mexico

ACKNOWLEDGMENTS

We gratefully acknowledge reviews, comments, and discussions of this Field Guide by R. W. Scott, R. Ginsburg, B. Bohor, W. Alvarez, J. Smit, and G. Ryder. We are thankful to J. Lyons for providing unpublished data on Mimbral glass particles and R. Rocchia and E. Robin for kindly providing unpublished iridium data. We owe a special thanks to V. Sharpton, who valiantly tried to coordinate and integrate the frequently opposing views of the authors and some of the reviewers.

Field work and laboratory research was supported by grants from the National Geographic Society (No. 4620-91), NSF OCE-9021338, EAR-9115044, ACS-PRF No. 26780-AC8, CONACYT No. L120-36-36, and the Swiss National Fund No. 8220-028367. Technical support was provided by Laboratoire de Géochemie et Petrographique de l'Institut de Géologie de Neuchâtel and by B. Kübler and C. Beck. Editorial and technical assistance of the manuscript was provided by Kim Beck at Princeton University.

Logistics and administrative and publications support for the field trip and conference were provided by the staff of the Publications and Program Services Department, Lunar and Planetary Institute.

TABLE OF CONTENTS

LIST OF FIGURES

INTRODUCTION

The controversy over the nature and causes of the global Cretaceous-Tertiary (KT) boundary faunal and floral changes was altered fundamentally with the discovery of the now-famous Ir anomaly at the KT boundary at Gubbio, Italy (*Alvarez et al.*, 1980). The identification of similar anomalies worldwide and the proposition that they and the KT extinctions resulted from the impact of a large extraterrestrial bolide have spurred over a decade of unprecedented research on the physical and biological events at and near the KT boundary. Within a short time, the controversy resolved itself into two contrasting schools of thought: (1) The KT events reflect the catastrophic effects of a large (10-km) bolide colliding with the Earth, and (2) the KT extinction was the culmination of long-term changes in the Earth's biota, reflecting major changes in the global climatic system, and resulted from extreme, but still normal, terrestrial processes, mainly volcanism, that may have been accelerated by a bolide impact at KT boundary time.

With the discovery of the buried Chicxulub structure on the north coast of Yucatan, Mexico, and its identification as a KT impact site (*Hildebrand et al.*, 1991; *Swisher et al.*, 1992; *Sharpton et al.*, 1992), outcrops of uppermost Cretaceous and lowest Tertiary strata around the Gulf of Mexico assume major importance as possible sources of direct evidence regarding the nature of both KT boundary events and the Chicxulub structure. Among the first such sites investigated, well before the discovery of the Chicxulub structure, are the KT sections along the Brazos River in southern Texas, which include a coarse-grained clastic unit at or near the KT boundary. This unit has been variously interpreted as reflecting a high-energy impact-generated tsunami (*Bourgeois et al.*, 1988) or a sea-level lowstand deposit unrelated to an impact (*Jiang and Gartner*, 1986; *Donovan et al.*, 1988; *Keller*, 1989). Subsequent investigation of KT sections at Beloc, Haiti, revealed the presence of glassy spherules with compositions suggesting formation involving the melting of carbonate rocks, consistent with the presence of thick Cretaceous carbonates at the Chicxulub site. Other sections in southern Mexico and Guatemala have been interpreted to show both conformable and unconformable relationships across the KT boundary *(Keller et al.*, 1993; *Stinnesbeck et al.*, 1994; *Montanari et al.*, 1994). However, outcrops in northeastern Mexico in the vicinity of Ciudad Victoria provide excellent, structurally uncomplicated, apparently conformable sections across the KT boundary over a distance of over 300 km.

These outcrops have been described and interpreted as yet in only a preliminary fashion (*Longoria and Gamper*, 1992; *Smit et al.*, 1992; *Stinnesbeck et al.*, 1993; *Bohor and Betterton*, 1993) and many aspects of their basic geology remain either unresolved or controversial. An important component of these sections is a 1–12-m-thick, sedimentologically complicated, coarse-grained clastic unit within thick sequences of fine-grained marls, and coincident with the KT boundary contact.

The objective of this field trip is to examine, sample, and discuss these important outcrops. It is hoped that some issues of basic geology might be resolved by discussions on the outcrops and that an interdisciplinary approach might be taken toward some of the more contentious issues of their interpretation. In the end, our discussions are likely to revolve around two fundamental issues: (1) Do the clastic layers occur precisely at the KT boundary or within either middle or latest Cretaceous strata, and (2) were the clastic layers deposited by a single or by closely spaced series of high-energy depositional events over a short period of time (days) or were they deposited by multiple events over a much longer interval of time (years to thousands of years)? Much of our observational effort is likely to be directed at collecting direct evidence pertinent to these questions.

In order to be of maximum use to both field-trip participants and others visiting these outcrops, this guidebook is divided into two major sections. The first provides descriptions of the outcrops. The second provides a summary of the major interpretations of the formation of these clastic units and KT events by proponents of both impact and nonimpact scenarios.

PART I: GEOLOGIC DESCRIPTIONS

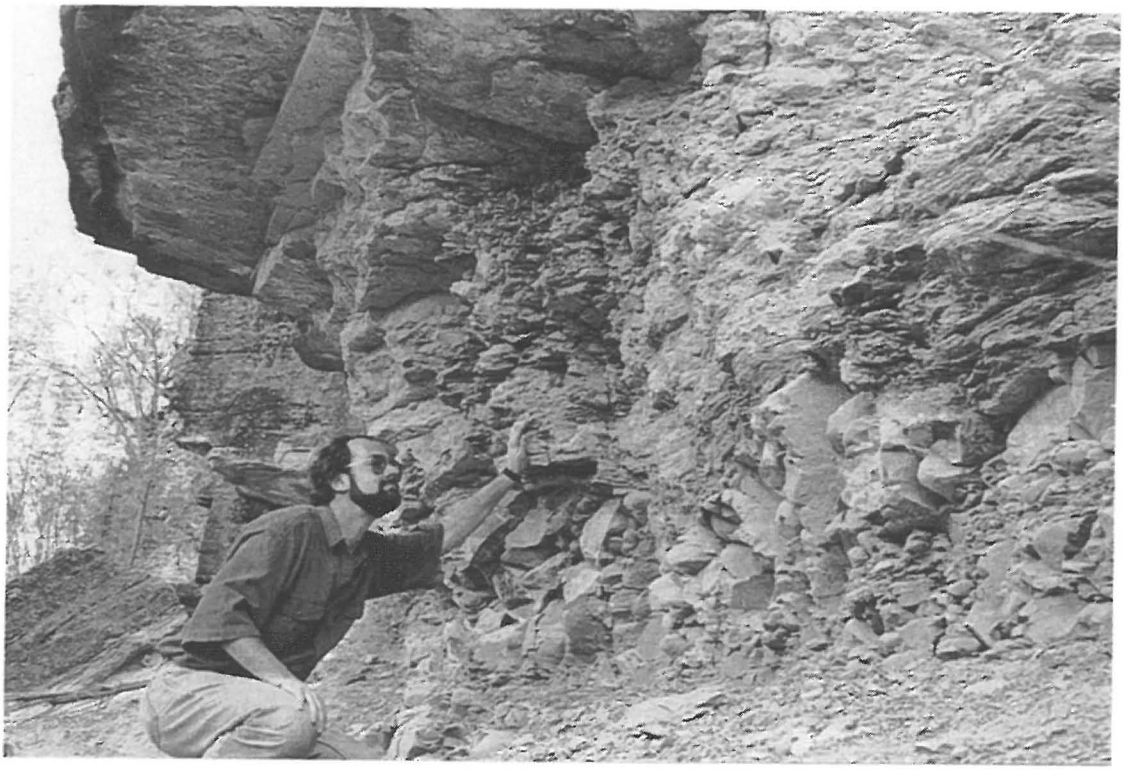

MAASTRICHTIAN TO PALEOGENE PALEOGEOGRAPHIC SETTING OF NORTHEASTERN MEXICO

During the Maastrichtian and Paleogene, northeastern Mexico was part of a shallow to moderately deepwater shelf-slope region that received a steady influx of terrigenous clastic sediments resulting from the Laramide Orogeny and uplift of the Sierra Madre Oriental to the west (Figs. 1 and 2) (*Sohl et al.*, 1991; *Galloway et al.*, 1991). Along the western Gulf of Mexico, a series of basins formed in the present states of Veracruz and Tamaulipas and in the southern and eastern parts of Nuevo León. Within these basins, rhythmically bedded marls and shales and thin layers of ash were deposited. These sedimentary rocks are correlated with the Campanian to Maastrichtian Mendez Formation and the Paleocene Velasco Formation. The contact between these formations is commonly interpreted as conformable (*Gamper*, 1977; *Longoria and Gamper*, 1993), although local disconformities have been reported by *Hay* (1960) and *Pessagno* (1969). The sediments were deposited in outer neritic to upper bathyal pelagic to hemipelagic environments.

In the region north and west of Monterrey deposition of terrigenous shallow-water to paralic sediments occurred during the Maastrichtian, now represented by the Olmas and Escondido Formations and the Difunta Group, which locally extends into the Eocene. Sediment influx was high, as for example in the Saltillo-Monterrey region, where the prodeltaic-deltaic wedge of the Difunta Group is several thousand meters thick and thins to the south and east (*Weidie et al.*, 1972).

At this time the western Gulf of Mexico was characterized by several large submarine paleocanyon systems that formed along the prograding unstable continental margin (Fig. 2). The best known of these submarine canyon systems are the Lavaca and Yoakum paleocanyons in Texas and the Chicontepec paleocanyon system in central-east Mexico (Fig. 2) (*Galloway et al.*, 1991). These paleocanyons are commonly connected by retrogradational or transgressive facies sequences (*Galloway et al.*, 1991).

In the Sierra de San Carlos to the north of El Mimbral, and the Sierra de Tamaulipas to the west, magmatic activity associated with extension began during the Eocene (and possibly Oligocene) along north-northwest/south-southeast-trending faults. At the same time, strong compression and thrusting accompanied the mountain building in the northern Sierra Madre Oriental. Subsequently, the whole area was uplifted during the late Tertiary to Recent. Uplift was accompanied by the formation of extensive fluvial fan systems and terraces and deposition of the Pleistocene conglomerates evident at El Mimbral and other sections (e.g., La Sierrita, Los Ramones).

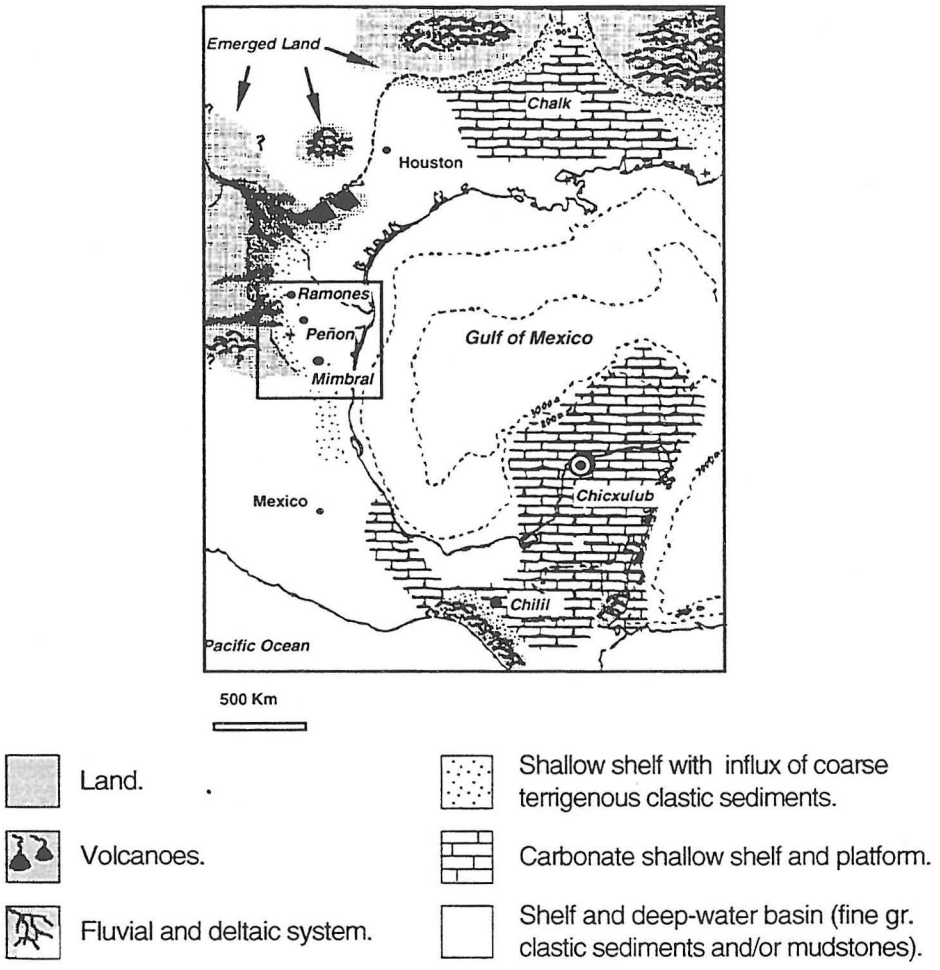

Fig. 1. *Paleogeography of the western Gulf of Mexico basin during the Maastrichtian (modified from Galloway et al., 1991; Sohl et al., 1991).*

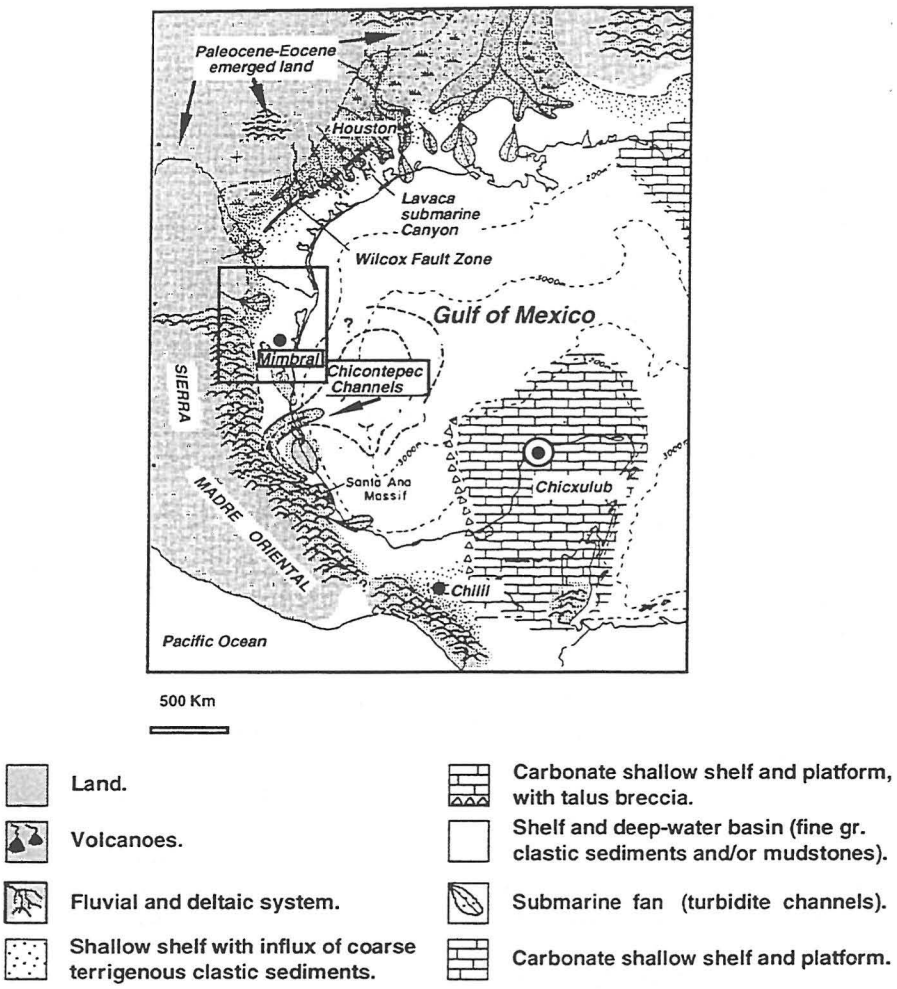

Fig. 2. Paleogeography of the western Gulf of Mexico basin during the Paleocene (modified from Galloway et al., 1991; Sohl et al., 1991).

KT BOUNDARY CLASTIC DEPOSITS IN NORTHEASTERN MEXICO

The clastic deposit of the Arroyo El Mimbral, located on the southwestern flank of the Sierra de Tamaulipas, was first described by *Muir* (1936), who interpreted it as marking a hiatus between the Maastrichtian Mendez and Paleocene Velasco Formations. *Hay* (1960) inferred that the deposit at Mimbral marked an angular unconformity. This outcrop was relocated by *Smit et al.* (1992) with the help of PEMEX geologists, and interpreted as an impact-generated tsunami or megawave deposit related to the bolide impact near Chicxulub on the north coast of Yucatan (Fig. 1).

Clastic deposits similar to Mimbral recently have been revisited by a field party including PEMEX geologists (*Alvarez et al.*, 1992) and independently by us at more than 12 other localities in northeastern Mexico (Fig. 3). All these sections show comparable depositional sequences and allow correlation (north-northwest/south-southeast) of three different lithological units and subunits over more than 300 km. We describe here the stratigraphic, biostratigraphic, depositional, lithological, mineralogical, and petrographic features of these clastic deposits at:

El Mimbral*	(latitude 23°12.6'N, longitude 98°40'W)
La Lajilla*	(latitude 23°40'N, longitude 98°43.9'W)
El Peñon*	(latitude 24°58'N, longitude 99°12.5'W)
El Mulato	(latitude 24°54'N, longitude 98°57'W)
La Sierrita (= Loma las Rusias)	(latitude 25°12.5'N, longitude 99°31.1'W)
Los Ramones	(latitude 25°42.1'N, longitude 99°36.5'W)

Other boundary sections not included in this Field Guide are known to occur at Rancho Nuevo (latitude 25°29.5'N, longitude 99°34.2'W), Los Cerritos (latitude 25°18'N, longitude 99°33'W), Cuauhtémoc (latitude 25°00.7'N, longitude 99°17.8'W), La Laja near China, El Porvenir (24°56.5'N, 99°11'W), and El Indio (latitude 24°54.6'N, longitude 99°00.0'W).

The geographic distribution of these localities indicates that the northeastern Mexico KT boundary clastic deposits were deposited in a north-northwest/south-southeast-trending area that is parallel to and 40–80 km east of the front range of today's Sierra Madre Oriental (Fig. 3). The southernmost section of this north-northwest/south-southeast is El Mimbral, which is located about 80 km southeast of Cd. Victoria, the capital of the State of Tamaulipas, Mexico. Los Ramones, the northernmost of the near-KT clastic deposits described here, is 40 km east of Monterrey, the capital of Nuevo León, Mexico.

Not all KT boundary outcrops in the region, however, appear to have clastic sediment deposition, as noted by *Gamper* (1977) and *Longoria and Gamper* (1992) in outcrops near Aldama (Arroyo Pedregoso) and Magiscatzin in the State of Tamaulipas (Fig. 3).

*To be visited on the February 5–9, 1994, field trip.

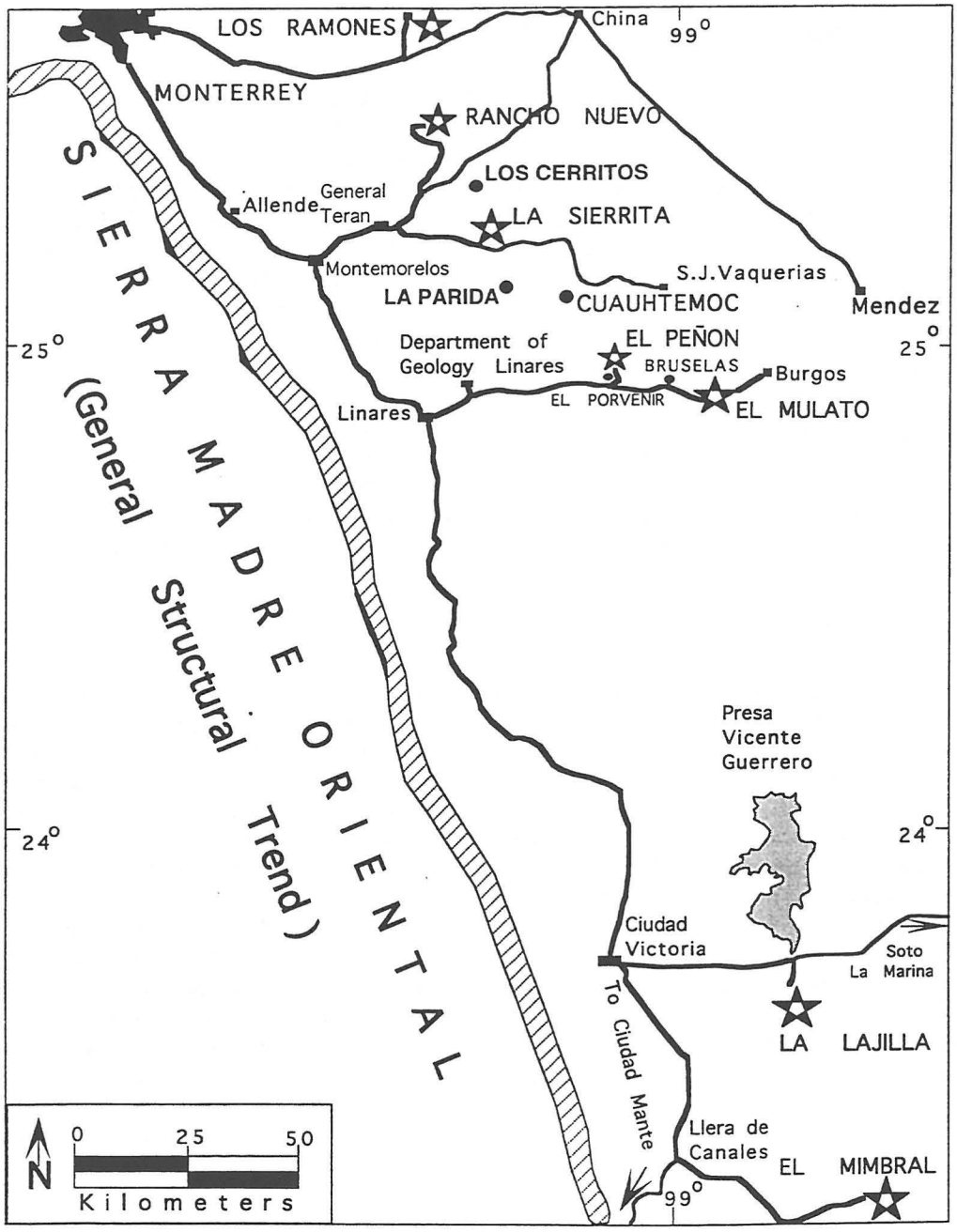

Fig. 3. Location map of near-KT-boundary clastic deposits in northeastern Mexico. Stars indicate sections included in this field guide, dots mark additional localities with clastic deposits in the region.

GENERAL DESCRIPTION OF OUTCROPS

The KT boundary in northeastern Mexico occurs within a thick sequence of fine-grained, marly sedimentary rocks of the Mendez (Upper Cretaceous) and Velasco (Paleocene) Formations. At or within a few decimeters of the actual KT boundary, the precise position of which is controversial, is a regionally developed clastic member ranging up to several meters thick. This member has been described by a number of investigators (*Smit et al.*, 1992; *Longoria and Gamper*, 1992; *Stinnesbeck et al.*, 1993; *Bohor and Betterton*, 1993; *Longoria and Grajales*, 1993) and interpreted both as a KT boundary deposit produced by an impact-generated tsunami or turbidity current (*Smit et al.*, 1992), as a series of normal high-energy turbidity-currents related to an impact (B*ohor and Betterton*, 1993) or as a series of gravity flows or turbidity currents related to the latest Maastrichtian sea-level lowstand and tectonic activity (uplift of Sierra Madre) (*Stinnesbeck et al.*, 1993).

This clastic member and its genesis represents the focus of KT boundary research in northeastern Mexico. It has been variously subdivided into a number of distinctive lithologic layers by *Smit et al.* (1992), *Stinnesbeck et al.* (1993), and *Longoria and Grajales* (1993). In this discussion, we employ the three-fold subdivisions of *Stinnesbeck et al.* (1993) Although the thickness and makeup of the clastic unit varies across individual outcrops, these subdivisions and their vertical arrangement are consistent and allow lithostratigraphic correlation of the deposit over the 300 km separating the outcrops in a north-south direction.

Unit 1: Spherule-rich Layer

The basal unit 1 of the clastic member is a soft, weathered sediment 10–30 cm thick that contains abundant spherules. This unit overlies marls of the Mendez Formation with an irregular contact representing an erosion surface. In addition to spherules, the unit contains foraminiferal tests, clasts of marl from the underlying Mendez Formation, clasts containing Turonian age foraminifera, and minor quartz. The spherules range from 1 to 5 mm in diameter, although *Longoria and Grajales* (1993, p. 73) report spherules up to 25 mm. Many spherules are filled with blocky calcite. Some spherules and foraminiferal tests are filled by greenish, microcrystalline phyllosilicates; possibly glauconite or smectite. Many contain fine internal spherical or radial structures and some are compound spherules. These spherules have been interpreted by some as oolites, oncolites, algal resting cysts, and volcanic spherules, transported from shallow-shelfal carbonate depositional settings (*Stinnesbeck et al.*, 1993 and herein); others have interpreted them as hollow, originally glassy, impact-produced microtektites that have been subsequently filled and replaced by calcite or phyllosilicate minerals (*Smit et al.*, 1992; *Bohor and Betterton*, 1993).

A possibly regional layer of well-cemented foraminiferal packstone, termed sandy limestone layer, occurs within or at the top of unit 1. The sedimentological significance and regional continuity of this sandy limestone layer remains uncertain.

Unit 1 is either massive or crudely stratified and locally shows large-scale trough cross-stratification.

Unit 2: Massive Sandstone

Unit 2 consists of a massive, commonly laminated sandstone with mudclasts at its base and less frequently discrete layers of plant debris. Sandbeds grade upward to slightly finer sands containing mica and a clay-rich matrix.

Unit 3: Interlayered Sand-Silt Beds

Unit 3 consists of interlayered sand, shale, and siltstone beds with diverse sedimentological features such as horizontal laminations, ripple marks, small scale crossbedding, flaser bedding, and convolute lamination. Thin layers with normal hemipelagic sedimentation and distinct layers containing zeolites were detected at El Mimbral, El Peñon, and La Lajilla within this unit. Rare plant debris is sometimes present. Where unit 3 directly overlies unit 1 or the Mendez Formation (e.g., Peñon II, La Lajilla I and II, La Sierrita III), mudclasts are commonly found near the base. Unit 3 is topped by one (or several) resistant rippled sandy limestone layer(s) containing bioturbation, most commonly *Chondrites, Zoophycos,* and Y-shaped *Thalassinoides* (?) burrowing networks.

SPECIFIC OUTCROP DESCRIPTIONS

ARROYO EL MIMBRAL

The Mimbral outcrop is located on the south bank of the Mimbral creek (or La Cañada) approximately 10 km east of the main road from Ciudad Victoria to Tampico at latitude 23°13'N and longitude 98°40'W. The outcrop is reached by a rough, unpaved, and often poorly graded dirt road that is difficult to navigate without a four-wheel drive. From the main road, the dirt road to Mimbral is best located by the high tower of a microwave station located about 1 km east of the main road. The dirt road to Mimbral leads past the microwave station, where it forks into two branches. The right branch leads downhill and directly to the Arroyo El Mimbral and the Mimbral outcrop (Fig. 5). There are several Ranchos to pass through on the way to the Mimbral outcrop. Prior to any visit, the owner of the Rancho Mimbral must be contacted and permission obtained to cross his Rancho. For permission contact Eng. Pedro Silva Rodriguez, Sierra Leone 120, fracc. Villa Real, Cd. Victoria, Tams., Mexico.

The Mimbral outcrop is 152 m long and of variable height, ranging from 1 m to 36 m (Figs. 6–8).

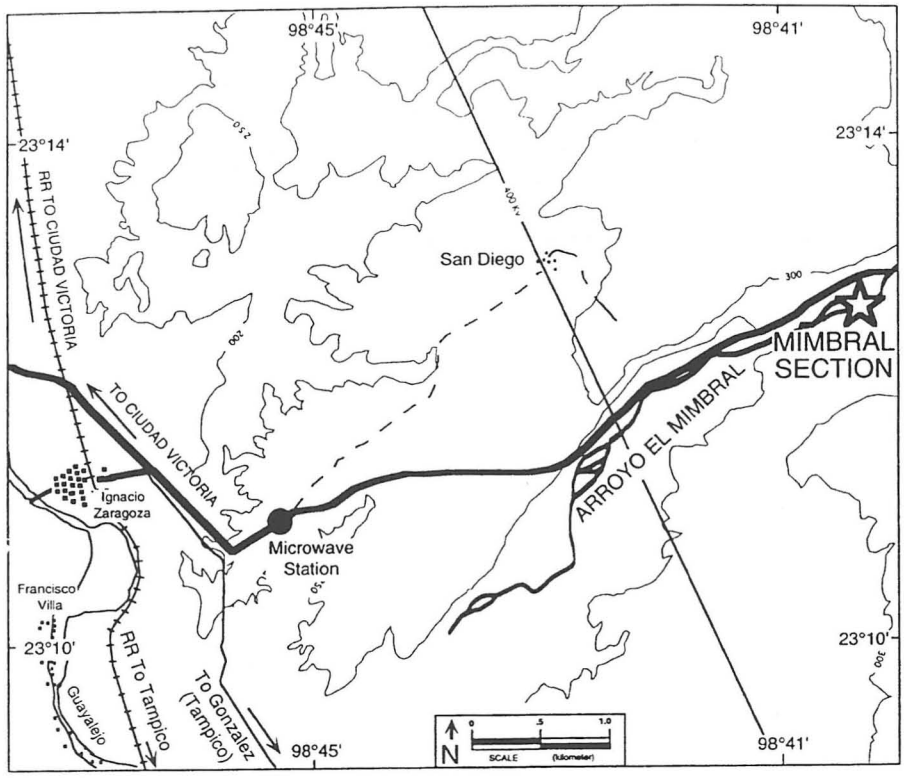

Fig. 4. *Location map: El Mimbral KT boundary section.*

The length of the outcrop is measured and marked by red letters at 2-m intervals along the outcrop (outcrop numbers courtesy of J. Smit, A. Montanari, and W. Alvarez). Most of the outcrop (30 m) exposes the upper Cretaceous Mendez Formation, which consists of rhythmically bedded marls and occasional thin bentonite layers (Fig. 7). A clastic deposit of variable thickness, ranging from 0.2 m to 3 m, extends for 60 m along the outcrop. This clastic deposit overlies an undulating erosional surface of the Mendez marls and contains rip-up mud clasts of Mendez lithologies near its base. The clastic deposit reaches 3 m in thickness at 28 m along the outcrop and shows all three lithologically and mineralogically distinct subdivisions. The El Mimbral outcrop is illustrated in Fig. 9.

Figure 10 shows the lithological columns across the center of the channel (Mimbral I) and at the right edge (Mimbral II). The basal unit 1 is characterized by a spherule-rich bed that contains a 20-cm-thick sandy limestone layer (SLL) containing fewer spherules. The middle unit 2 consists of laminated sandstone with mud-clasts and discrete layers of plant debris near its base. The upper unit 3 consists of alternating sand, silt, and mud layers topped by a rippled sandy limestone (RSL) that is also characterized by bioturbation (*Chondrites* burrows). Grey marine shales of the Tertiary Velasco Formation discontinuously overlie unit 3 (Fig. 9).

At the west edge of the deposit only the topmost 25 cm of unit 3, the rippled sandy limestone layer, is present. The most continuous KT transition is found at 150–152 m along the outcrop (Figs. 7 and 10). At this location the KT boundary is marked by a thin (2–4 cm) clay layer containing a 2–4-mm red oxidized layer that overlies the rippled sandy limestone of unit 3. Planktic foraminifera are dissolved in the clay layer, which represents Zone P0 at other KT boundary localities. The first Tertiary planktic foraminifera, including *Eoglobigerina fringa, E. edita, Woodringina hornerstownensis, Parvularugoglobigerina eugubina,* and *P. longiapertura,* appear just above (4–9 cm) the thin clay layer. These Tertiary species indicate the presence of Zone P1a (see Biostratigraphy section) beginning at the top of the clay layer. The clay layer grades into 2.2 m of exposed gray shales and marls of the lower Tertiary (Danian Zones P1a to P1b) Velasco Formation (Fig. 7). Thin ash (bentonite) layers are present about 30 cm below the top of the Mendez Formation and at 6–8 cm and 2.0 m above the base of the Velasco Formation.

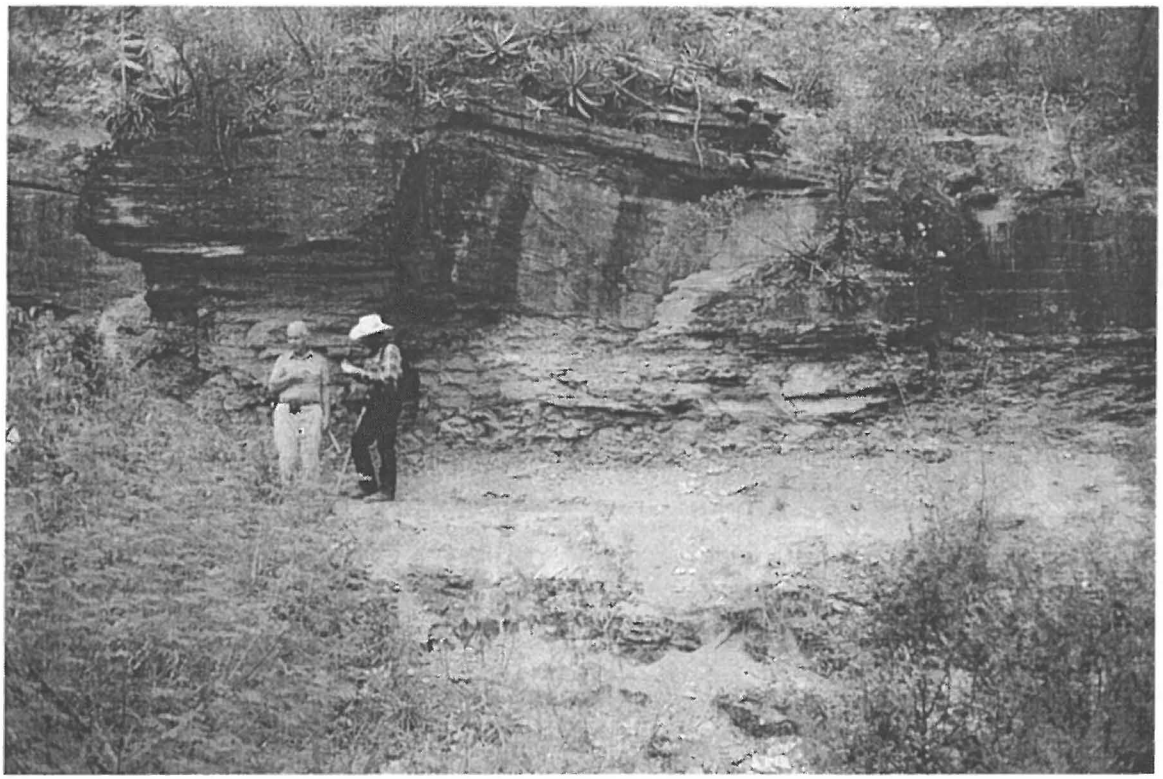

Fig. 5. *Outcrop of channelized clastic deposits at Mimbral.*

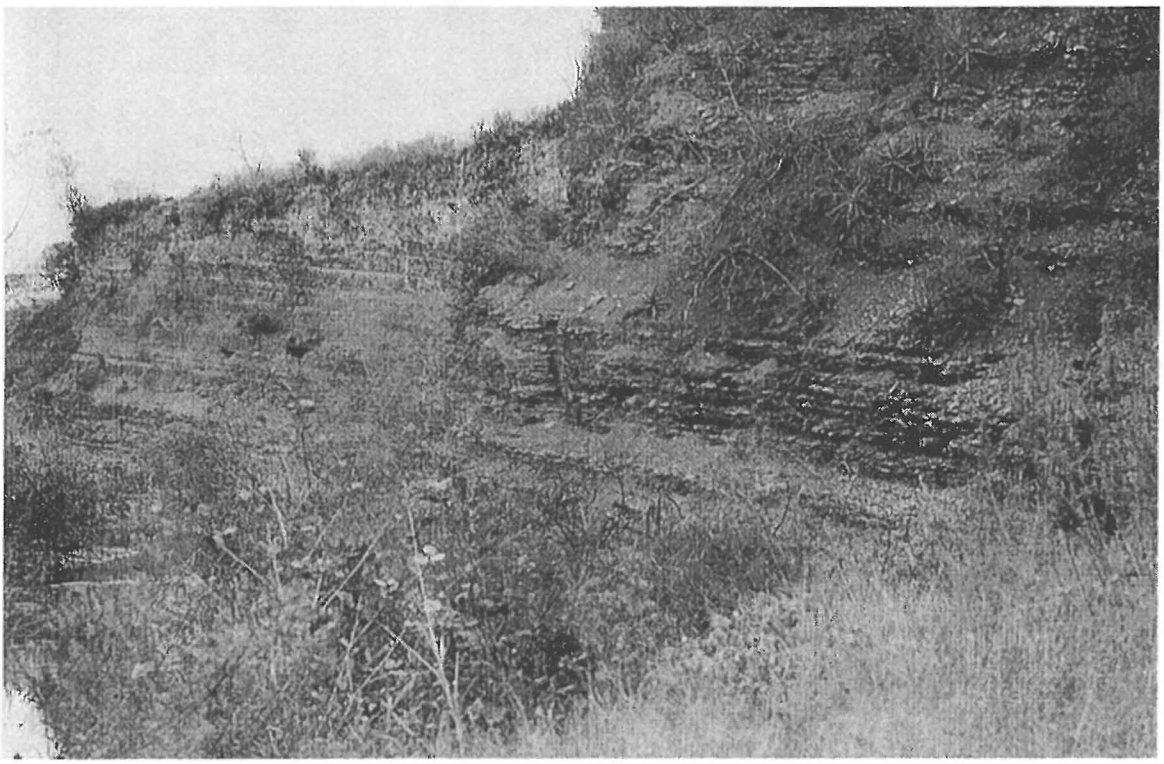

Fig. 6. *Rhythmically bedded hemipelagic marls of the Maastrichtian Mendez Formation.*

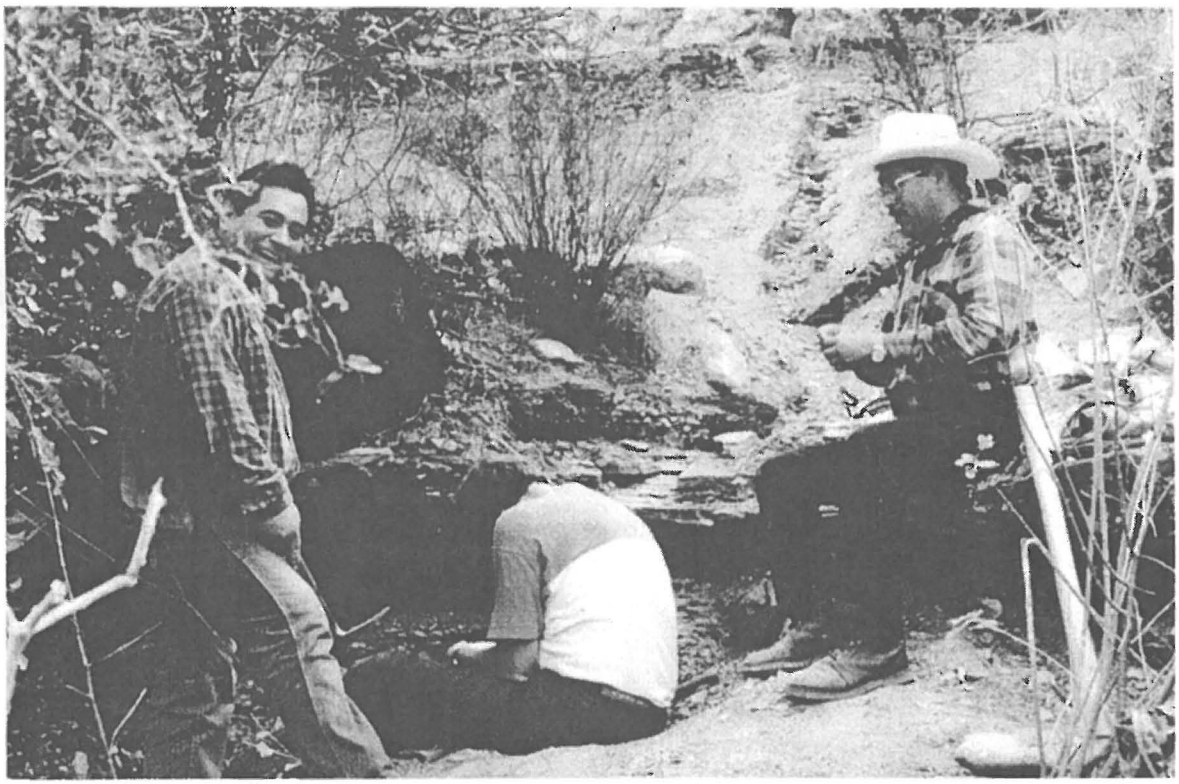

Fig. 7. KT boundary transect at right edge of channel deposit at El Mimbral II.

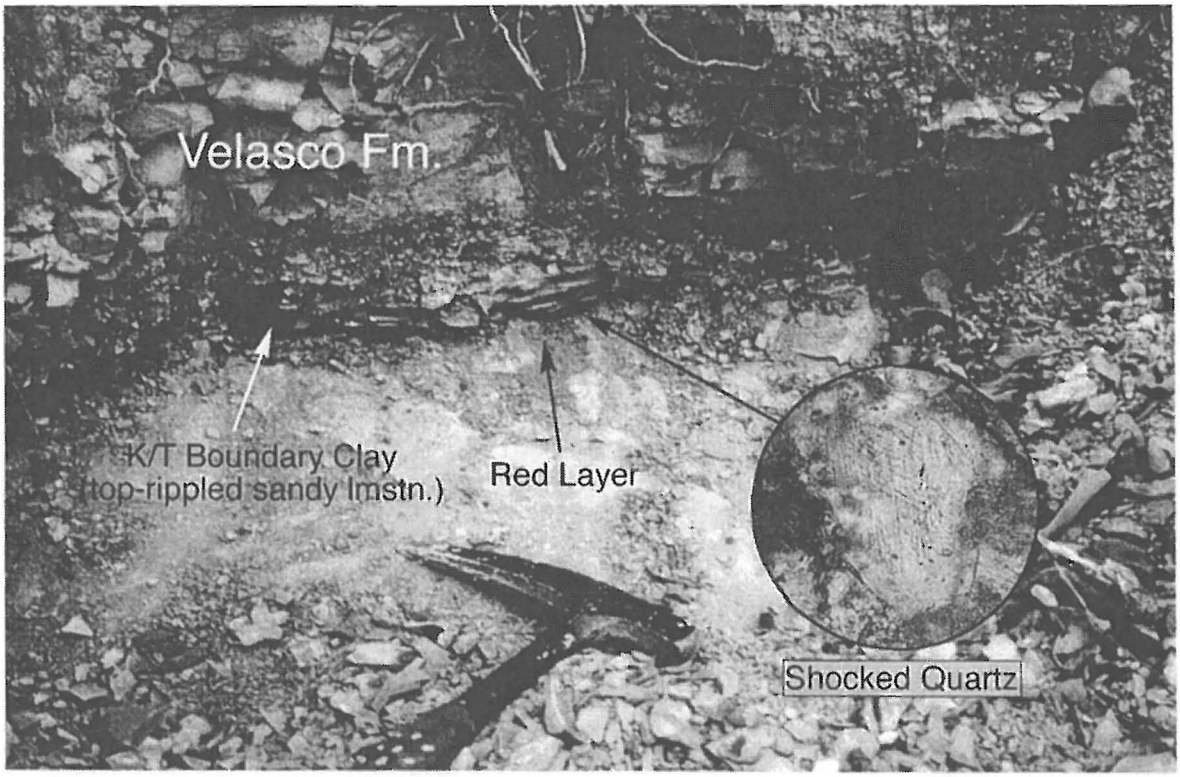

Fig. 8. Close-up of KT boundary and red layer at El Mimbral II with insert of shocked quartz grain from the red layer.

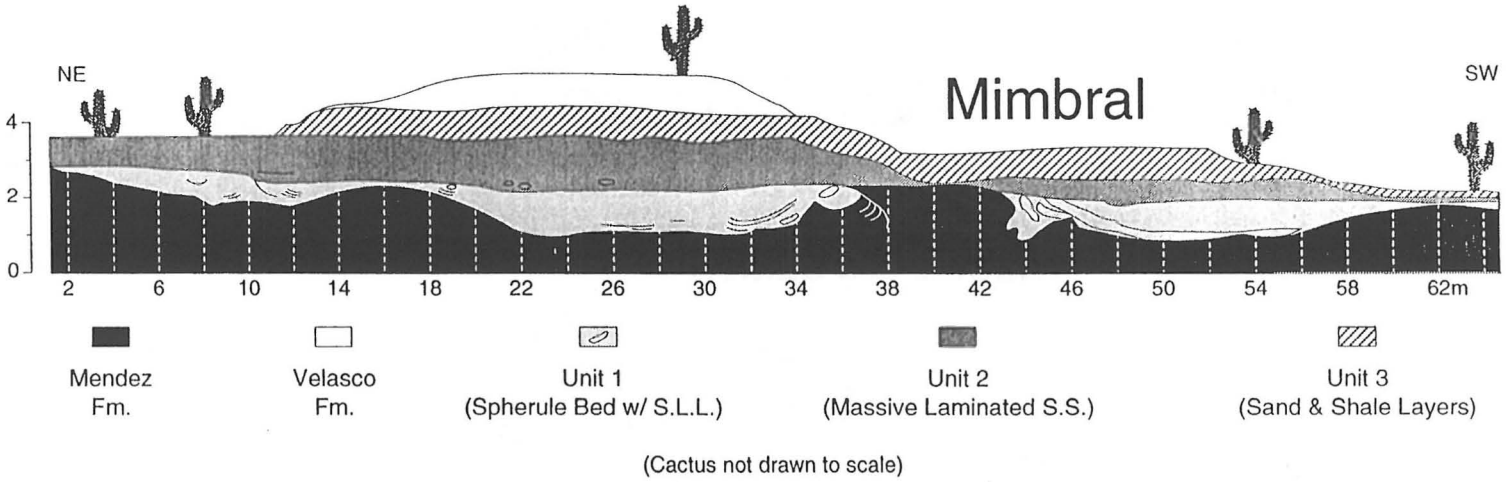

Fig. 9. *Sketch of El Mimbral outcrop based on measured sections at 2-m intervals. SLL refers to sandy limestone layer. (Meter numbers are painted on outcrop, courtesy of J. Smit, A. Montanari, and W. Alvarez).*

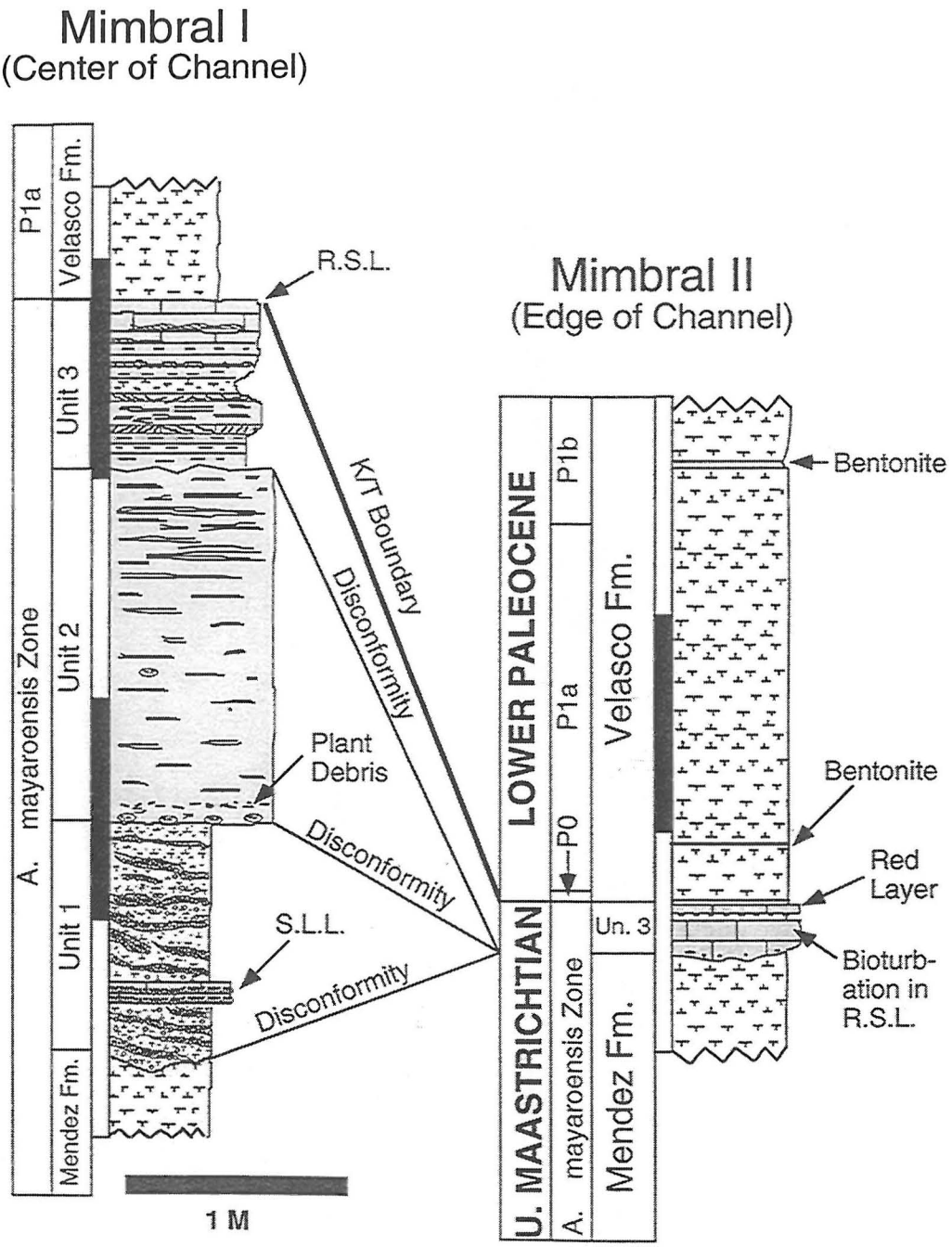

Fig. 10. *Stratigraphic correlation of two KT boundary transects across the clastic channel deposit at 28 m along the outcrop and at the right edge of the channel at 150 m along the outcrop. Note that at the edge of the channel, only the topmost rippled sandy limestone layer (RSL) of the clastic deposit is present and the stratigraphic sequence between Mendez and Velasco Formations is more continuous. SLL = sandy limestone layer, RSL = rippled sandy limestone.*

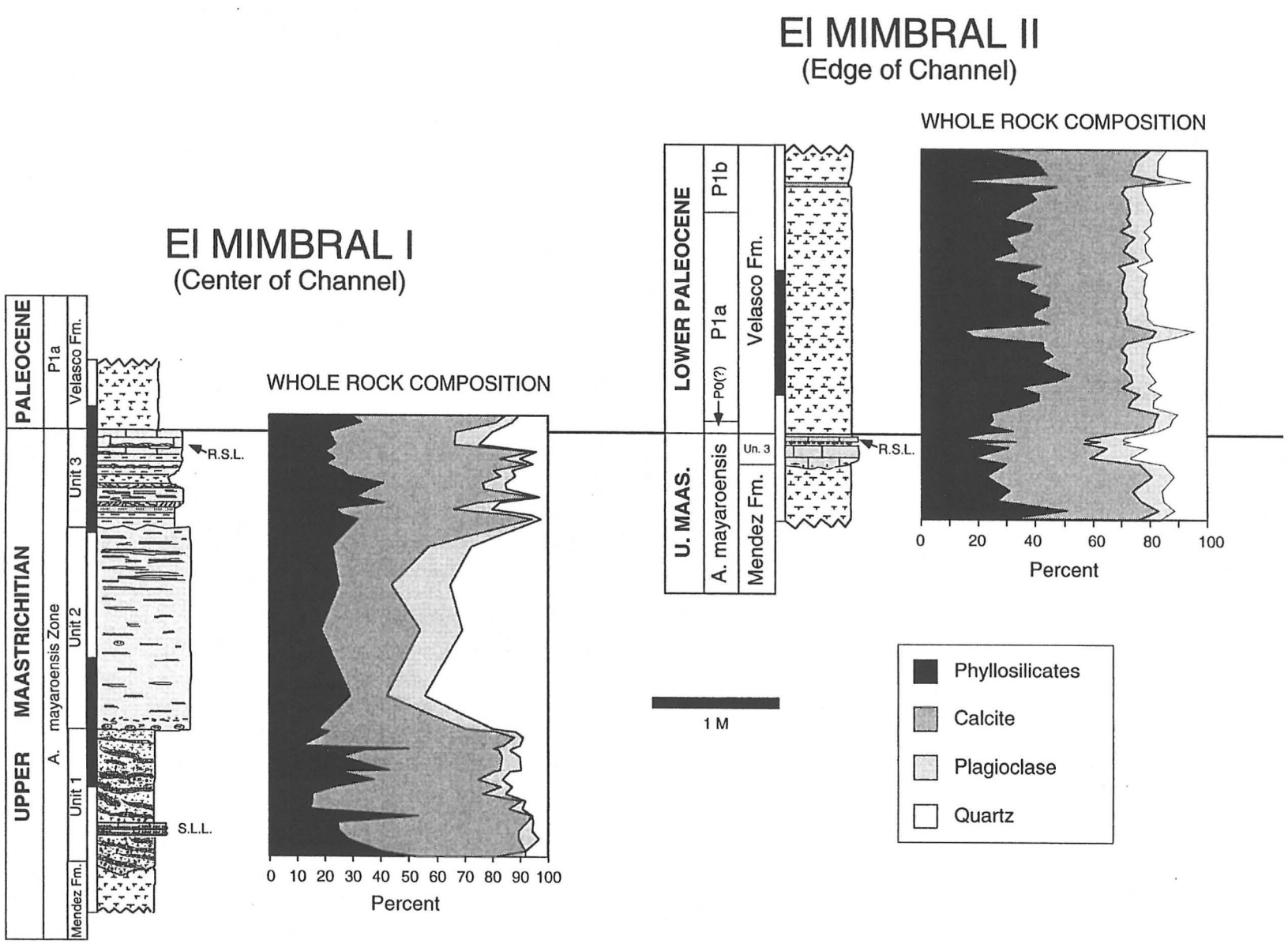

preparation). Measured by estimation from whole-rock XRD (Kübler, 1987). SLL = sandy limestone layer, RSL = rippled sandy limestone.

UNIT 1

Spherule Layer:	Friable, rich in calcareous spherules, glauconite particles and glauconite infillings of spherules and foraminifera, large mud clasts of Mendez Formation, and discrete sandy limestone layer (SLL, Fig. 12).
Thickness:	Variable, between 100 cm in the center of channel (Mimbral I) thinning to 0 cm at right edge of channel (Mimbral II, Fig.10).
Lower Contact:	Disconformably overlies the Mendez Formation, contact characterized by undulating erosional surface (Fig. 14).
Upper Contact:	Disconformable with massive sandstone of unit 2 in center of outcrop (Mimbral I), and with unit 3 at the edge (Figs. 15 and 16).
Sedimentological Features:	Oblique bedding and groove casts.
Sandy Limestone Layer (SLL):	Present in center of outcrop.
Position:	Variable, due to slump and convolute bedding, contact with unit 2 at 34 m along outcrop (Figs. 13 and 16a,b).
Thickness:	25 to 0 cm.
Characteristics:	Undulating surface due to convolute bedding, gradation of spherule abundance (Figs. 13, 15, and 16).
Mudclasts:	Rounded clasts of Mendez marls, ranging up to tens of centimeters in size, some mud clasts contain Foraminifera of Turonian age *(Marginotruncana sigali, M. pseudolinneiana).*
Mineralogy:	Calcite 66%, plagioclase 4%, quartz 11%, phyllosilicates 19% (Fig. 11).
Bioturbation:	None observed.

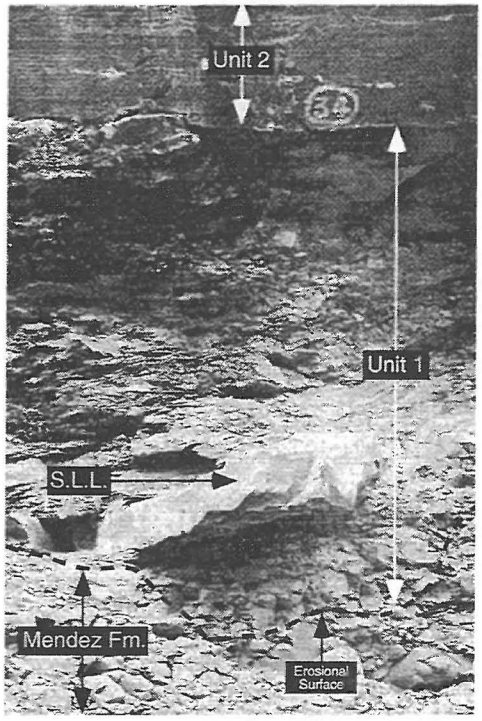

Fig. 12. Unit 1, lower part of clastic deposit.

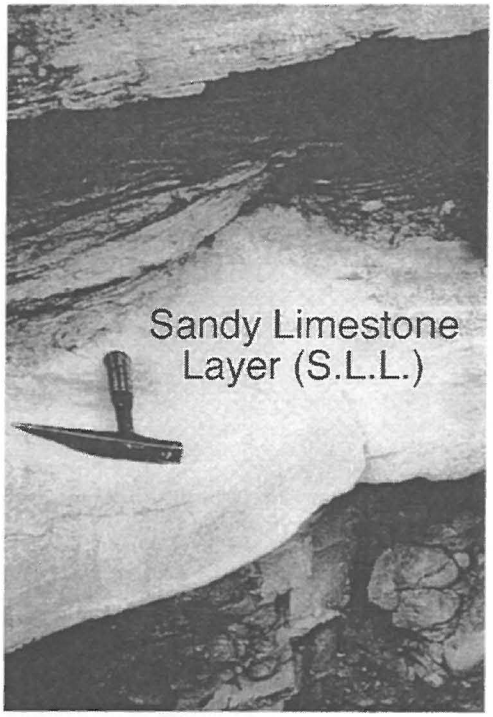

Fig. 13. Drapes of spherules over SLL.

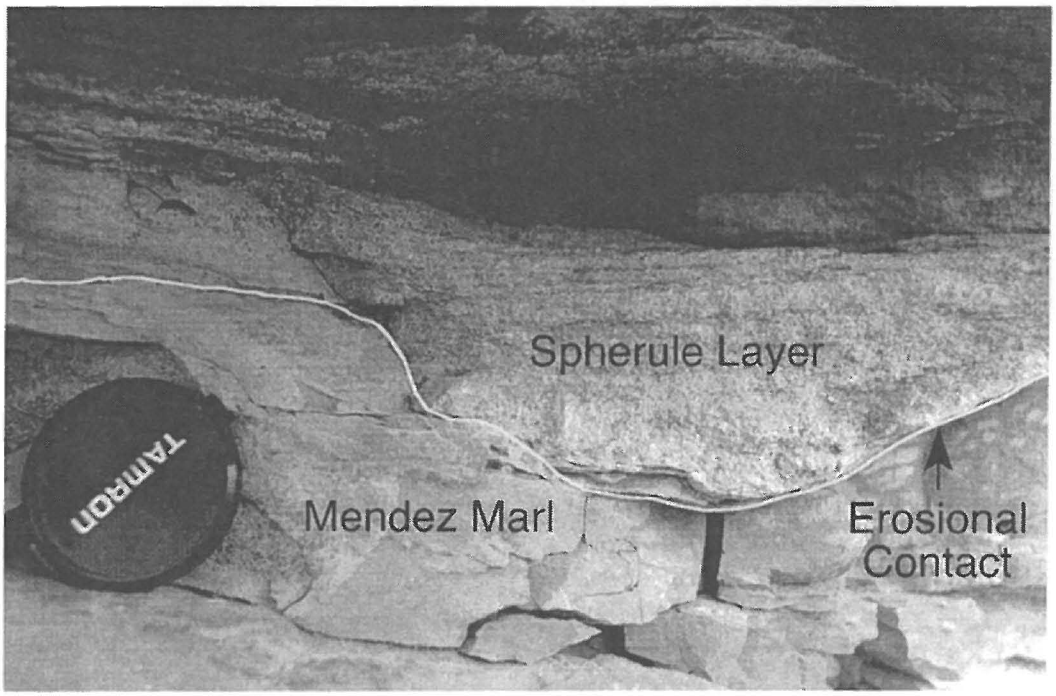

Fig. 14. Note absence of mixing of spherules into Mendez marls at contact between Mendez Formation; unit 1 suggests partial lithification prior to deposition of spherule unit.

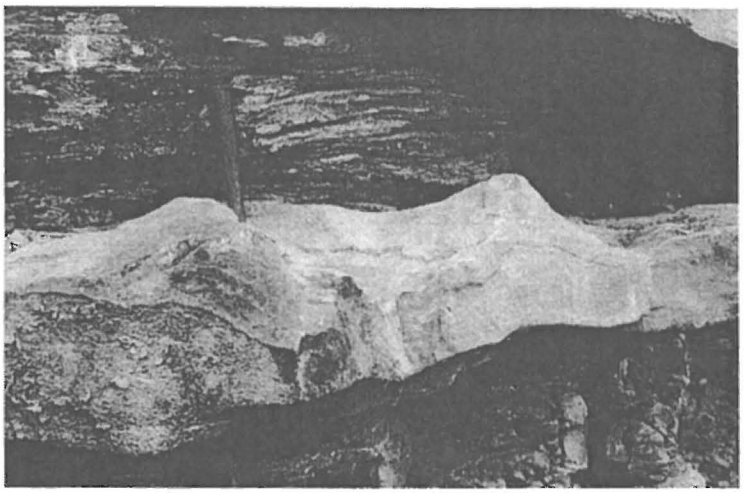

Fig. 15. *Sandy limestone layer (SLL) with convolute bedding within unit 1.*

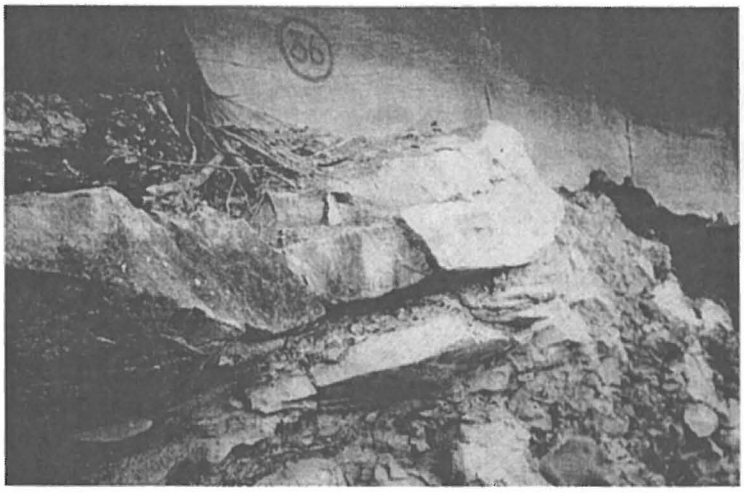

Fig. 16a. *Sandy limestone layer (SLL) of unit 1 in contact with basal unit 2; note that contact is disconformable.*

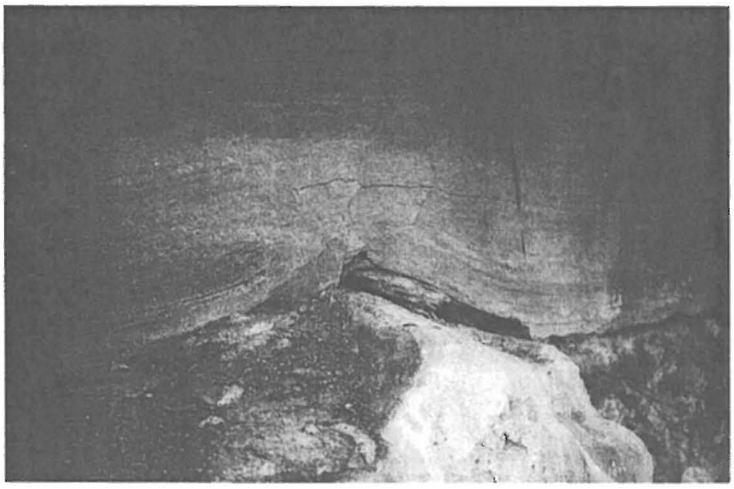

Fig. 16b. *Close-up of Fig. 16a. Note draping of sandstone layer indicating partial lithification of sandy limestone prior to deposition of overlying unit.*

Other Characteristics:

Spherules: 2–5 mm ranging up to 15 mm in size, shiny, easily detectable, consisting of infillings of blocky calcite, glauconite, mineral grains, and foraminifera. Many spherules have organic shells that may represent algal resting cysts, and many large spherules are composites containing multiple smaller spherules. No glassy spherules have been found, but rare glass fragments are present (Fig. 23).

Quartz Grains: Unshocked quartz is abundant in the spherule layer of unit 1. Very rare (<1%) quartz grains exhibit deformation features but some of these grains are rounded. Sets of lamellae are commonly curved and irregularly spaced and some lamellae are decorated with trains of fluid inclusions (Figs. 21 and 22).

Fig. 17. *Composite spherule.*

Fig. 18. *Spherule with opaque mineral (rutile?).*

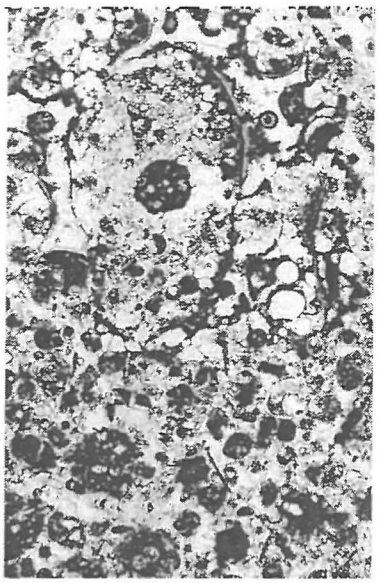

Fig. 19. *Spherules containing foraminifera with glauconite infilling.*

Fig. 20. *Spherules containing foraminifera with glauconite infilling.*

Figs. 21. *Quartz grains with lamellar features.*

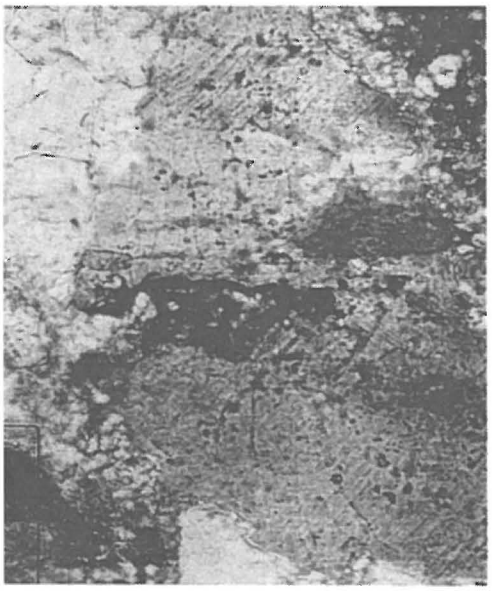

Fig. 22. *Quartz grains with lamellar features.*

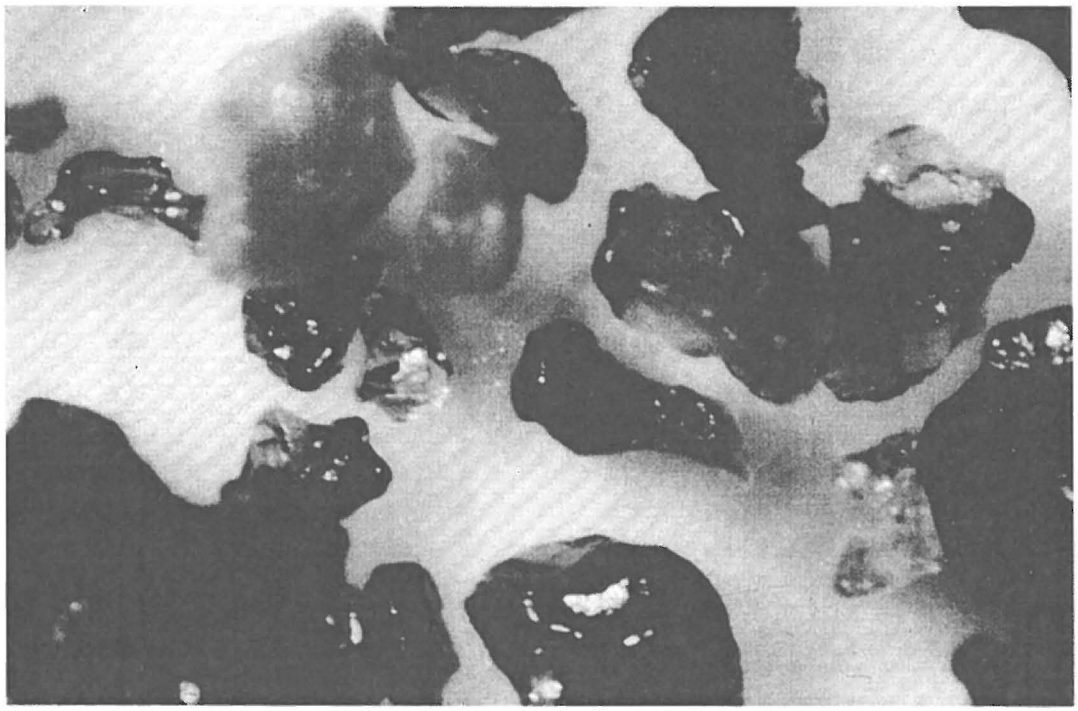

Fig. 23. *Glass shards from unit 1 (courtesy of A. Hildebrand).*

UNIT 2

Massive Sandstone: Horizontally laminated sandstone, with mudclasts and plant debris at its base. No indication of upward fining.

Thickness: Variable, up to 140 cm, thinning out and disappearing toward channel edges (Fig. 24).

Lower Contact: Disconformable with spherule unit 1.

Upper Contact: Disconformable with unit 3.

Sedimentological Features: Horizontal laminations (Fig. 25).

Mudclasts: Common at base, with some containing Turonian-age Foraminifers.

Plant Debris: Abundant wood and leaves in distinct layers near the base; no charcoal observed (Fig. 26).

Mineralogy: Quartz 41%, plagioclase 23% (mostly oligoclase and albite), calcite 24%, phyllosilicates 11% (Fig. 11).

Bioturbation: None observed.

Other Characteristics: No glass, shocked quartz, spherules, or Ir.

UNIT 3

Sand-Siltstone: Interlayered sand, shale, and siltstone beds topped by rippled sandy limestone layer that is commonly bioturbated (Fig. 27).

Thickness: 100 cm in outcrop center thinning to 20 cm at edge.

Lower Contact: Disconformable with unit 2 in center of outcrop and unit 1, or even Mendez Formation near edge of outcrop.

Upper Contact: Disconformable (?) overlain by shales of the Velasco Formation.

Sedimentological Features: Diverse, including laminated intervals and upward fining, ripple marks, flaser bedding, convolute laminations, and thin layer of normal hemipelagic sedimentation.

Rippled Sandy Limestone (RSL): Thickness between 20 and 25 cm, resistant to weathering, contains climbing ripples; layer continues outside the channel.

Mudclasts: None observed.

Bioturbation: *Chondrites* near top and within rippled sandy limestone layer.

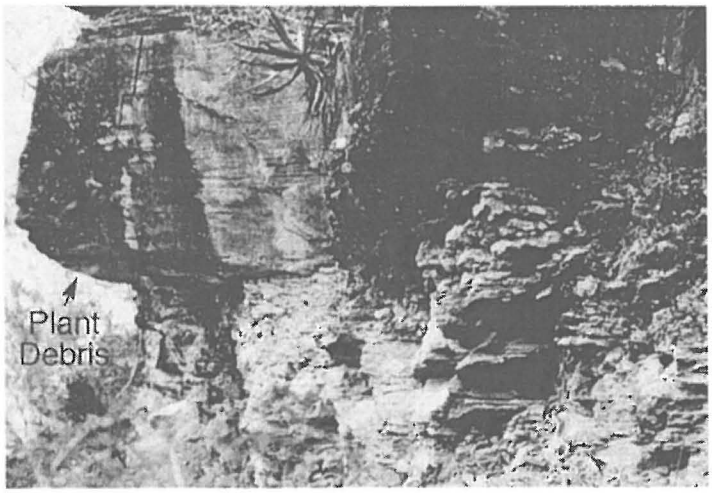

Fig. 24. *Unit 2, massive sandstone overlying spherule layer.*

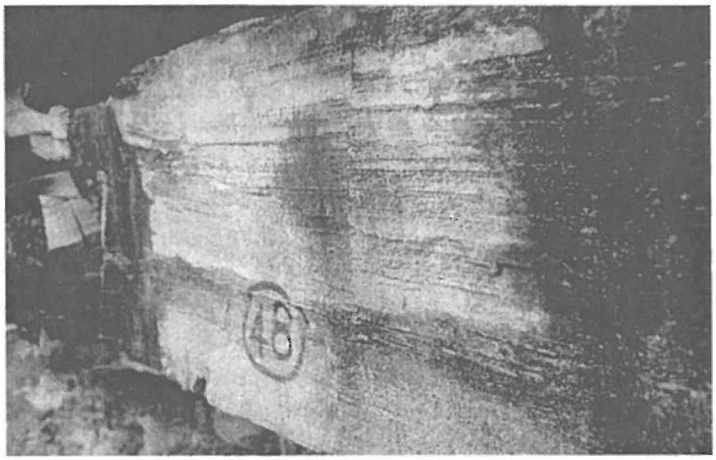

Fig. 25. *Unit 2, massive sandstone with horizontal laminations.*

Figs. 26. *Plant debris in discrete layers near the base of unit 2. See Fig. 24 for location.*

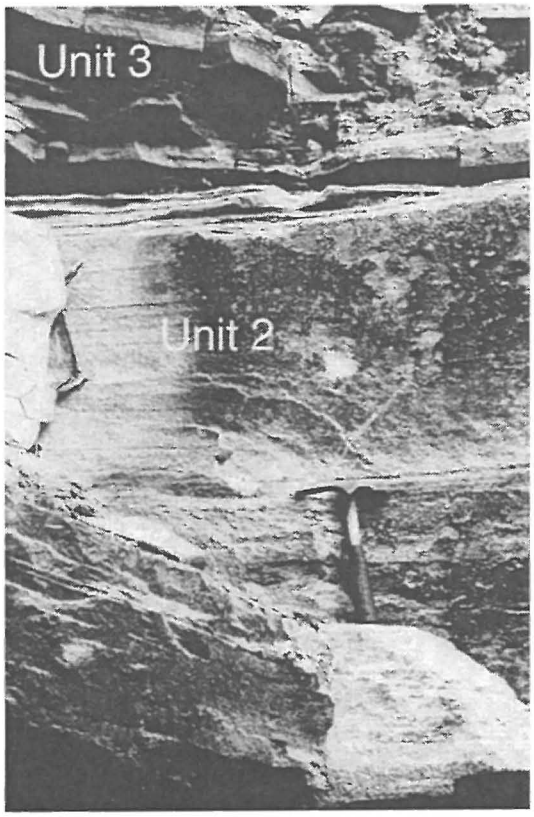

Fig. 27. Mimbral I, units 2 and 3.

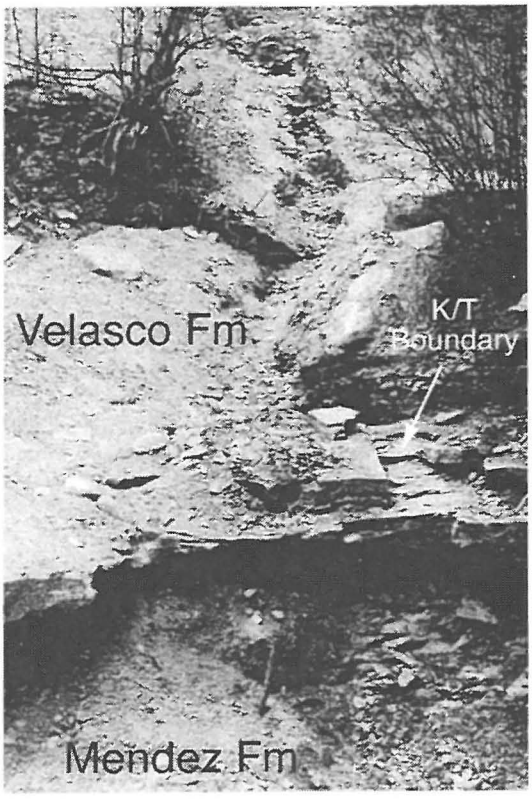

Fig. 28. Mimbral II, right edge of outcrop.

Mineralogy: Mineralogical contents vary from layer to layer. Thin hemipelagic sediment layers with high carbonate content can be correlated with similar layers of unit 3 in other outcrops. Zeolite-enriched layers are present and can be correlated with other outcrops.

Other Characteristics: No glass, spherules, shocked quartz, or Ir observed (see Fig. 98 for Ir profile).

(Putative) KT Boundary Layer:

Thickness: 2–4 cm observed only at right edge of Mimbral outcrop. A 2–4-mm-thick red layer is present about 1 cm above the base of the clay layer (Figs. 8 and 28).

Lower Contact: Probably disconformable with sandy limestone layer of unit 3 as indicated by bioturbation.

Upper Contact: Conformable, grades into shales and marls of the Velasco Formation.

Mineralogy: Randomly interstratified smectite (80%) and illite (20%) (Fig. 11).

Other Characteristics: Very rare small subrounded quartz grains with two sets of planar deformation features were found in the red layer (Fig. 9). Boundary clay layer is enriched in zeolites.

Smit et al. (1992) reported Ir concentrations of 0.9 ppb in the basal Velasco shale overlying unit 3 near meter mark 28 along the outcrop. (The age of this Velasco shale is Zone P1a.) Rocchia and Robin (in *Stinnesbeck et al.*, 1993) measured maximum Ir concentrations of 0.8 ppb in the boundary clay or Zone P0 and in Zone P1a. No elevated levels of Ir and no Ni-rich spinels were found in the red layer at the base of the boundary clay, or the sandy limestone (see Fig. 98).

ARROYO LA LAJILLA

The KT boundary transition crops out along the river outlet of the La Lajilla Lake dam about 200 m north of the village of La Lajilla at latitude 23°40'N and longitude 98°43.9'W (Fig. 1). The section is approached by the main road from Cd. Victoria to Soto La Marina (Fig. 29). Five hundred meters east of the small village of Casas is an electrical transform station on the south side of the road. Immediately beyond this electrical station to the south is an unpaved dirt road leading 8 km to the La Lajilla village. The dirt road is well graded and passable with ordinary cars. KT boundary outcrops are easily accessible and seen from the road and bridge across the Arroyo La Lajilla just before entering the village. Boundary outcrops are found on the north and south sides of the banks of the arroyo (Figs. 30 and 31). Additional outcrops are located on the shores of La Lajilla Lake. Specifically, one nearby outcrop (La Lajilla II) can be easily reached on a trail to the south side of the lake about 150 m beyond a small pedestrian bridge.

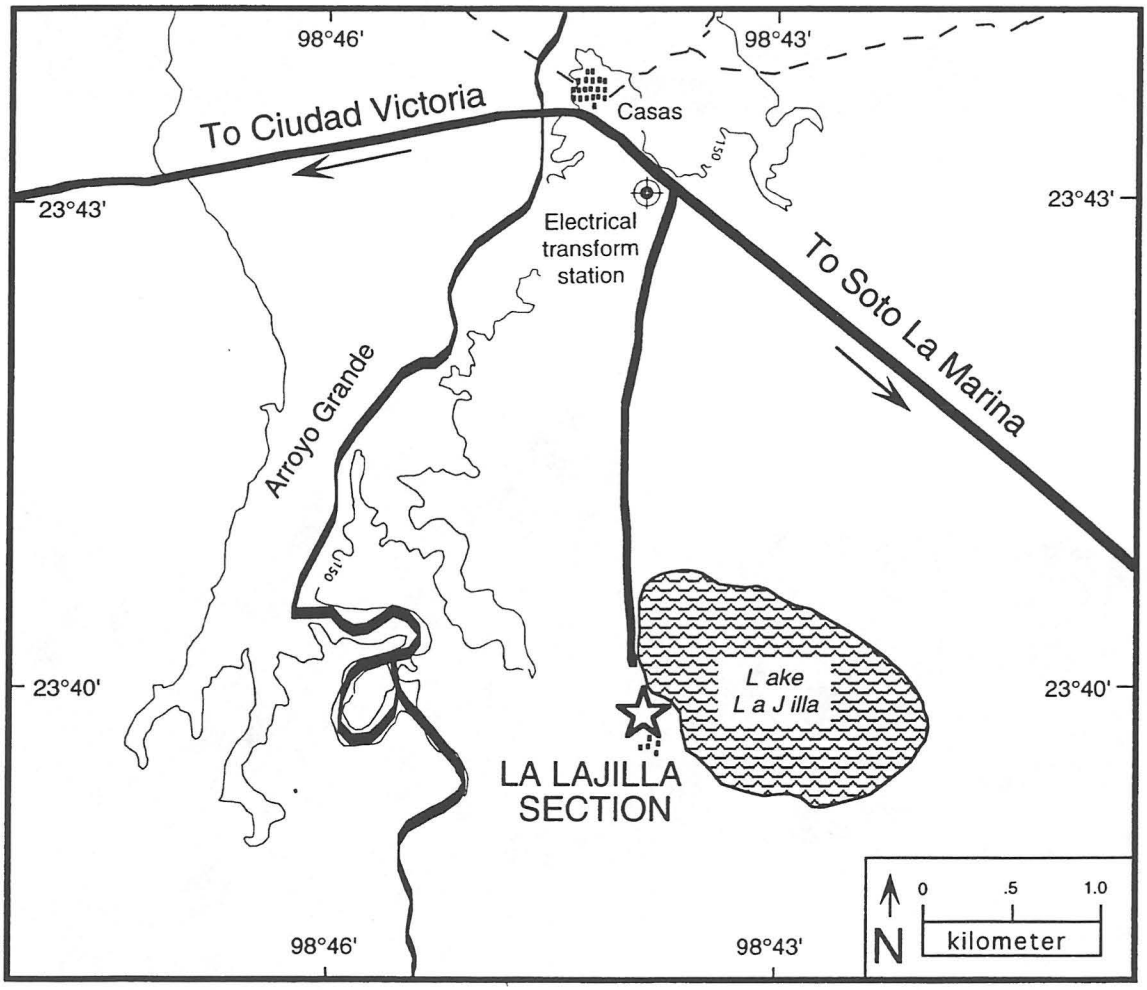

Fig. 29. Location map of Arroyo La Lajilla KT boundary outcrops.

Fig. 30. *La Lajilla KT boundary outcrop I on the north side of the arroyo with view of pedestrian bridge in background.*

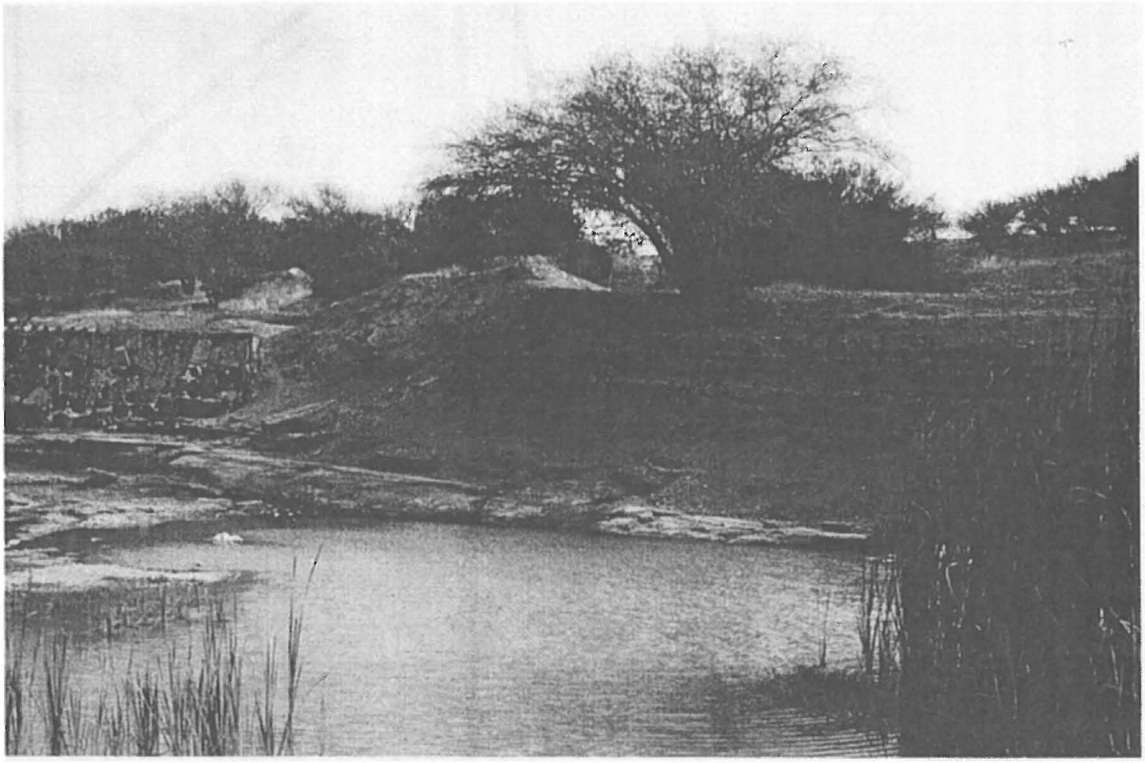

Fig. 31. *La Lajilla KT boundary outcrop I on the south side of the arroyo with trail in background leading to La Lajilla II outcrop along the lake shore.*

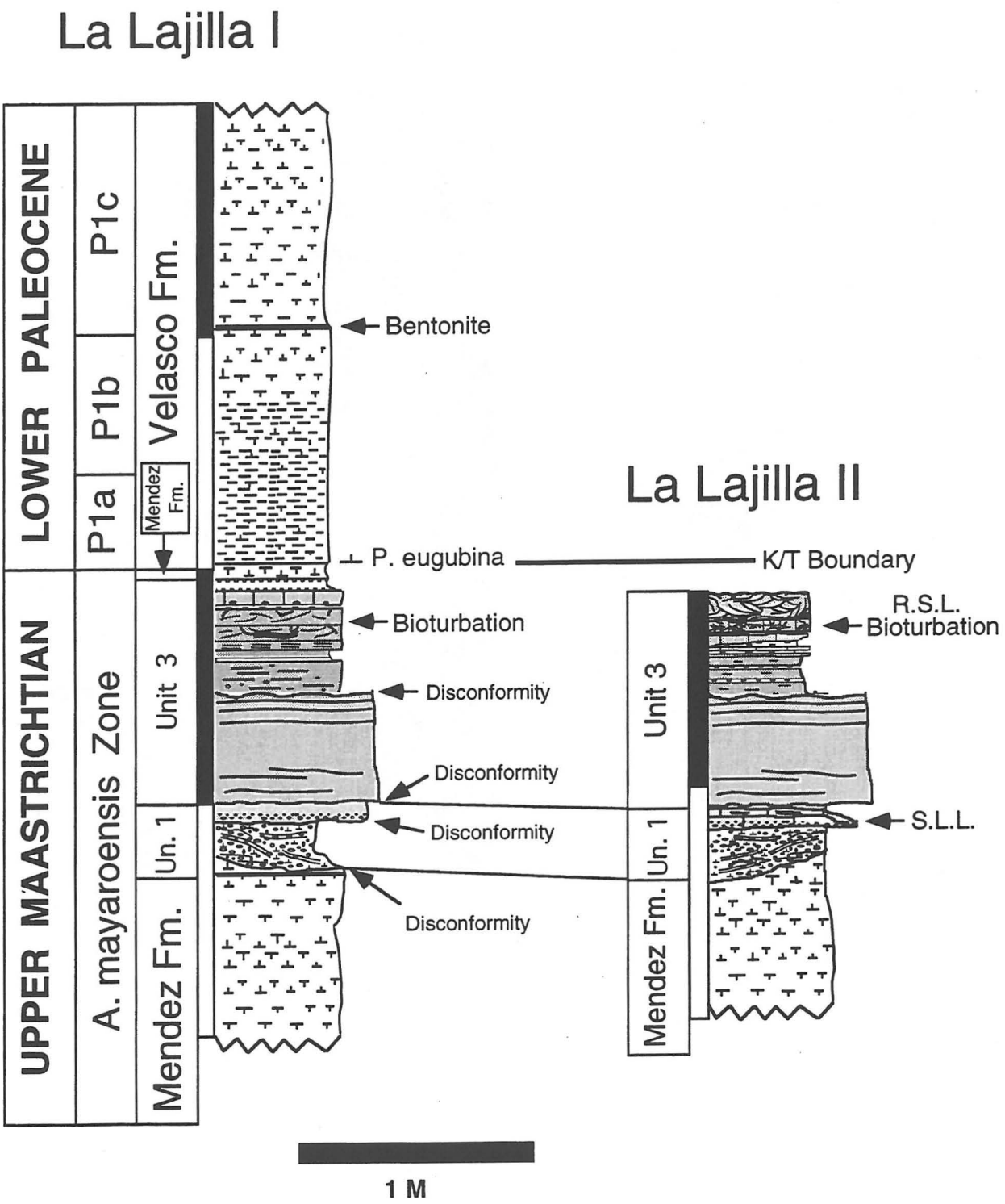

Fig. 32. Lithostratigraphic columns of La Lajilla I and II. Note the thin layer of Mendez marl with A. mayaroensis-zone foraminifera on top of unit 3 at La Lajilla I indicates that the clastic member was deposited prior to the KT boundary event. RSL = rippled sandy limestone, SLL = sandy limestone layer.

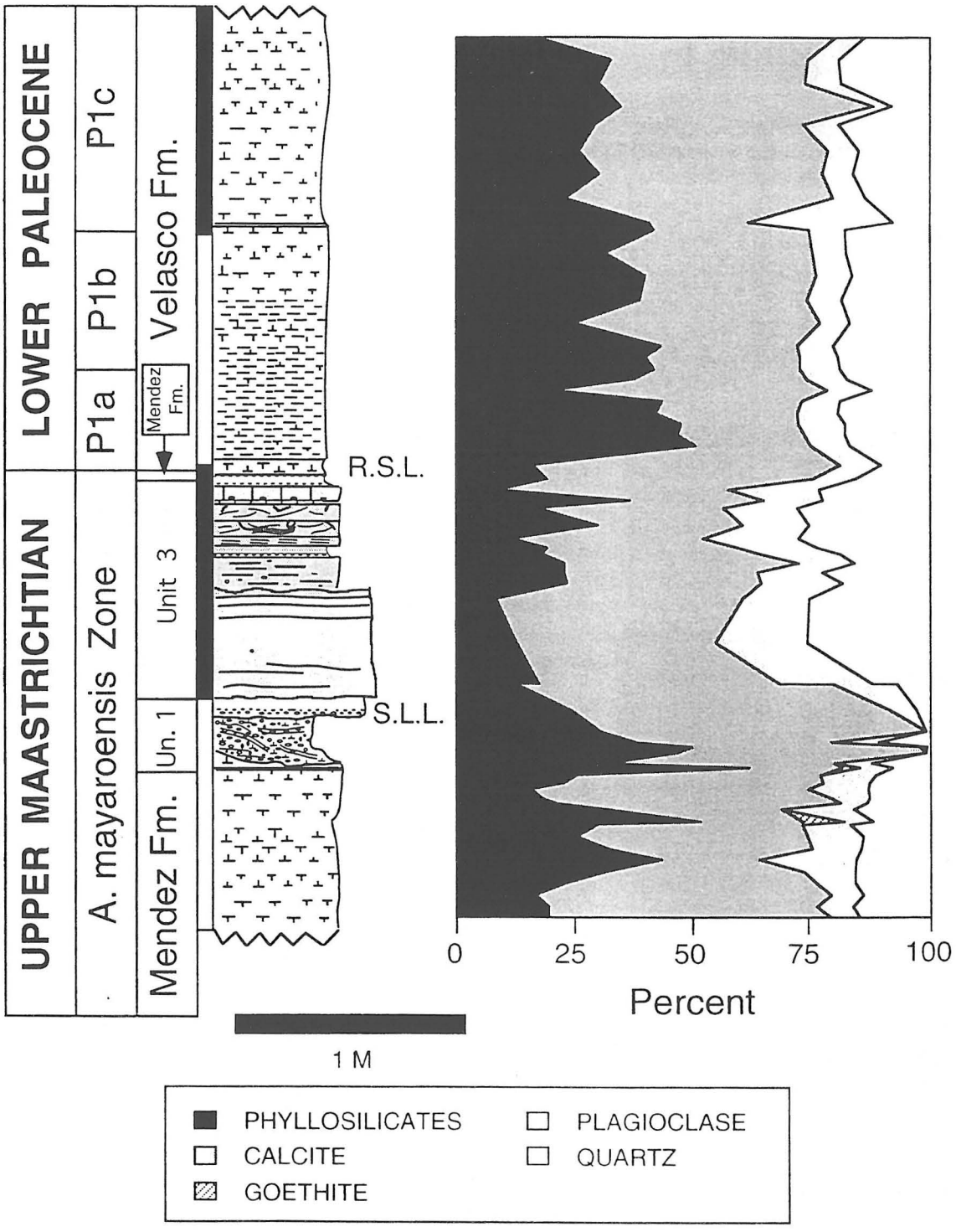

Fig. 33. *Whole-rock composition of the La Lajilla I KT boundary outcrop (from Adatte et al., in preparation). Measured by estimation from whole-rock XRD (Kübler, 1987).*

La Lajilla I and II Sections

At La Lajilla I the KT boundary transition is exposed on both the north and south sides of the arroyo; however, on the south side more of the Tertiary Velasco Formation is exposed. The basal part of the outcrop (75 cm) consists of gray marls of the upper Maastrichtian Mendez Formation (Figs. 30 and 31). An erosional contact separates the Mendez Formation from the overlying spherule-rich sediments that are topped by the sandy limestone layer (SLL) of unit 1 that is characterized by spherules at its base and top. The spherule-rich sediments are variable in thickness and reach a maximum of 35 cm. The sandy limestone layer at the top of unit 1 is a maximum of 8 cm thick and locally disappears. Both the upper and probably lower contacts of the sandy limestone layer appear to be disconformable (Fig. 32). Above the apparent disconformity at the top of unit 1 is a 1-m-thick sequence of horizontally laminated and cross-bedded sandstone intercalated with siltstone and topped by bioturbated rippled sandy limestones (RSL, Fig. 31). This sedimentary sequence correlates with unit 3 of Mimbral. Unit 2 (the laminated sandstone) is missing. Above unit 3 (RSL) a thin layer of Mendez marls is present (Fig. 32) containing a well-developed assemblage of the *A. mayaroensis* zone including the index taxon. This layer of Mendez marl indicates that unit 3 of the clastic deposit was deposited during the latest Maastrichtian prior to the KT boundary event. No clay layer is present between the top of this Mendez marl and the overlying Velasco Formation, which is of Zone P1a *(P. eugubina)* age. About 2 m of Lower Tertiary marls of the Velasco Formation are exposed. La Lajilla II, which crops out along the lake shore, is very similar to La Lajilla I except that several meters of the Mendez Formation are exposed.

UNIT 1

Spherule Layer:	Friable, rich in calcareous spherules, glauconite particles, and glauconite infilling of spherules and foraminifera, mud-clasts of the Mendez Formation and discrete layer of sandy lime stone.
Thickness:	Variable, ranging between 5 cm and 35 cm including 8-cm-thick sandy limestone (Fig. 37).
Lower Contact:	Disconformably overlies the Mendez Formation, contact characterized by undulating erosional surface (Fig. 39).
Upper Contact:	Disconformable with laminated and cross-bedded sandstone of unit 3 (Fig. 39).
Sedimentological Features:	Oblique bedding, laminations.
Sandy Limestone Layer (SLL):	Discontinuously present.
Position:	At top of spherule-rich sediments of unit 1. In contrast, at Mimbral and Peñon I the sandy limestone layer is within unit 1.
Thickness:	Variable, ranging from 0 to 10 cm.
Characteristics:	Undulating surfaces on top and bottom of layer due to convolute bedding (Fig. 37). Gradation in spherule abundance and size.
Spherules:	Size mostly 2–5 mm, spherules usually weathered in sandy limestone and replaced by blocky calcite.
Mudclasts:	Rounded clasts of Mendez marls up to 15 cm in size.

Mineralogy: Calcite 35–60%, plagioclase 10–20%, quartz 15–30%, phyllosilicates 20–40%.

Bioturbation: None observed.

UNIT 2

Massive Sandstone: Not present at La Lajilla I or II.

UNIT 3

Sand-Siltstone: Interlayered sand, shale, and siltstone beds topped by rippled sandy limestone layers that are commonly bioturbated (Figs. 38–40).

Thickness: 90–100 cm.

Lower Contact: Disconformable with unit 1 and generally overlies the sandy limestone layer (Fig. 37).

Upper Contact: Disconformable with overlying marls of the Mendez Formation, sometimes with oxidation crusts at the top of unit 3.

Sedimentological Features: Diverse, including laminated intervals, ripple marks, and small-scale cross-bedding, coarse-grained layers separated by thin muddy layers that could represent long intervals of hemipelagic sedimentation.

Rippled Sandy Limestone (RSL): Two or three very resistant beds separated by thin interlayers of siltstone (Figs. 38 and 40), pronounced small-scale bedding, total thickness between 20 cm and 25 cm.

Mudclasts: None observed.

Bioturbation: Abundant *Chondrites* and Y-shaped (? *Thalassinoides*) burrowing networks near the top of unit 3 within sandy limestone layers.

Lithology: Mineralogical contents vary from layer to layer. Zeolites present in distinct layers.

Other Characteristics: Glass reported by *Bohor and Betterton* (1993).

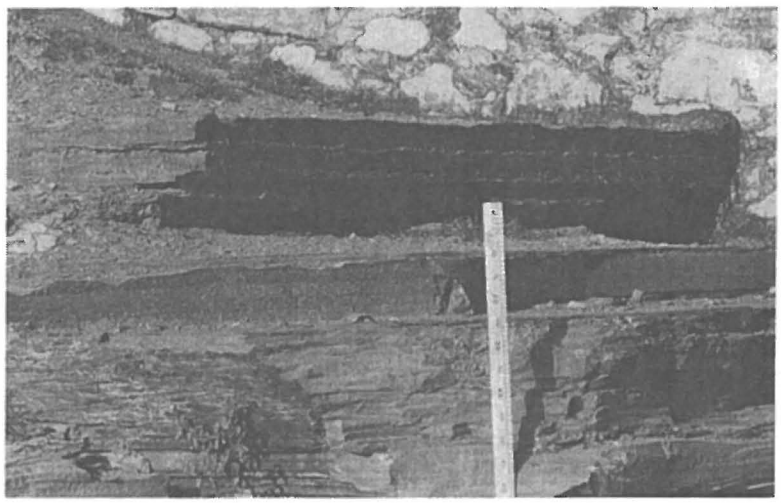

Fig. 34. *La Lajilla I, unit 3 on north side of arroyo.*

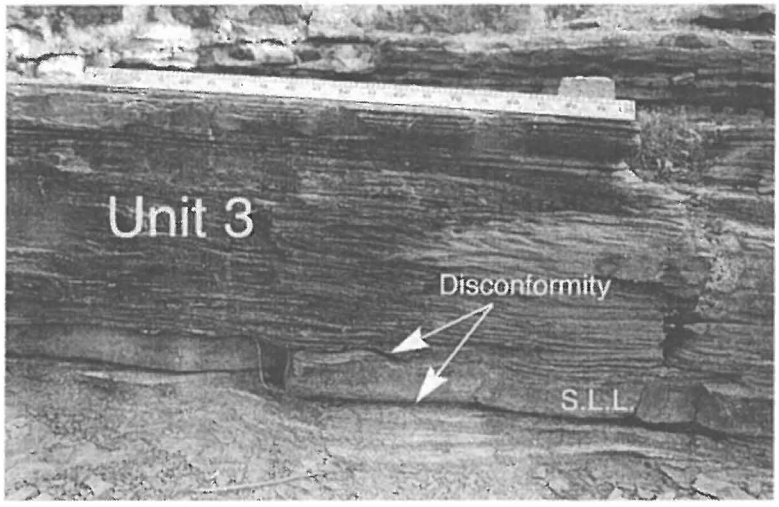

Fig. 35. *La Lajilla I, note disconformities above and below the SLL of unit 1.*

Fig. 36. *La Lajilla I, on south bank of arroyo. Unit 3 and overlying Velasco Formation.*

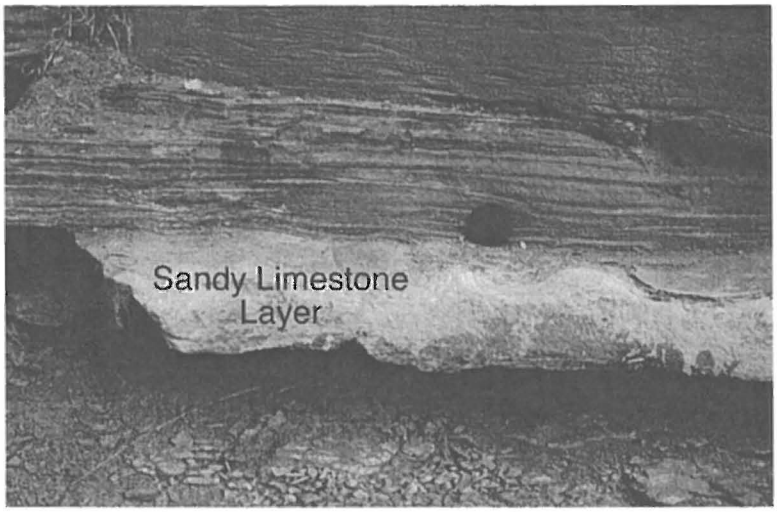

Fig. 37. *La Lajilla I, sandy limestone of unit 1 with convolute bedding.*

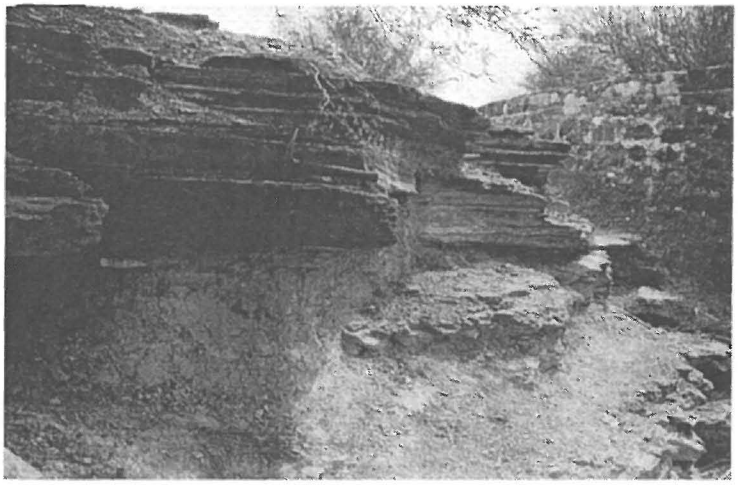

Fig. 38. La Lajilla II, KT boundary outcrop showing top of Mendez marl, reduced spherule-rich unit 1 topped by sand-silt alternations of unit 3.

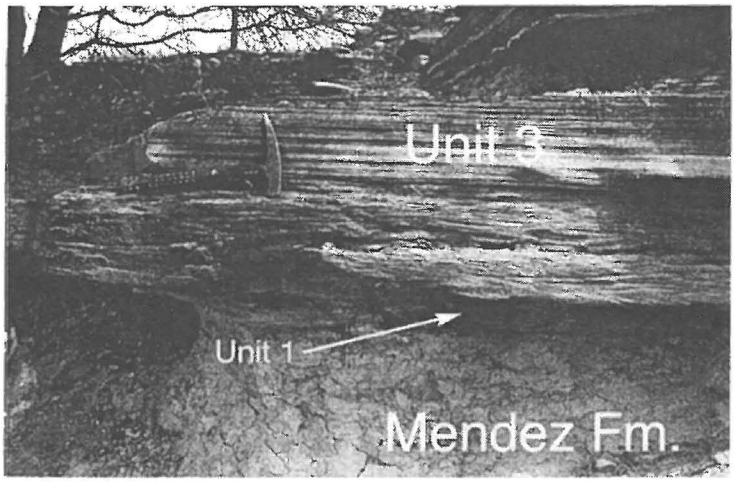

Fig. 39. La Lajilla II, with Mendez marls, spherule-rich unit 1 and lower part of unit 3.

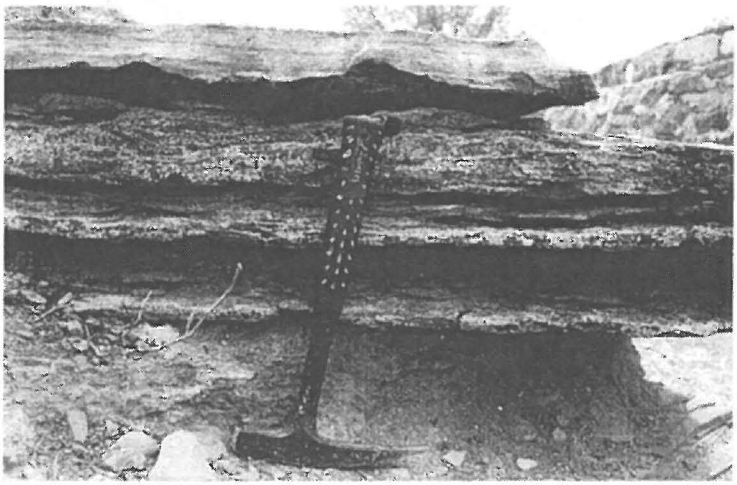

Fig. 40. La Lajilla II, several beds of the sandy limestone layer that cap unit 3.

EL PEÑON

The El Peñon KT boundary outcrop is located 40 km east of Linares at latitude 24°58'N and longitude 99°12.5'W (Fig. 41). To locate the El Peñon section take the road to Cerro Prieto and follow it along the lake shore to Cascajoso. There take the unmarked dirt road that branches to the south leading to Burgos. (If lost, ask for the road to Burgos.) Follow the dirt road for about 20 km to reach Porvenir Lake. Near the lake, the road bifurcates: The right branch leads to El Mulato, the left branch to El Peñon. Follow the left branch for 3 km to El Peñon. At this point the electrical power lines take a turn east to a trail that leads off the main dirt road to the west. Follow this trail for about 1 km across a dry creek, curving to the right for about 200 m. Stop and park. (This last kilometer is not always accessible without four-wheel drive.) The main El Peñon I outcrop is to the left, extending for about 100 m and dipping 8° to the northeast (Fig. 42). The second outcrop, El Peñon II, is 200 m north of the main outcrop on a small hill (Fig. 43).

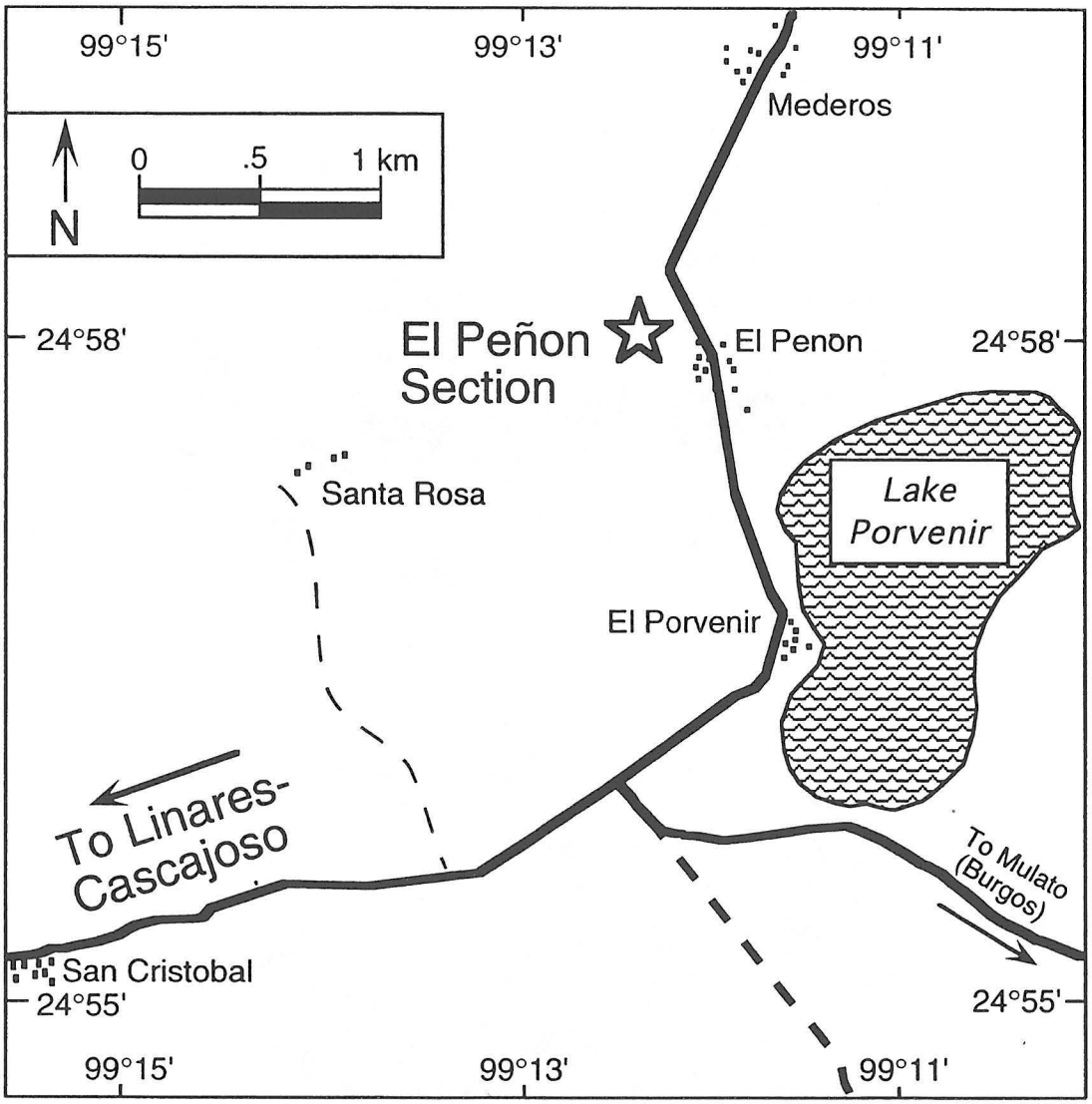

Fig. 41. Location map of El Peñon KT boundary outcrops.

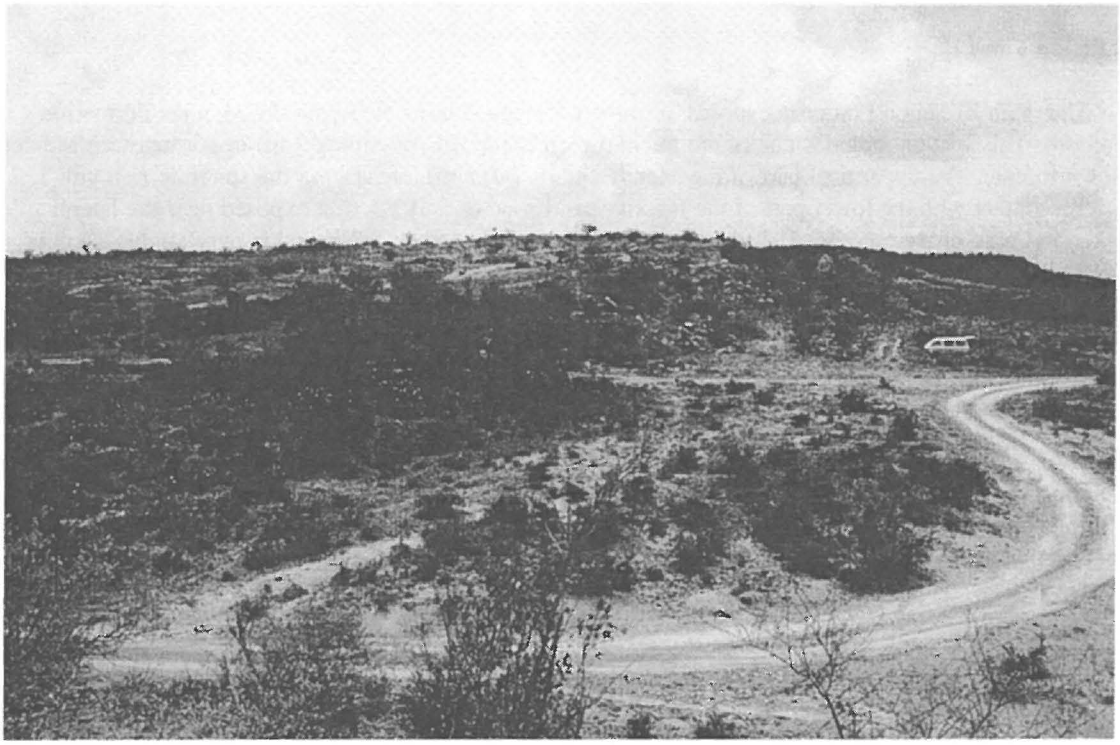

Fig. 42. General view of El Peñon with KT boundary outcrop in background to the left of parked car.

Fig. 43. Near-KT clastic deposit of El Peñon II.

El Peñon I and II

The main El Peñon I outcrop exposes all three lithological units overlying the Mendez Formation (Fig. 44). This section includes one of the thickest clastic deposits (spanning 7 m) in northeastern Mexico known to date. The uppermost part of the Mendez marls (<0.5 m), underlying the spherule-rich unit 1, and the contact with the lower part of the massive sandstone of unit 2 is best exposed near the lateral center and base of the outcrop. The massive sandstone of unit 2 spans 3.7 m and is overlain by 2.7 m of alternating sand and siltstone beds of unit 3. The top of unit 3 is bioturbated and exposed over a large parking-lot-sized area. The top of this bioturbated interval is correlatable with the rippled sandy limestone layer that characterizes the top of the clastic deposit in other KT boundary sections. No Velasco Formation is present.

The Peñon II section is located 200 m north of the main Peñon I outcrop and to the (north) side of the trail. The section exposes about 5 m of weathered marls of the Mendez Formation (Fig. 44) followed by a 2.5-m-thick clastic deposit (Fig. 43). Only units 1 and 3 are present, which are correlatable with the main outcrop. About 20 cm of spherule-rich sediments topped by a 5-cm-thick sandy limestone form unit 1. Unit 3 consists of 2.7 m of alternating sand and siltstone beds that disconformably overlie unit 2. No Velasco Formation is present. Additional outcrops showing sequences similar to El Peñon II are found nearby.

UNIT 1

Spherule Layer:	Friable, rich in calcareous spherules and glauconite particles and infillings of foraminiferal shells, discrete layer of sandy limestone (SLL, Fig. 46).
Thickness:	Variable, ranging from 65 to 75 cm in El Peñon I and 25 cm at El Peñon II.
Lower Contact:	Disconformably overlies the Mendez Formation, contact characterized by undulating erosional surface.
Upper Contact:	Disconformable with massive sandstone of unit 2 at El Peñon I and disconformable contact with cross-bedded sandstone of unit 3 at El Peñon II (Fig. 44).
Sedimentological Features:	Oblique bedding and groove casts on base (Fig. 47).
Sandy Limestone Layer (SLL):	Present in the upper part of the spherule-rich layer of unit 1 at El Peñon I, and at the top of unit 1 at El Peñon II (Fig. 48). Undulating upper and lower surfaces due to convolute bedding at El Peñon II. Gradation of spherule abundance observed at El Peñon I.
Thickness:	5–8 cm.
Spherules:	2–5 mm in size, usually weathered in friable sediments and replaced by blocky calcite in sandy limestone layer (SLL).
Mineralogy:	Calcite 60%, plagioclase 9%, quartz 15–20%, and phyllosilicates 15–20% (Fig. 45).

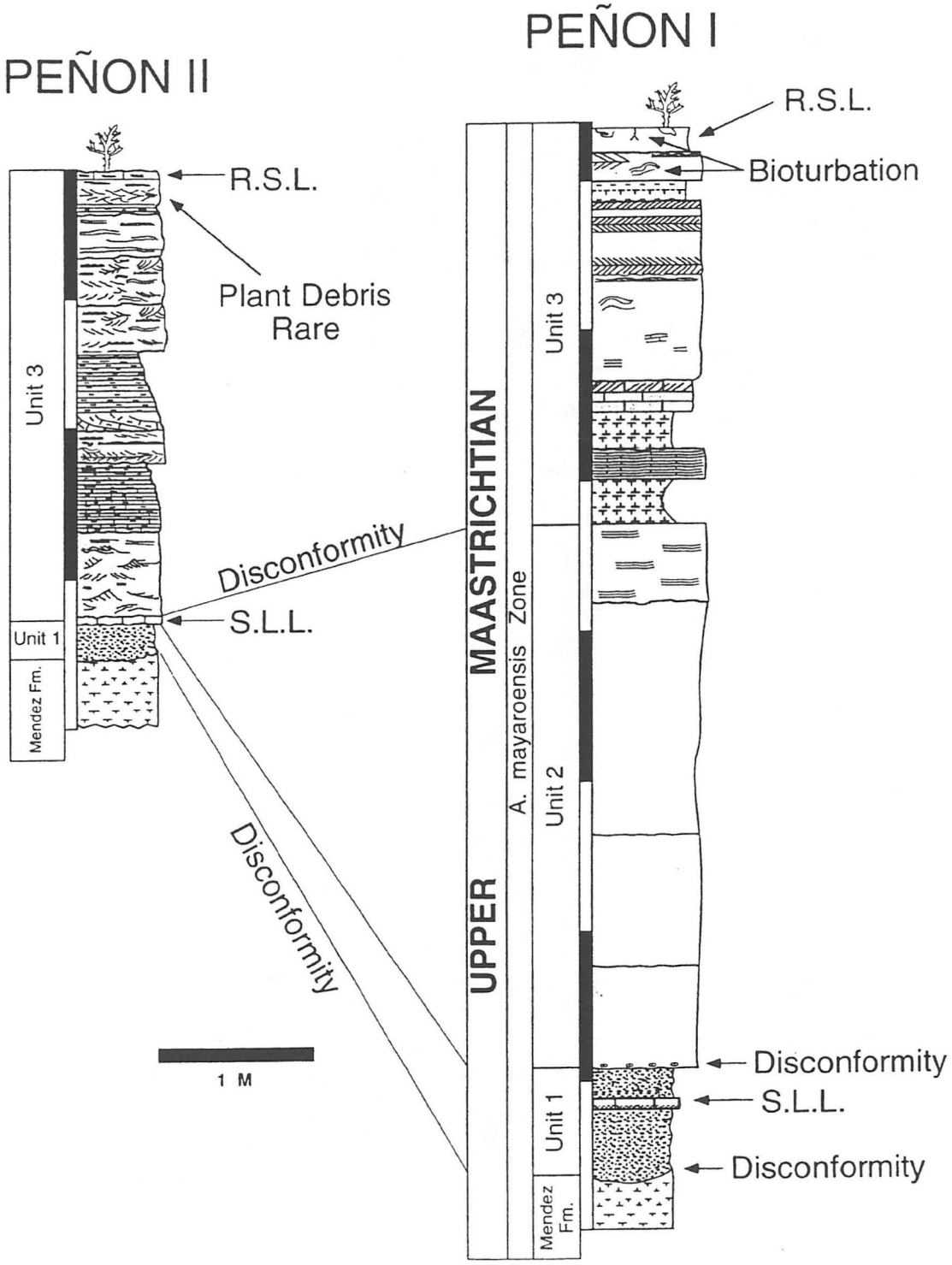

Fig. 44. *Lithostratigraphic columns of near-KT-boundary outcrops at El Peñon I and II. RSL = rippled sandy limestone, SLL = sandy limestone layer.*

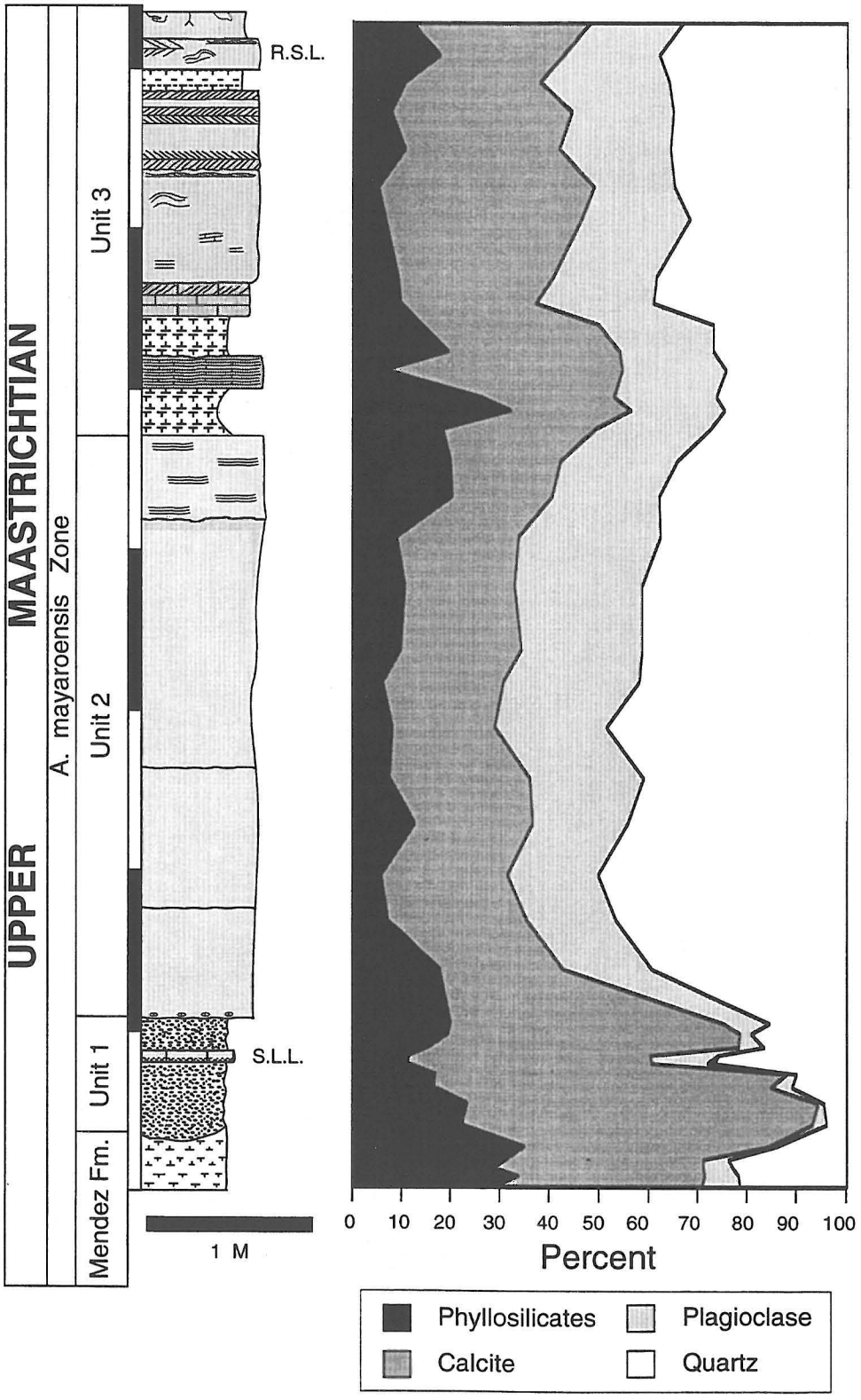

Fig. 45. Whole-rock composition of near-KT-boundary deposits at El Peñon I, measured by estimation from whole-rock XRD (Kübler, 1987).

UNIT 2

Massive Sandstone: Horizontal laminations, mudclasts at base, upward fining of sediments observed (Fig. 49).

Thickness: Variable, up to 3.7 m at El Peñon I, not present at El Peñon II.

Lower Contact: Disconformable with spherule-rich unit 1.

Upper Contact: Conformable (?) with unit 3 at El Peñon I.

Sedimentological Features: Horizontal laminations, weak upward fining.

Mudclasts: Common at the base of unit 2, up to 10 cm in size (Fig. 51).

Plant Debris, Bioturbation: None observed.

Mineralogy: Calcite 25–30%, plagioclase 10–20%, phyllosilicates 10–20%, quartz 40% (Fig. 45).

UNIT 3

Sand-Siltstone: Interlayered sand, shale, and siltstone beds, topped by rippled and bioturbated limestone (Figs. 50, 52, and 53).

Thickness: 2.6–2.7 m at El Peñon I and II.

Lower Contact: Conformable (?) with unit 2 at El Peñon I and disconformable with sandy limestone layer of unit 1 at El Peñon II (Fig. 52).

Upper Contact: Contact with Velasco Formation not present.

Sedimentological Features: Diverse, including laminations, convolute bedding (Fig. 56), ripple marks (Fig. 55), flaser bedding, and thin fine-grained muddy layers.

Rippled Sandy Limestone (RSL): Not well characterized in comparison with clastic deposits at El Mimbral or La Lajilla. Top 15 cm of unit 3 at El Peñon I and II has high carbonate content.

Mudclasts: Rare mudclasts and spherules at the base of unit 3, which unconformably overlies unit 1 at El Peñon II.

Plant Debris: Rare wood and leaf debris in upper 50 cm of unit 3.

Bioturbation: Common in discrete layers near top of unit 3, abundant *Chondrites, Zoophycos,* and Y-shaped *Thalassinoides*(?) burrowing networks (Figs. 57–59).

Mineralogy: Mineralogical contents vary from layer to layer. Zeolites present in distinct layers.

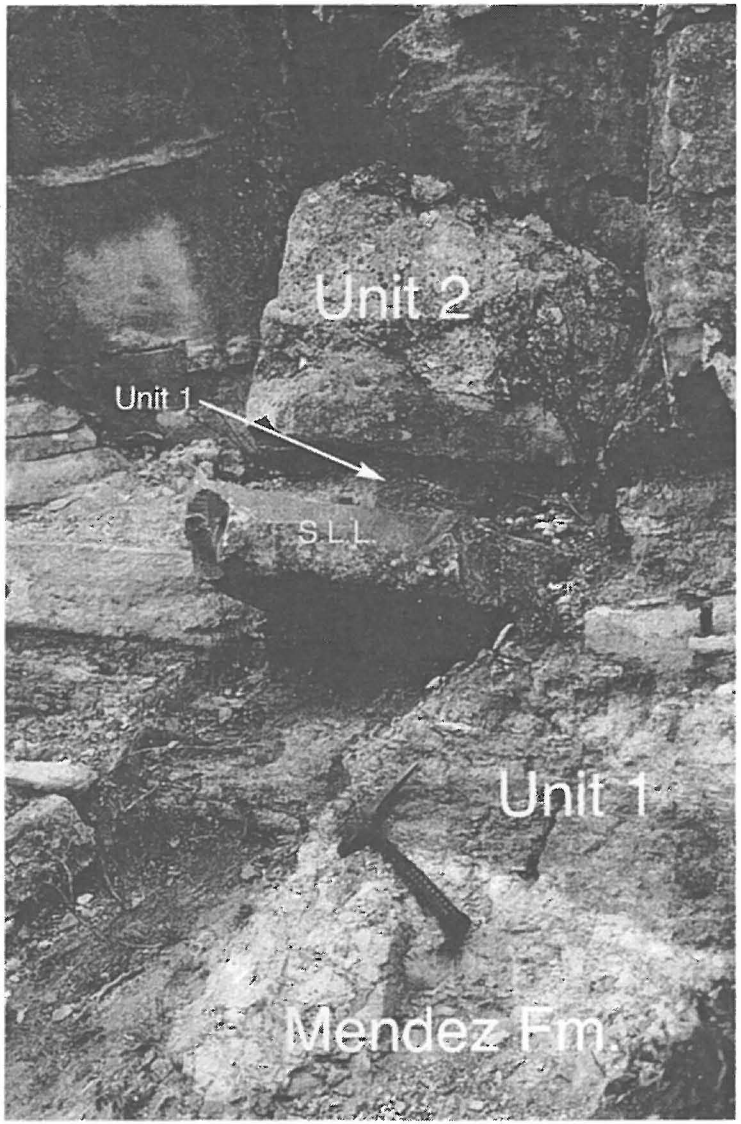

Fig. 46. *El Peñon, lower part of clastic deposit.*

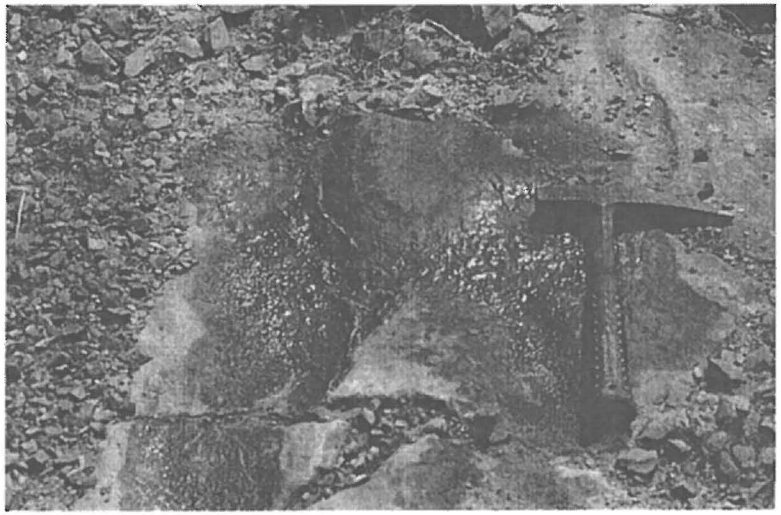

Fig. 47. *El Peñon I, groove casts at the base of unit 1.*

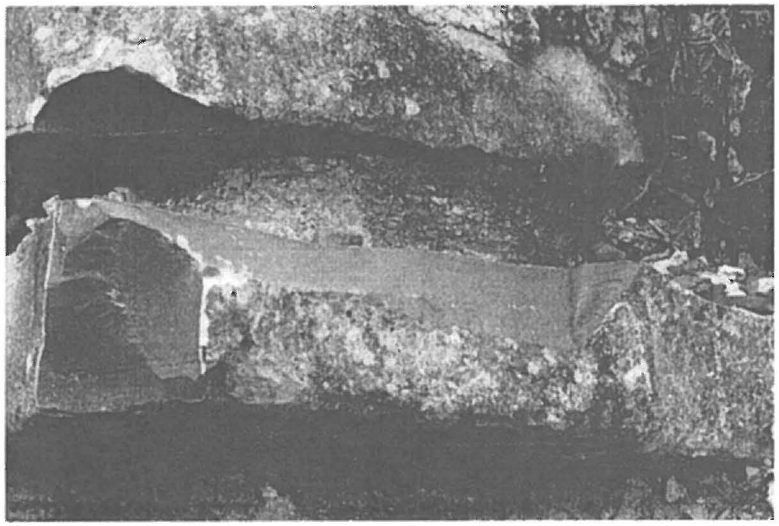

Fig. 48. *El Peñon, sandy limestone in unit I and gradation of spherules.*

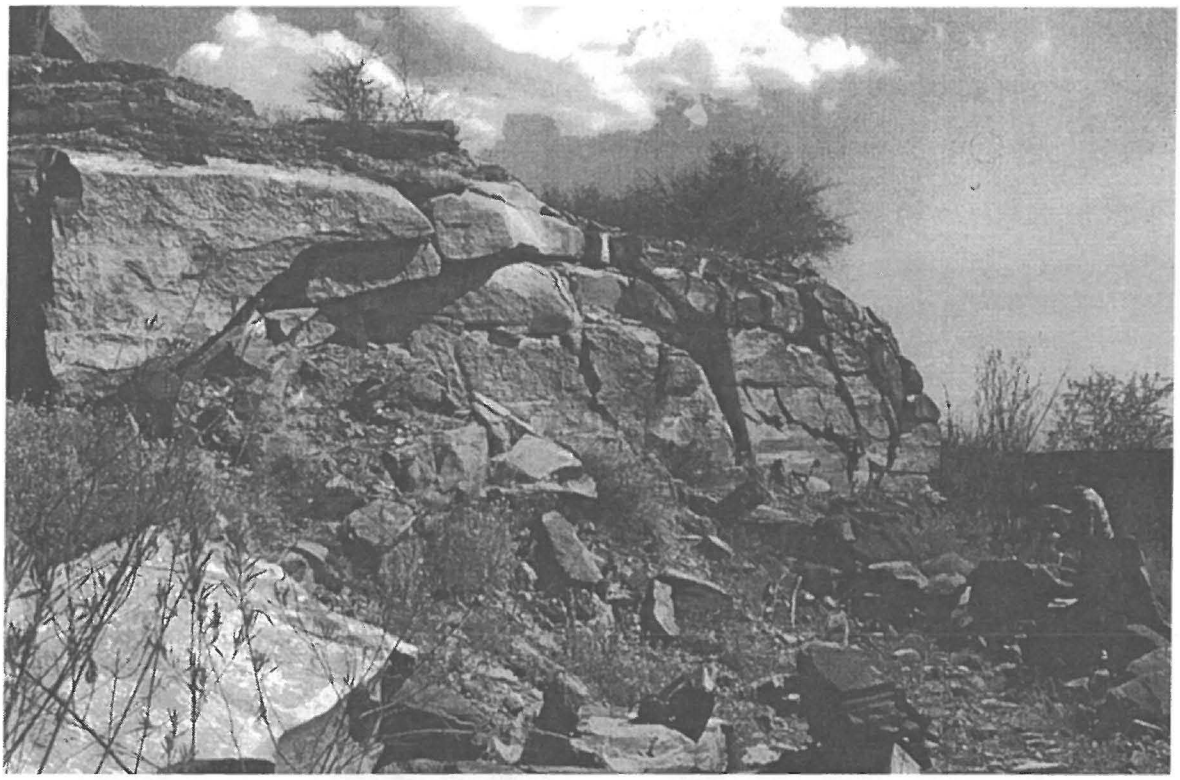

Fig. 49. *El Peñon I, massive sandstone of unit 2.*

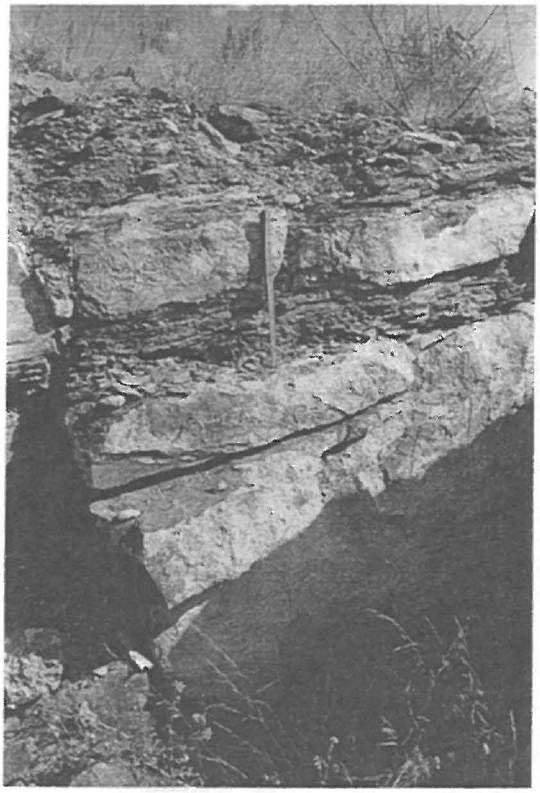

Fig. 50. *El Peñon I, alternating beds of sand and siltstone of unit 3.*

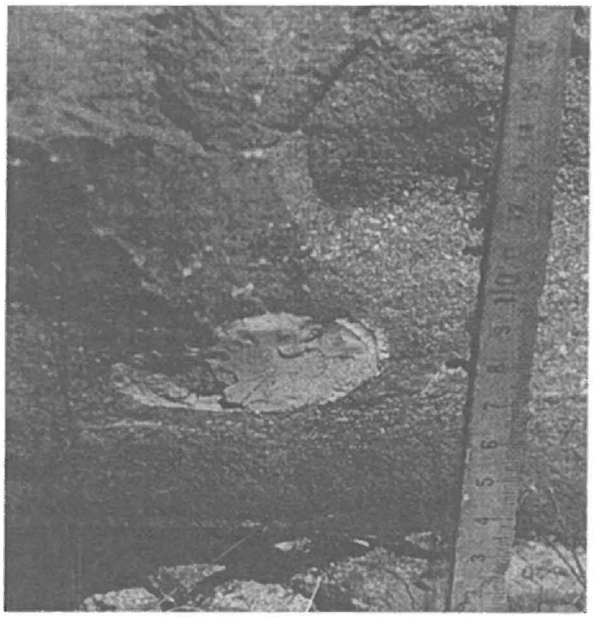

Fig. 51. *El Peñon I, rounded mudclast near the base of unit 2.*

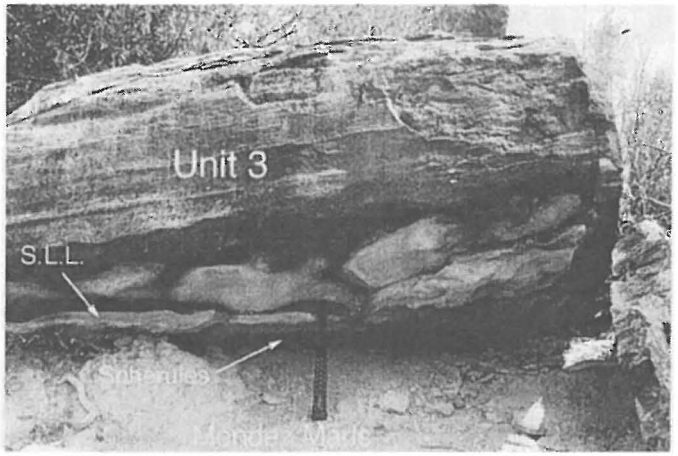

Fig. 52. *El Peñon II, unit 1 with SLL on top disconformably underlying unit 3.*

Fig. 53. *El Peñon II showing variable sedimentary features of unit 3.*

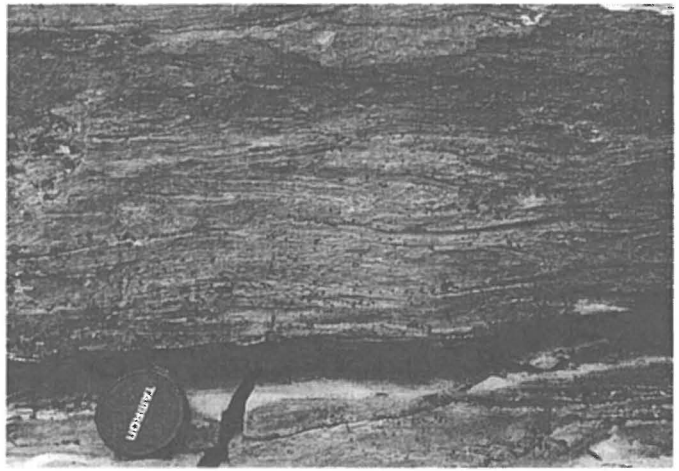

Fig. 54. *El Peñon II, wavy bedding of sandstone within unit 3.*

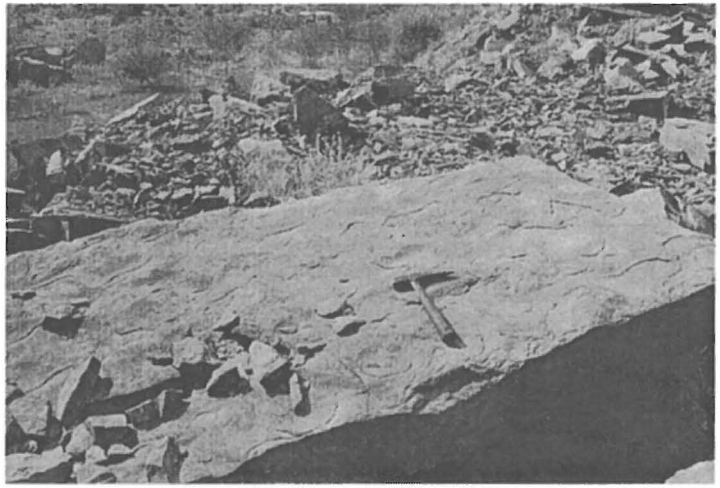

Fig. 55. *El Peñon I, ripple marks near top of unit 3.*

Fig. 56. *Convolute bedding within unit 3 at El Peñon I.*

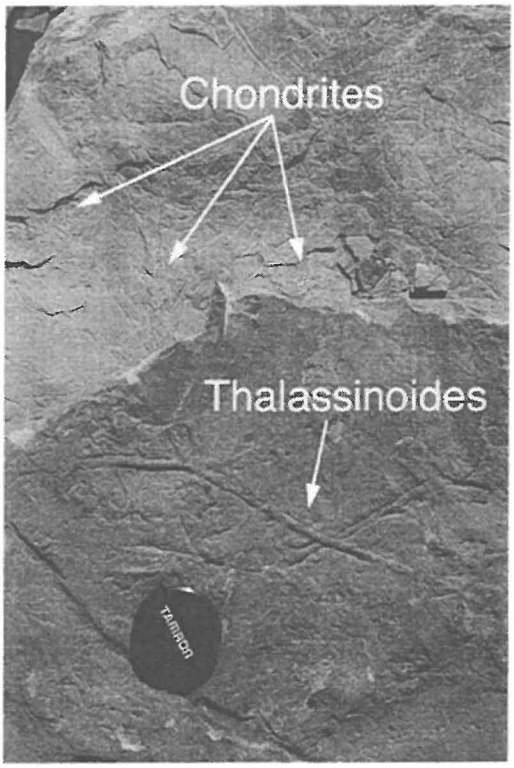

Fig. 57. *Unit 3 at El Peñon I with two different bioturbated sediment layers.*

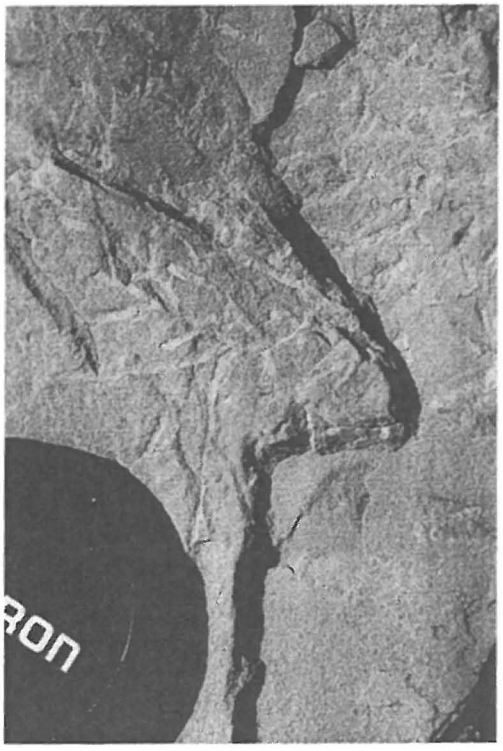

Fig. 58. *Chondrites burrows near top of unit 3 at El Peñon I.*

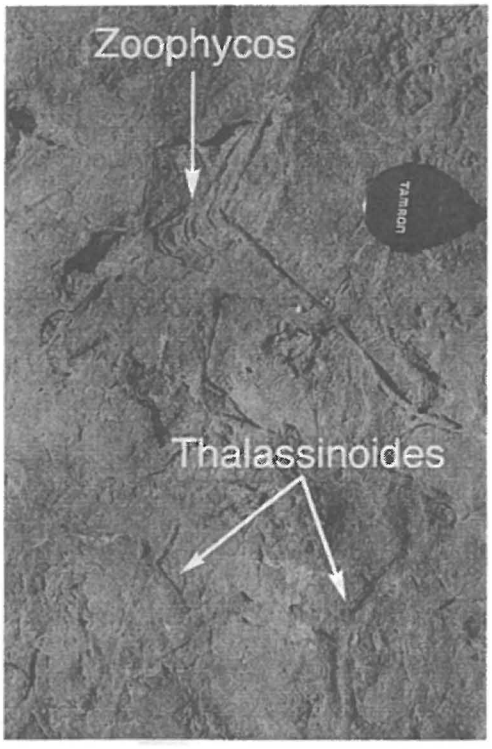

Fig. 59. *Zoophycos and Thalassinoides(?) burrows near top of unit 3 at El Peñon I.*

EL MULATO

The KT boundary outcrop is located north of the village of El Mulato (Fig. 60) (latitude 24°54'N, longitude 98°57'W). The village is situated on the unpaved road from Linares to Burgos about 60 km east of Linares (the road is serviceable in dry periods only). For directions to the dirt road to Burgos, see road information for El Peñon. Near Lake Porvenir take road to Mulato-Burgos (roads are not marked). About 500 m after the turn-off to El Peñon, the road branches again. Here take the northeast (left) branch to Burgos (if in doubt, ask). Follow this road for 20 km past the state border between Nuevo León and Tamaulipas into the village of El Mulato and park. The KT boundary section is in a canyon reached by a trail about 0.5 km north of the village. Note that on the road to El Mulato you will see resistant layers of basalt on top of the hills to the north that may be mistaken for the near-KT clastic deposit (Fig. 62); however, some clastic KT age sediments are exposed below the basalt layers.

The El Mulato KT boundary transition is well-exposed over 50 m along the hillside (Fig. 61). Most of the outcrop consists of gray marls of the Maastrichtian Mendez Formation (~20 m), followed by a 2-m-thick clastic deposit that contains all three lithological units (units 1, 2, and 3). This clastic deposit is overlain by a thin layer of Mendez marl containing a well-developed *A. mayaroensis*-zone fauna including the index taxon, similar to La Lajilla. At both La Lajilla and El Mulato sections the presence of this Mendez marl indicates that deposition of the top of the clastic deposit occurred during the latest Maastrichtian prior to the KT boundary. Several tens of meters of the Tertiary Velasco Formation overlie this deposit.

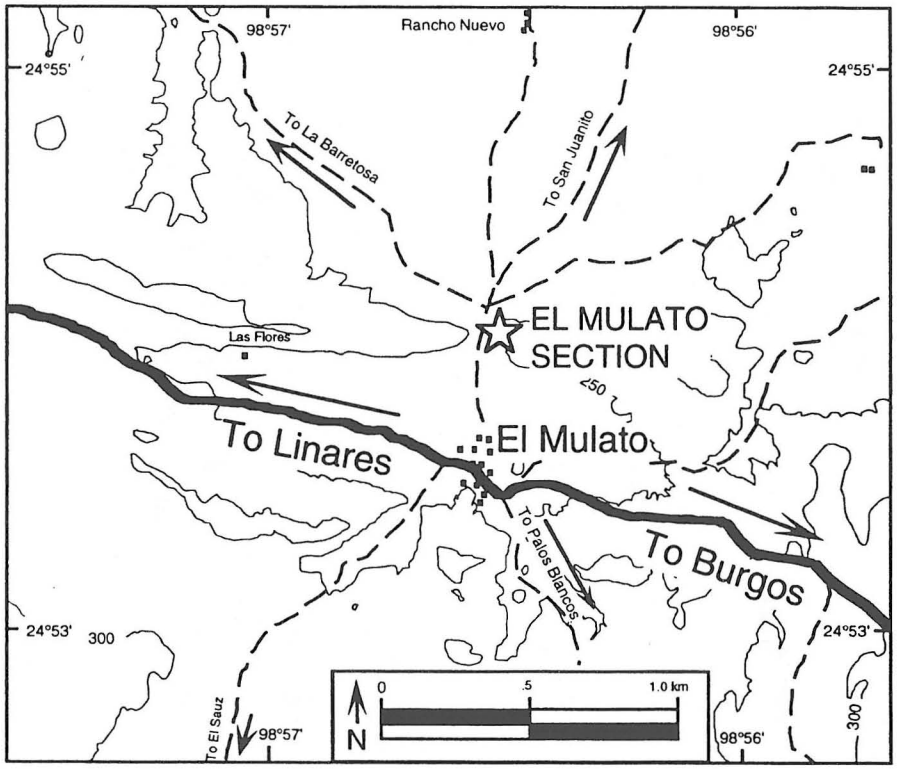

Fig. 60. *Location map of El Mulato KT boundary outcrop.*

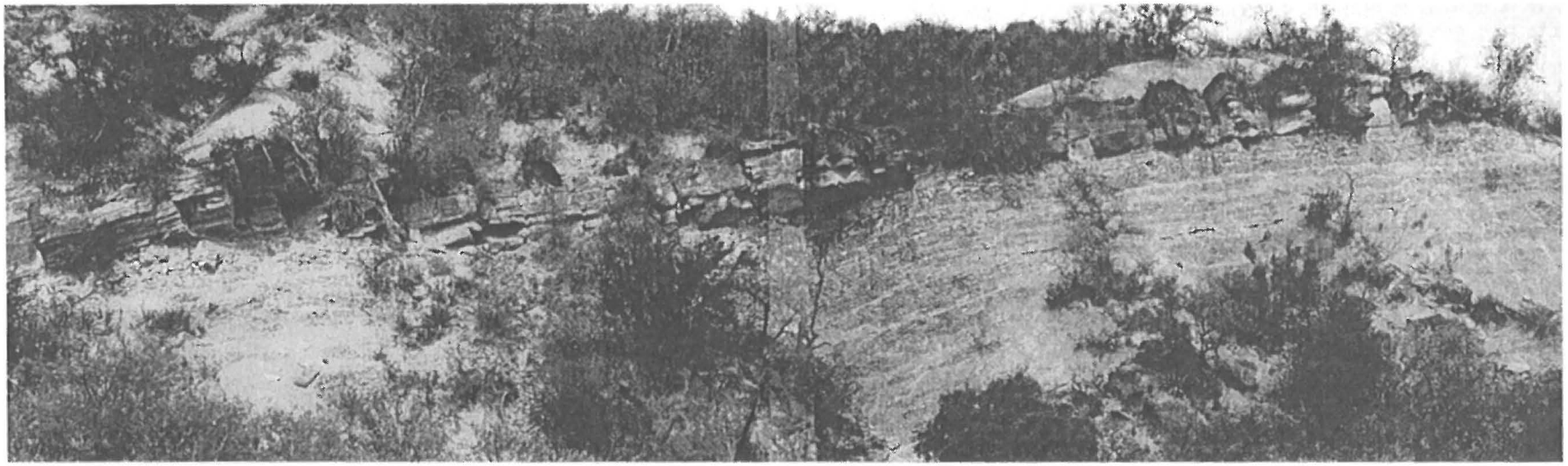

Fig. 61. *El Mulato, composite photograph of outcrop.*

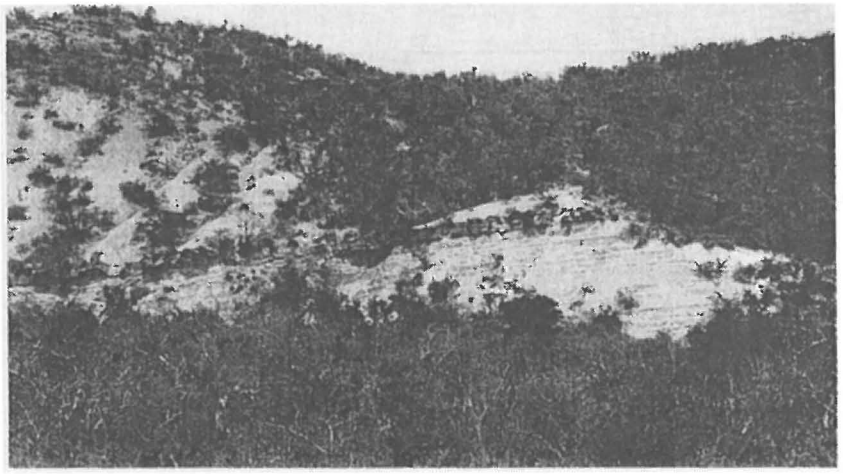

Fig. 62. *View of El Mulato KT boundary outcrop seen from the north of the village. Note basalt flows on top of hill to the right.*

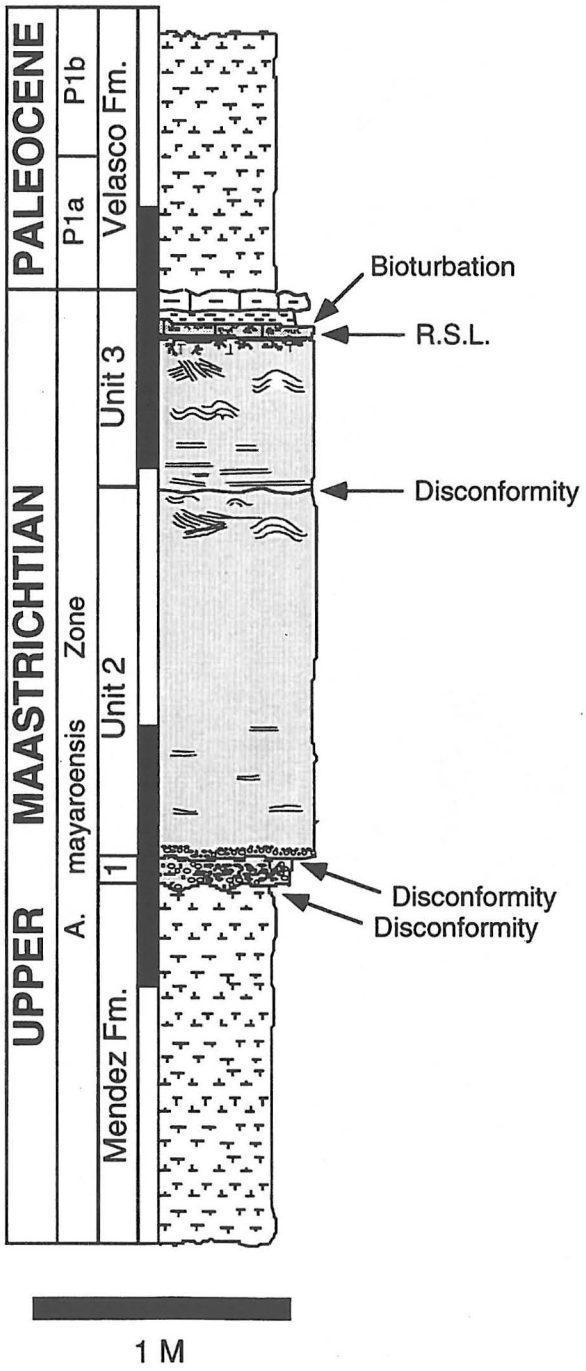

Fig. 63. *Lithostratigraphic column of the El Mulato KT boundary section. Note presence of thin layer of Mendez marl on top of clastic deposit, which indicates deposition prior to the KT boundary event. RSL = rippled sandy limestone, SLL = sandy limestone layer.*

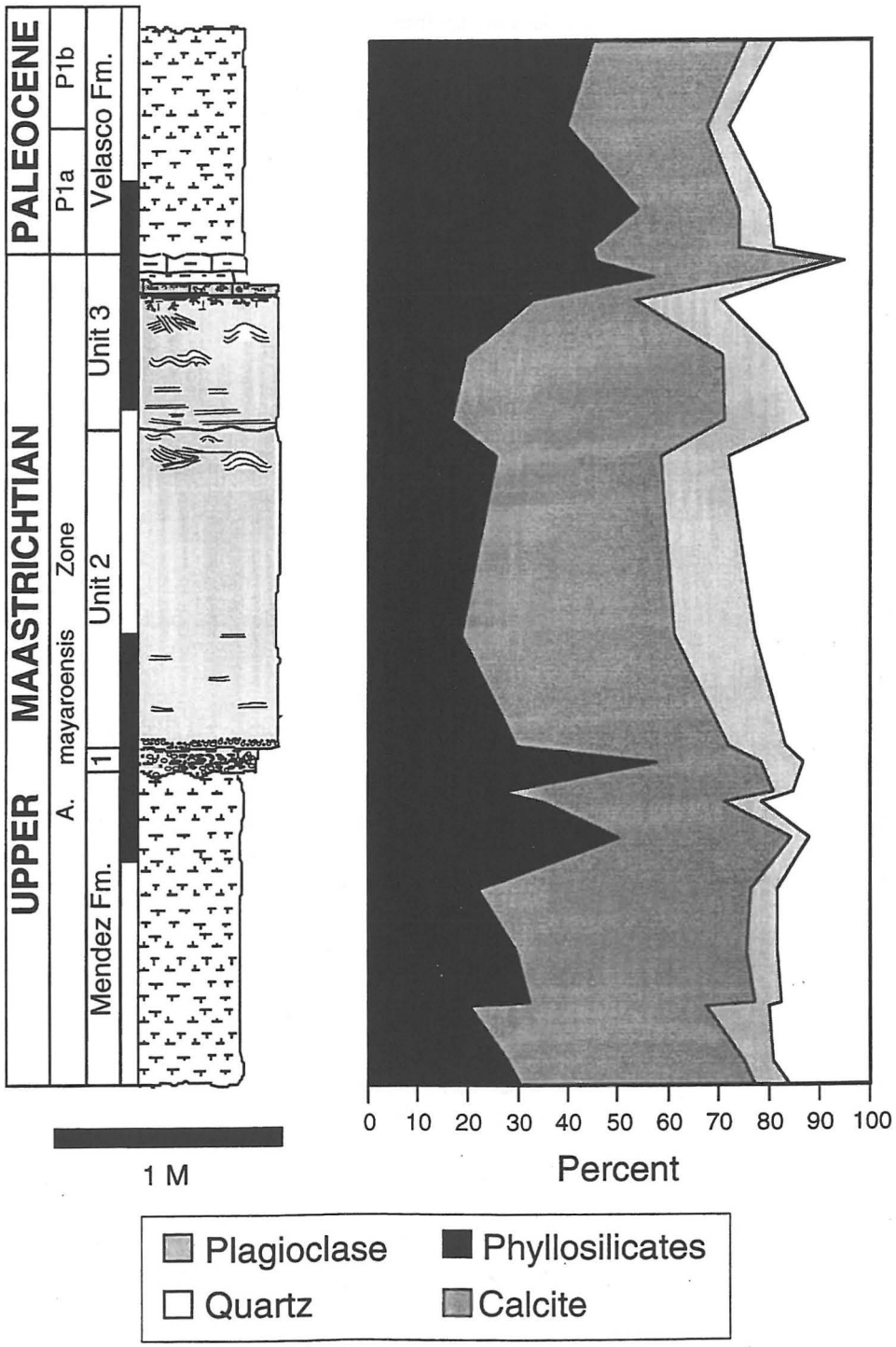

Fig. 64. Whole-rock composition of KT boundary deposits at El Mulato (from Adatte et al., in preparation). Measured by estimation from whole-rock XRD (Kübler, 1987).

UNIT 1

Spherule Layer:	Friable, rich in calcareous spherules, glauconite particles, and infillings of foraminiferal tests (Figs. 65 and 66).
Thickness:	Variable, ranging from 0 to 10 cm.
Lower Contact:	Disconformably overlies the Mendez Formation, contact characterized by undulating erosional surface.
Upper Contact:	Disconformable with massive sandstone of unit 2 (Fig. 65).
Sedimentological Features:	Weak horizontal laminations.
Sandy Limestone Layer (SLL):	None observed.
Spherules:	2–5 mm in size, usually weathered.
Mudclasts:	Rounded clasts and lenses of Mendez marls.
Mineralogy:	Calcite 20–40%, plagioclase 5–10%, quartz 15%, phyllosilicates 40–80%, (Fig. 64).

UNIT 2

Massive Sandstone:	Laminated sandstone with spherules near base.
Thickness:	1.4 m.
Lower Contact:	Disconformable with unit 1 or locally with Mendez Formation.
Upper Contact:	Disconformable with sandstone of unit 3.
Sedimentological Features:	Horizontal laminations, convolute bedding in upper part and weak upward fining.
Mudclasts:	None observed.
Spherules:	Common near base of unit 2.
Plant Debris:	None observed by us, but mentioned by Smit (personal communication, 1993).
Bioturbation:	None observed.
Mineralogy:	Calcite 50%, plagioclase 15%, phyllosilicates 15–25%, quartz 25%, (Fig. 64).

UNIT 3

Sand-Siltstone: Interlayered sand and thin siltstone beds, topped by rippled sandy limestone layers.

Thickness: 77 cm.

Lower Contact: Disconformable (?) with unit 2.

Upper Contact: Disconformable (?), overlain by shales of lower Tertiary Velasco Formation.

Sedimentological Features: Diverse, including laminated intervals, and rippled, wavy, oblique, and convolute bedding (Figs. 67 and 68).

Rippled Sandy Limestone (RSL): Two beds, 15–20 cm thick, rippled bedding.

Mudclasts: None observed.

Spherules: None observed.

Plant Debris: Rare wood and leaf debris.

Bioturbation: Abundant *Chondrites*, *Zoophycos*, and Y-shaped *Thalassinoides* (?) burrowing networks near top of sandy limestone layer (Figs. 69–71).

Mineralogy: Mineralogical contents vary from layer to layer. Zeolites in distinct layer(s).

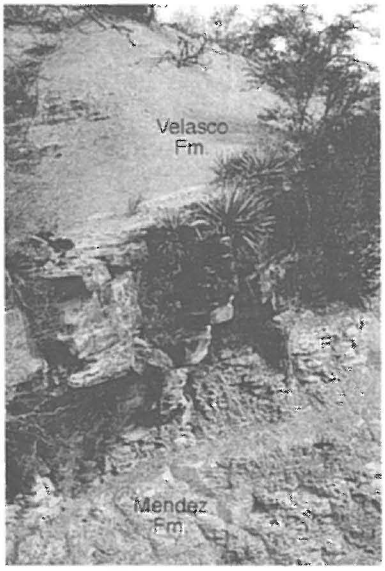

Fig. 65. *El Mulato, clastic deposit with Mendez and Velasco Formations.*

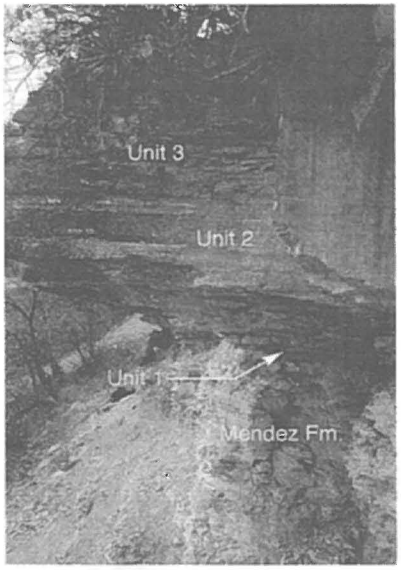

Fig. 66. *El Mulato, clastic deposit showing lower contact with Mendez marls.*

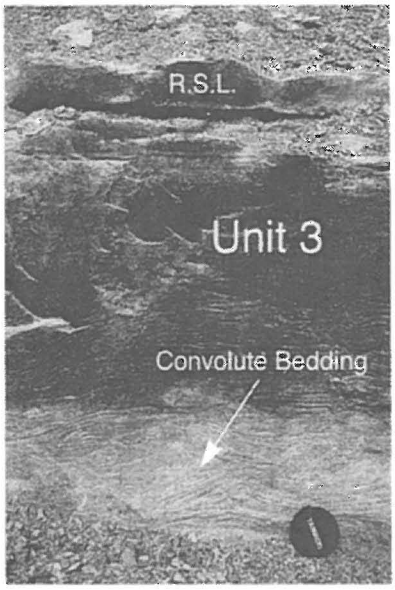

Fig. 67. *El Mulato, upper part of unit 3 with convolute bedding.*

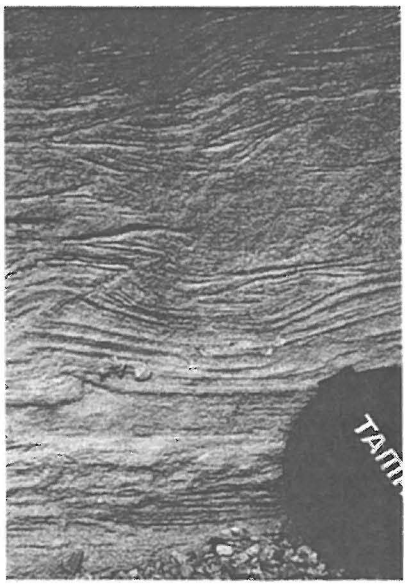

Fig. 68. *Close-up of Fig. 67 showing convolute bedding.*

Fig. 69. *El Mulato, top of unit 3; Chondrites feeding tubes.*

Fig. 70. *El Mulato, top of unit 3; Y-shaped Thalassinoides(?).*

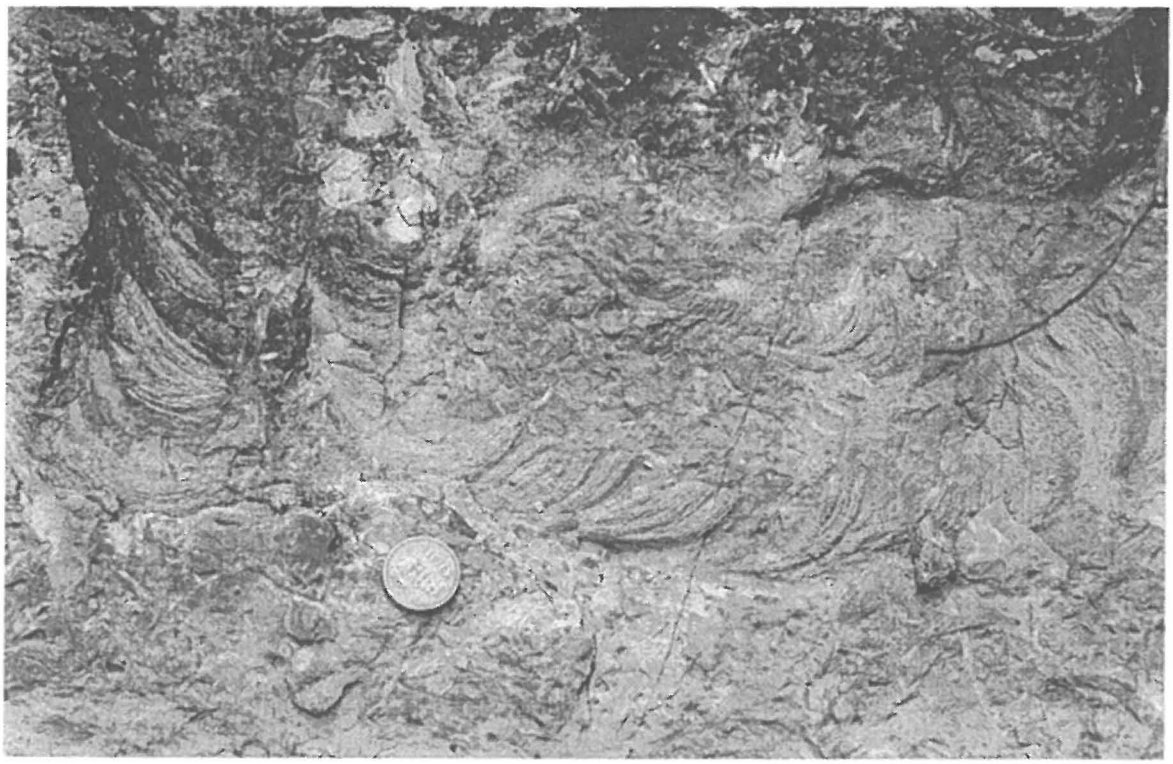

Fig. 71. *El Mulato, top of unit 3, bioturbation by Zoophycos (spreiten structures).*

LA SIERRITA

The KT boundary outcrops are located near the hamlet of La Sierrita on the road from Montemorelos to Vaquería (latitude 25°12.30'N and longitude 99°31.1'W, Fig. 3). From Montemorelos, take the road in the direction of Reynosa. About 5 km beyond General Terán take a right (south) turn toward the village of Vaqueria. Follow this (paved) road for about 17 km to the hamlet of La Sierrita (Fig. 72). At La Sierrita take the unpaved road south (right turn) for 2–3 km toward the hills. A gate spans the road. If it is closed, park the car and continue on foot 500 m to outcrop.

La Sierrita KT boundary outcrops are found over several kilometers along hill tops and valleys trending in a north-south direction. The La Sierrita outcrops described here, also known as Loma Las Rusias, are found at the dirt road and along a north-south-trending ridge. We illustrate three near-KT boundary clastic deposits beginning near the dirt road and continuing 500 m to the south (Fig. 78). Three transects illustrate the variable thickness and sedimentological features within the clastic deposit. All three lithologic units (units 1, 2, and 3; Fig. 73) are present, although not always at the same outcrop location.

La Sierrita I, located near the dirt road, is poorly exposed at the base with a 20-cm-thick spherule layer that is apparently overlain by Mendez marls (~30 cm). Mendez marls have not been observed above the spherule-rich layer in any of the other outcrops, and it is possible that its presence at La Sierrita I is due to faulting or postdepositional deformation. The massive laminated sandstone of unit 2 is well represented (~2.3 m) and disconformably overlies unit 1 (Fig. 71). No sediments are exposed above unit 2 at the outcrop at La Sierrita I, but at outcrops II and III unit 3 is present (Fig. 73).

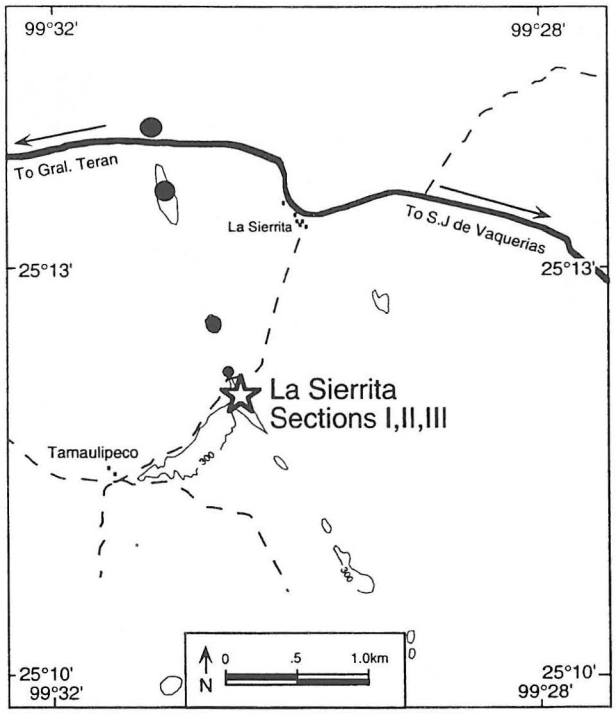

Fig. 72. Location map of La Sierrita KT boundary outcrops.

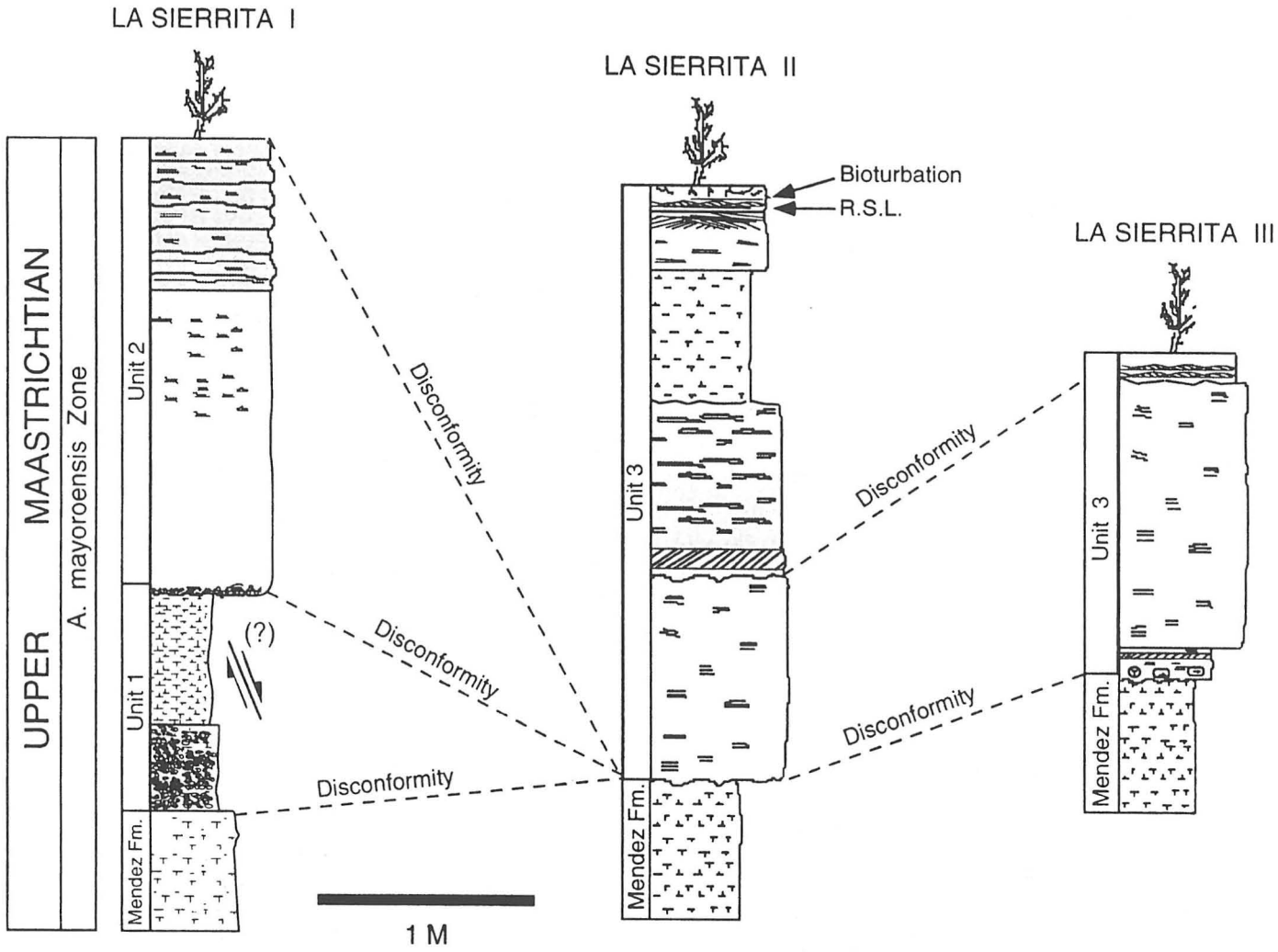

Fig. 73. Lithostratigraphic columns of La Sierrita I, II, and III.

UNIT 1

Spherule Layer:	Weathered, friable, rich in calcareous spherules, glauconite particles, and infillings of foraminiferal shells. Not present at La Sierrita II and III outcrops.
Thickness:	Variable, between 0 and 20 cm.
Lower Contact:	Disconformable, overlies Mendez Formation at La Sierrita I, but contact not well exposed.
Upper Contact:	Disconformable, not well exposed.
Sedimentological Features:	None observed.
Sandy Limestone Layer (SLL):	Not present.
Spherules:	2–5 mm in size, highly weathered.
Mineralogy:	Phyllosilicates 10%, calcite 80%, quartz 8%, plagioclase 2%.
Other Characteristics:	Not investigated.

UNIT 2

Massive Sandstone:	Sandstone with horizontal laminations, not present in La Sierrita III outcrops (Fig. 74).
Thickness:	Variable, 2.3 m in La Sierrita I, and not present in La Sierrita II and La Sierrita III.
Lower Contact:	Not clearly exposed at La Sierrita I.
Upper Contact:	Not exposed at La Sierrita I, not present at La Sierrita II and III.
Sedimentological Features:	Horizontal laminations, weak upward fining.
Mudclasts:	None observed.
Spherules:	Common near the base at La Sierrita I.
Plant Debris:	None observed.
Bioturbation:	None observed.
Mineralogy:	Phyllosilicates 10–25%, calcite variable 20–40%, quartz 10–35%, plagioclase 5–20%.

UNIT 3

Sandstone Dominated: Sequence with varying sedimentological features (laminations, ripples, cross-bedding, convolute bedding; Fig. 75).

Thickness: Variable, 1.0–2.8 m in La Sierrita II and III. Not present in La Sierrita I.

Lower Contact: Disconformable with Mendez Formation at La Sierrita II and III.

Upper Contact: Not present.

Sedimentological Features: Laminations, ripple marks, convolute and cross bedding.

Rippled Sandy Limestone (RSL): 20 cm thick, bioturbated at La Sierrita II and III. Not present at La Sierrita I and III (Fig. 73).

Mudclasts: Common near the base of unit 3 in La Sierrita III (Fig. 77).

Plant Debris: None observed.

Bioturbation: Common near top of unit 3, abundant *Chondrites*, *Zoophycos*, and Y-shaped *Thalassinoides* (?) burrowing networks (Fig. 77).

Mineralogy: Phyllosilicates 20–30%, calcite variable 30–50%, quartz 15–25%, plagioclase 5–20%. Zeolites in discrete layers.

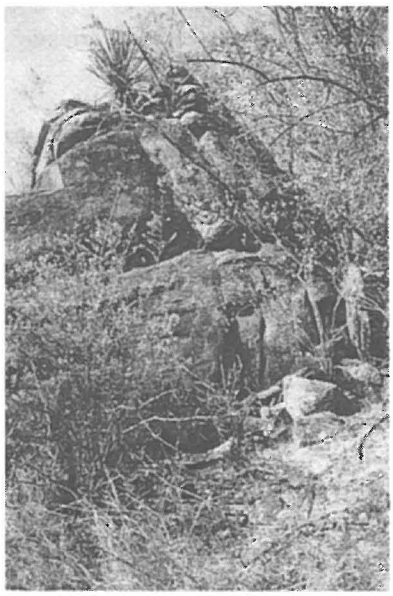

Fig. 74. *La Sierrita I, outcrop with clastic deposit of unit 2 disconformably overlying Mendez marls and unit 1.*

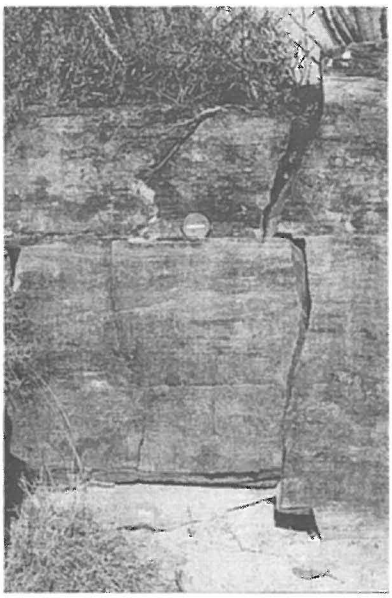

Fig. 75. *La Sierrita III, outcrop with clastic deposit of unit 3 disconformably overlying Mendez Formation.*

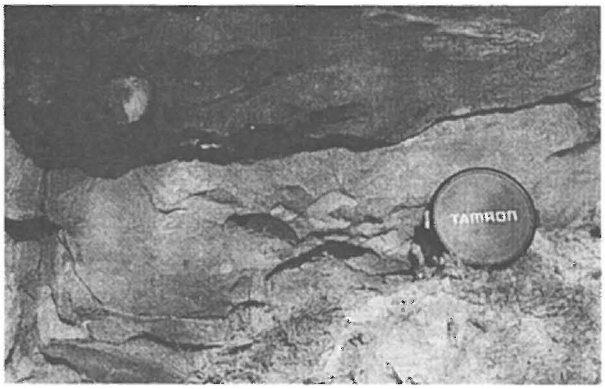

Fig. 76. *La Sierrita III, mudclasts at the base of unit 3.*

Fig. 77. *La Sierrita II, Thalassinoides(?) burrows at the top of unit 3.*

LOS RAMONES

The near KT boundary clastic deposit outcrops 500 m east of the town of Los Ramones at the eastern bank of the Pesquería River (latitude 25°42.1'N, longitude 99°36.5'W) (Figs. 3 and 78). The town of Los Ramones is easily reached by car on the old highway from Monterrey to Reynosa (the new highway lacks an exit to Los Ramones). The turn-off to Los Ramones is 50 km east of Monterrey. Follow sign to Los Ramones. After crossing river (at edge of town) continue to gas station (~500 m), then turn right (east) on next street to exit town and continue to river and park. Section is on opposite riverbank (river can usually be crossed easily during the dry season). Excellent outcrops of the upper Cretaceous Mendez Formation are found along the river banks and around the big river bend. The near KT boundary clastic deposit is easily recognized by its resistant and blocky outcrops overlying the Mendez marls (Figs. 79 and 80).

The outcrop spans about 50 m and dips northeast, where it disappears in the river bed (Fig. 79). The clastic deposit is about 4 m thick and disconformably overlies the Mendez Formation In contrast to all other near-KT boundary clastic deposits known to us, the Los Ramones deposit does not permit positive identification of the lithologic units (units 1, 2, and 3) observed at other locations. For instance, no spherule-rich layers are present at Los Ramones, and we can only tentatively identify undifferentiated units 2 and 3 consisting of generally structureless sandstones with some upward fining. Within these units are numerous zones marked by mudclasts of probable Mendez marls that suggest the presence of disconformities. The top of the clastic deposit is bioturbated by shallow-water crabs and underlies a thin microconglomeratic bed that is topped by a sandstone layer with unidirectional ripples. Trace fossils and lithological characteristics suggest that deposition of the clastic deposit at Los Ramones occurred in a shallower water environment than at the other locations to the south.

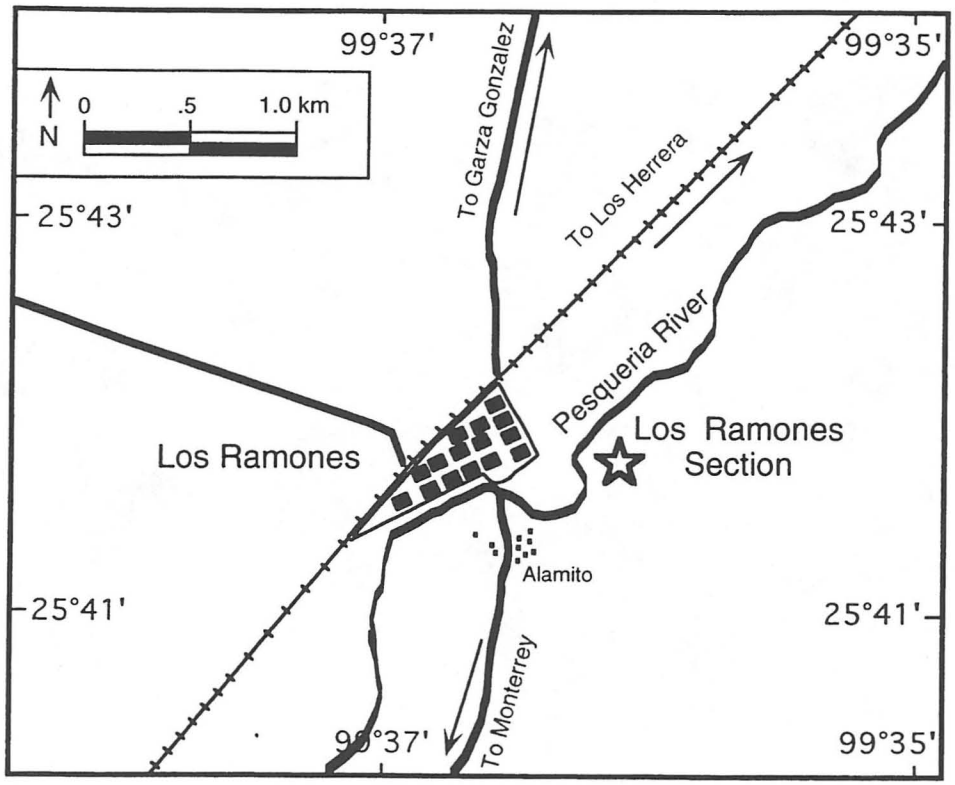

Fig. 78. Location map of Los Ramones KT boundary sections.

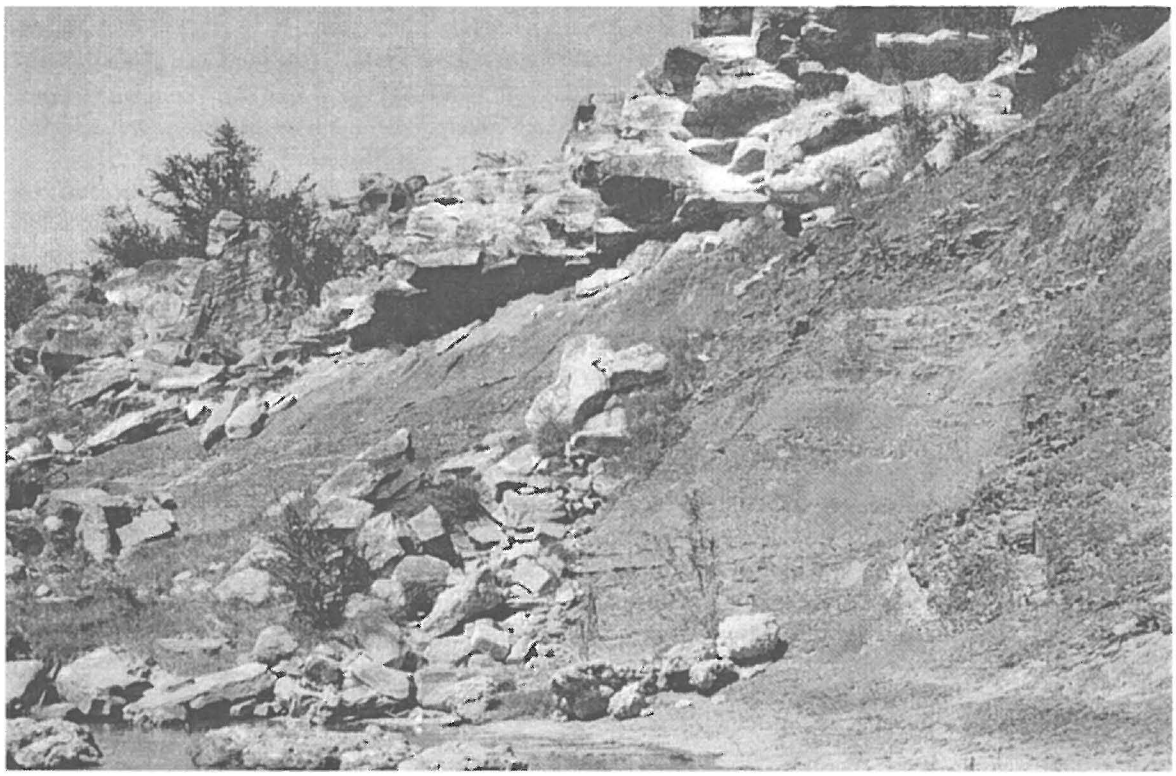

Fig. 79. Los Ramones, general view of near-KT-boundary clastic deposit overlying Mendez Formation.

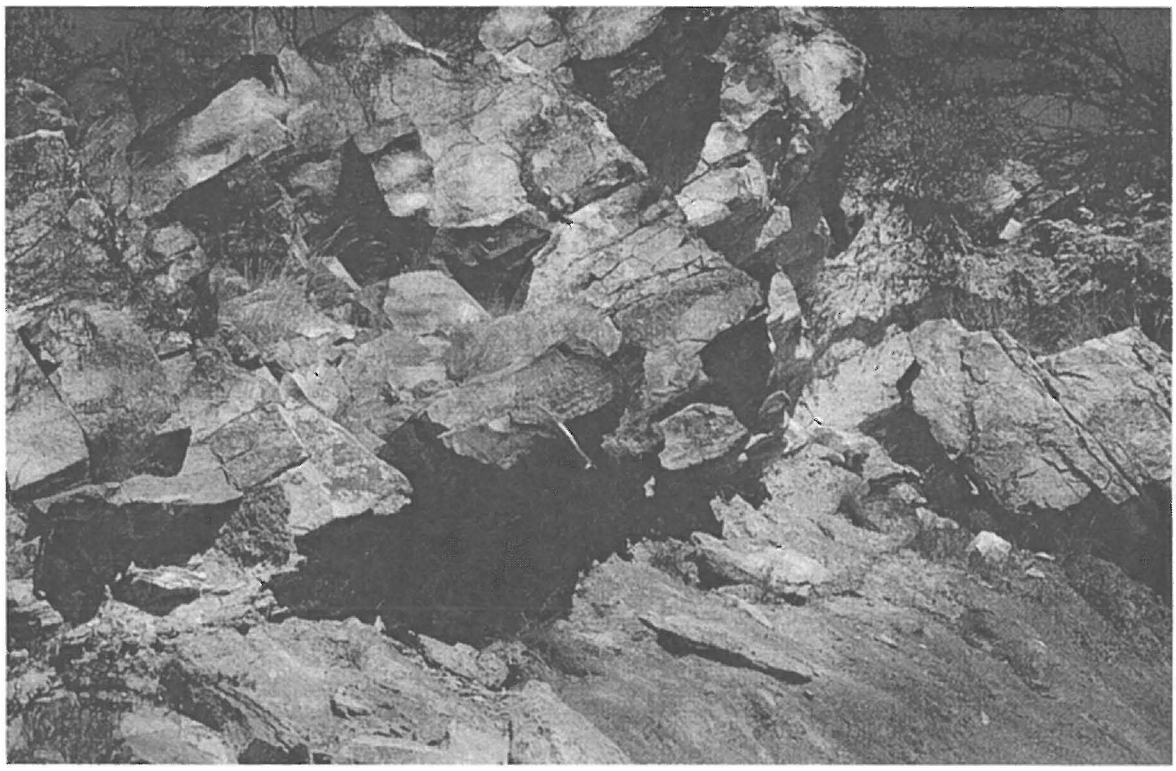

Fig. 80. Los Ramones, view of massive sandstones overlying Mendez Formation.

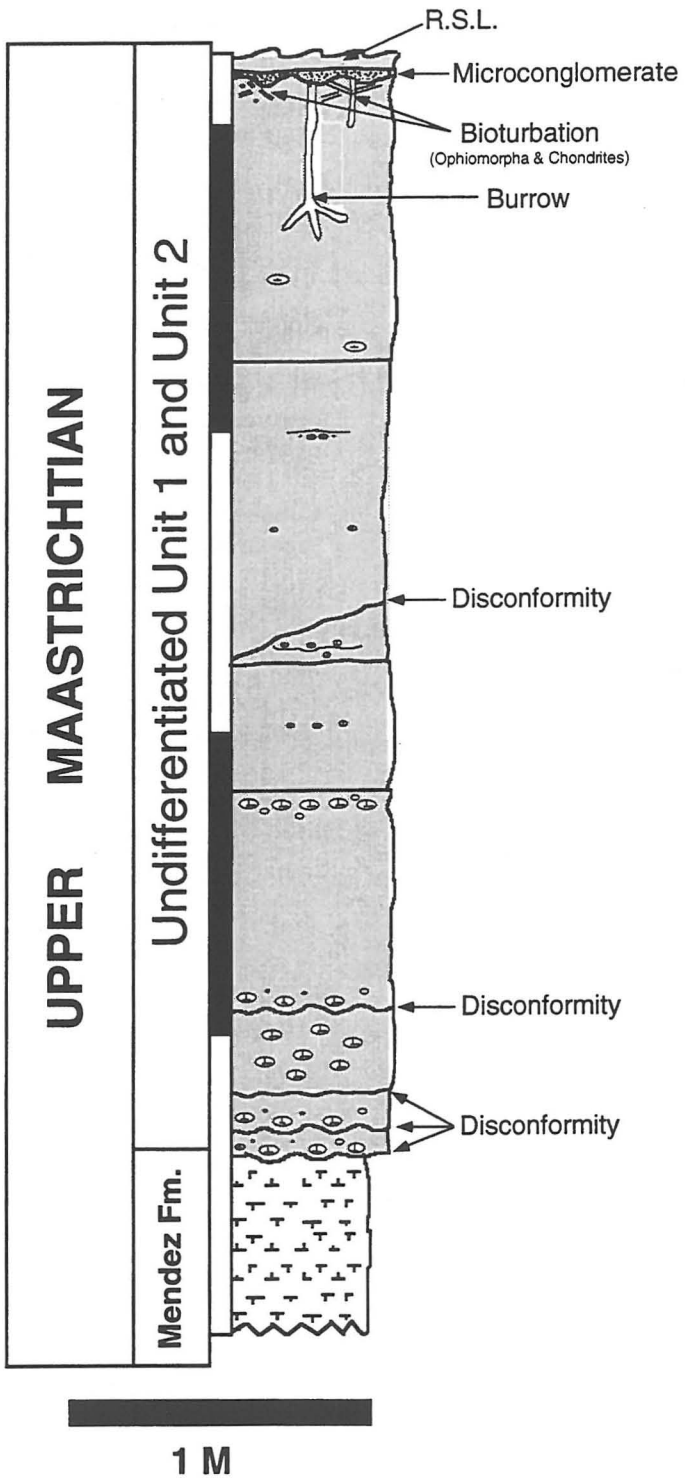

Fig. 81. Lithostratigraphic column of the Los Ramones section.

UNIT 1

Not recognized.

UNITS 2 AND 3

Undifferentiated.

Massive structureless sandstone with mudclasts and bioturbation; microconglomerate and rippled sandstone at the top (Fig. 81).

Thickness: 4 m.

Lower Contact: Disconformable with Mendez marls.

Upper Contact: Not present at this location.

Sedimentological Features: Weak upward fining, size gradation of mudclasts; numerous discontinuities, unidirectional rippled sandstone at top of outcrop.

Mudclasts: Common throughout clastic deposit, well rounded or subrounded, graded (Figs. 82 and 83).

Plant Debris: None observed.

Bioturbation: *Ophiomorpha* burrowing networks, *Chondrites*, and unidentified branched, vertical tubular structures. Bioturbation restricted to top 30 cm of clastic deposit (Figs. 84 and 85).

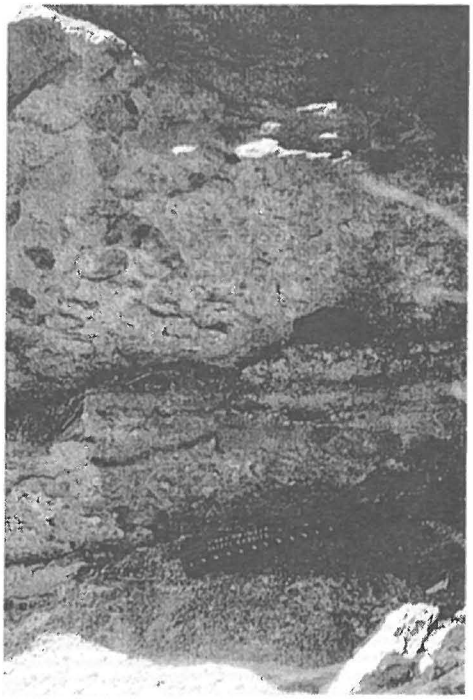

Fig. 82. *Los Ramones, mudclasts at base of clastic deposit.*

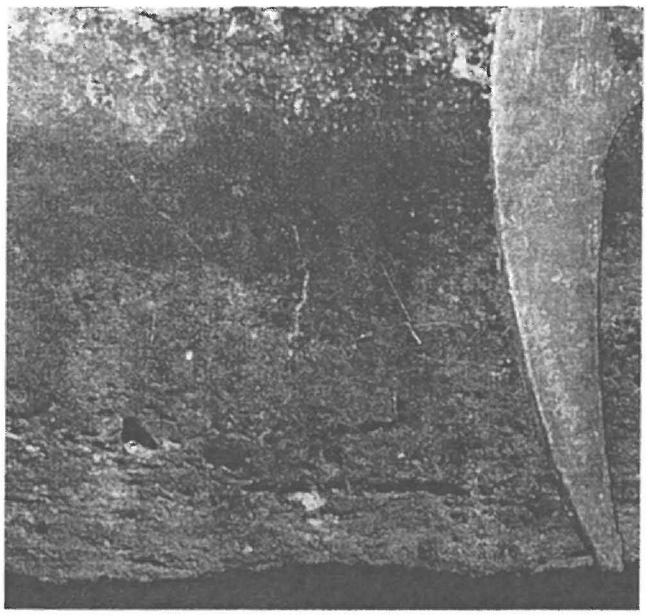

Fig. 83. *Los Ramones, gradation of mudclasts near base of clastic deposit.*

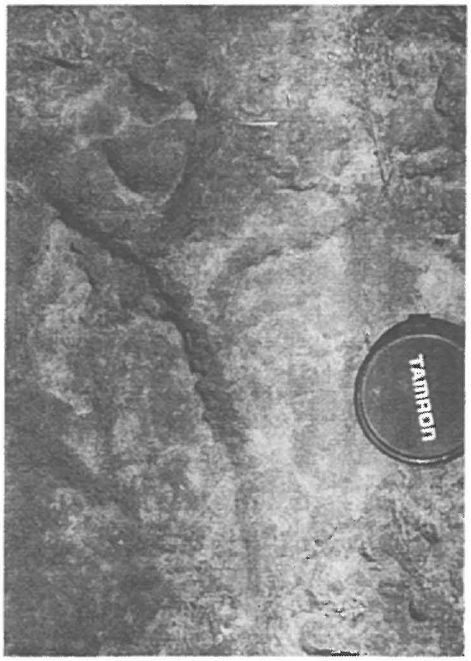

Fig. 84. *Los Ramones, Ophiomorpha burrows near top of clastic deposit.*

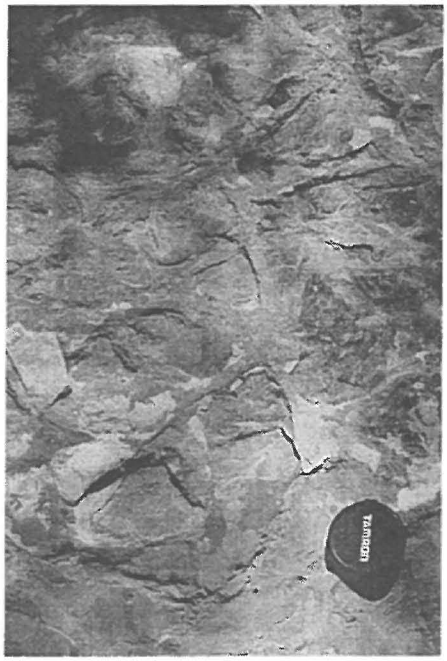

Fig. 85. *Los Ramones, Ophiomorpha burrows near the top of clastic deposit.*

PART II: INTERPRETATIONS

THE KT BOUNDARY CLASTIC DEPOSITS IN NORTHEASTERN MEXICO AS PRODUCT OF NONCATASTROPHIC GEOLOGIC PROCESSES?

G. Keller, W. Stinnesbeck, T. Adatte, J. G. Lopez-Oliva, and N. MacLeod

BIOSTRATIGRAPHY

Definition of the KT Boundary Based on the El Kef Stratotype Section

The El Kef section of Tunisia was officially designated the Cretaceous-Tertiary (KT) boundary global stratotype section and point (GSSP) at the XXVIII International Geological Congress in Washington in 1989. Chosen for its apparently continuous and expanded sedimentary record, excellent preservation of microfossils, and geochemical and mineralogical marker horizons, the stratotype provides an ideal sequence by which other sections can be compared and correlated worldwide. As such the El Kef stratotype has become the single most important KT boundary section and the standard by which the completeness of the faunal, floral, and sedimentary records are judged worldwide. Such a comparison was recently published by *MacLeod and Keller* (1991) based on graphic correlation of over 30 KT boundary sections worldwide. Results show that the El Kef section indeed represents the most expanded and stratigraphically complete KT boundary transition known to date. Similar nearly complete sections also occur at Brazos River (Texas), Agost and Caravaca (Spain), Nye Kløv (Denmark), Mimbral (Mexico), and ODP Site 738C.

Placement of the KT boundary: The KT boundary is easily identified in the El Kef stratotype or elsewhere based on the following criteria: (1) a lithologic break from chalk or marl deposition of the Cretaceous to a thin layer of dark organic-rich and $CaCO_3$-poor clay, known as the boundary clay. At El Kef this layer is 55 cm thick and represents the most expanded boundary clay observed to date in any KT boundary sections. More frequently, the boundary clay is only 4–6 cm thick [e.g., Agost, Caravaca, Stevns Klint, Nye Kløv, El Mimbral (*Smit*, 1990; *Canudo et al.*, 1991)];. (2) a 2–3-mm oxidized red-layer at the base of the boundary clay (this red layer is present at El Kef as well as in all complete KT boundary sections); (3) maximum Ir concentrations generally concentrated in the red layer and boundary clay although they may trail several tens of centimeters above the boundary clay [at El Kef, maximum Ir concentrations are found in the red layer and values decrease through the boundary clay (*Robin et al.*, 1991)];. (5) a negative ^{13}C shift in marine plankton of low and middle latitudes as also present at El Kef (*Smit and ten Kate*, 1982; *Kuslys and Krähenbühl*, 1983; *Keller and Lindinger*, 1989); (6) the first appearance of Tertiary planktic foraminifera at the base or within a few centimeters of the boundary clay, red layer, Ir anomaly, and Ni-rich spinels [at El Kef, the first Tertiary species *(G. conusa)* appears at the base of the boundary clay and three other new species *(E. fringa, E. edita,* and *W. hornerstownensis)* appear within the basal 15 cm of the boundary clay (*Keller*, 1988; *Ben Abdelkader*, 1992; Keller et al., in preparation)]; and (7) the gradual disappearance of Cretaceous tropical taxa.

In the stratotype section at El Kef all these criteria are met (Fig. 86) and most of them are present in all the best and most complete KT boundary sequences (e.g., Agost, Caravaca, Nye Kløv, Brazos River, El Mimbral, ODP Site 738C). Coincidence of these lithological, geochemical, and paleontological criteria is unique in the geological record and virtually ensures that the placement of the KT boundary is uniform and coeval in marine sequences across latitudes. Any of these criteria used in isolation, however, diminish the stratigraphic resolution of the KT boundary.

Some workers have suggested that the sudden extinction of all but one or at most three planktic foraminiferal species should define the KT boundary (*Smit*, 1982, 1990; *Berggren and Miller*, 1988; *Olsson and Liu*, 1993; *Liu and Olsson*, 1992). This is not practical, however, since such a sudden extinction horizon has only been observed in sections with a KT boundary hiatus (*MacLeod and Keller*, 1991a,b; *Keller et al.*, 1993a). In temporally continuous low-latitude sections such as El Kef, Brazos, Mimbral, Agost, and Caravaca, only specialized tropical to subtropical forms disappeared, whereas most cosmopolitan taxa survived (*Keller*, 1988, 1989a,b; *Keller et al.*, 1994; *Canudo et al.*, 1991). Moreover, in high-latitude sections such as Nye Kløv and ODP Site 738C, where no tropical taxa are present, there are

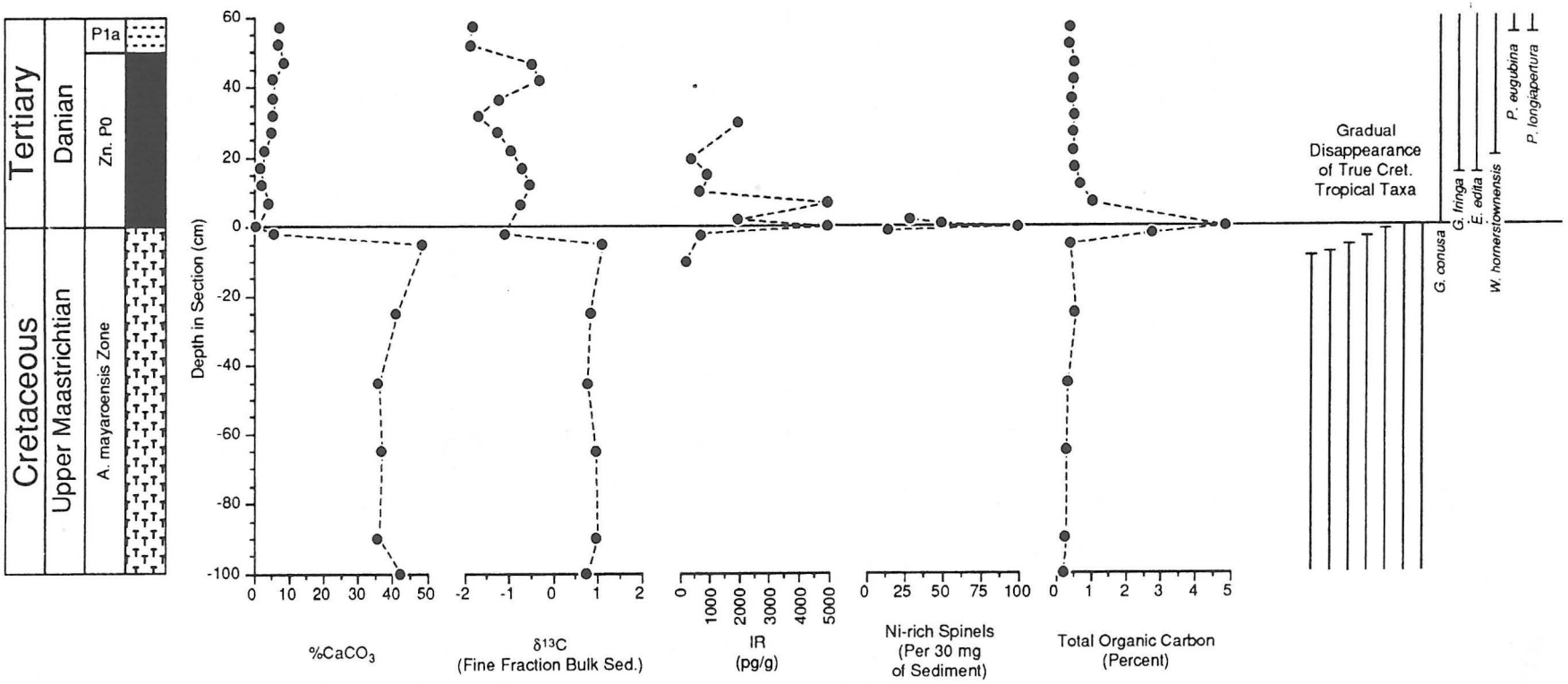

Fig. 86. *Lithostratigraphic, geochemical, mineralogical, and biostratigraphic criteria that identify the KT boundary at the El Kef stratotype section.*

no significant species extinctions at the KT boundary (*Keller*, 1993; *Keller et al.*, 1993b). Equally impractical is the suggestion that the first abundance increase of *Guembelitria* spp. define the KT boundary as suggested by *Smit* (1982, 1990), *Liu and Olsson* (1992), and *Olsson and Liu* (1993), because species abundance peaks are not unique events, but rather reflect favorable environmental conditions for the particular species. For instance, at El Kef and Brazos such conditions prevailed through Zones P0 and P1a and reoccurred in Zone P1c (*Keller*, 1988, 1989a,b). At Mimbral, Agost, and Caravaca the first *Guembelitria* abundance peak is near the base of Zone P1a, and in the Spanish sections the maximum abundance occurs in Zone P1c (*Canudo et al.*, 1991; *Keller et al.*, 1994). In the high-latitude Nye Kløv sections *Guembelitria* is abundant in the uppermost Cretaceous as well as early Tertiary Zones P0 and P1a and rare at the KT boundary (*Keller et al.*, 1993b). Similarly, in the southern high-latitude ODP Site 738C, *Guembelitria* is rare at the boundary and common in the upper part of Zone P0 and in Zone P1a (*Keller*, 1993). These data indicate that *Guembelitria* abundance peaks are highly unreliable markers for the KT boundary.

Biostratigraphic zonation of the KT boundary transition is generally based on first and last appearances (local originations and extinctions) of species and sometimes relative species abundance changes. However, diachronous occurrences of some species and preservation factors occasionally prevent precise placement of zonal boundaries. This is usually a minor problem when compared with artificial errors introduced by other biases such as sampling technique (including sample spacing and collection method), laboratory processing (e.g., large vs. small size fractions, which results in the loss of small taxa), type of faunal analysis (qualitative vs. quantitative), differing taxonomic concepts (lumpers vs. splitters), and the use of alternative zonal schemes. For the nonpaleontologists, evaluating contrasting biostratigraphies is often difficult, but clues to the reliability of individual studies are inherent in the type of analysis. For instance, the most accurate age determinations and biostratigraphic correlations for KT boundary deposits are obtained from high-resolution sampling practices (e.g., centimeter-scale sampling of outcrops), laboratory processing of samples to retain small species (e.g., size fraction >38 mm in KT boundary clay and >63 mm above and below), and quantitative rather than qualitative faunal analysis. In addition, the investigator needs to know how the various zonal schemes correlate.

The most commonly used planktic foraminiferal zonal schemes are illustrated in Fig. 87 along with first and last appearances of taxa with index species that define zonal boundaries in bold type. The zonal schemes by *Keller* (1988, 1993), *Smit* (1982), *Smit et al.*, 1992), and *Berggren and Miller* (1988) differ largely in the degree of stratigraphic resolution, with Keller's zonation providing the highest resolution. *Longoria and Gamper*'s (1992) zonal scheme is unique (see also *Gamper*, 1977; *Longoria*, 1977, 1984) in that they continue to place the KT boundary at the first appearance of *P. eugubina*, which places the early Danian (Zone P0) in the late Maastrichtian. This practice has been discontinued by other workers since the early 1980s with the advent of high-resolution KT boundary studies, and in particular since the acceptance of the El Kef stratotype, where *P. eugubina* first appears well above the KT boundary. In their zonal scheme the actual KT boundary is within a transition zone characterized by the co-presence of unspecified "Globigerinas" and Cretaceous species (Fig. 87).

As discussed in the previous section, based on the KT boundary stratotype at El Kef, Tunisia, the KT boundary is characterized by the first appearance of Tertiary species (e.g., *Eoglobigerina fringa, E. simplicissima, E. edita, Globoconusa conusa, W. hornerstownensis*) with *G. conusa* first appearing in the 1 cm above the KT boundary and the other Tertiary species first appearing in the 10–15 cm of the basal boundary clay (of Zone P0). In addition, the KT boundary is generally characterized by a major lithological change from Maastrichtian carbonate-rich sediments to the "boundary clay," often with a red oxidized layer at its base. The boundary clay, and in particular the red oxidized layer, generally contains elevated Ir concentrations, Ni-rich spinels, and carbon isotopic values of surface waters that rapidly decrease to near bottom-water values. These biological, geochemical, and mineralogical signatures provide an unequivocal marker horizon for the KT boundary (Fig. 86).

Of the sections discussed in this field guide, only El Mimbral has been biostratigraphically studied in detail and published (*Smit et al.*, 1992; *Longoria and Gamper*, 1992; *Keller et al.*, 1994). Data from La Lajilla is presented herein. In addition to La Lajilla, biostratigraphic studies of Rancho Nuevo, La Parida, Peñon, Ramones, La Sierrita, and Mulato have also been completed (Lopez-Oliva and Keller, in preparation), and the results are briefly discussed in this field guide.

Arroyo El Mimbral

Smit et al. (1992) first reported that the El Mimbral clastic deposit is of KT boundary age. They placed the boundary at the top of the clastic deposit, which they interpreted as a bolide impact-generated tsunami deposit. Subsequently, they placed the KT boundary at the base of the clastic deposit based on their interpretation of the clastic sediments as an impact-generated tsunami deposit (see this volume). *Longoria and Gamper* (1992) challenged this KT boundary age assignment, claiming that the clastic deposit is middle Maastrichtian in age. They based their argument on the fact that they could not find the late Maastrichtian index taxon *Abathomphalus mayaroensis* in the Mendez marl samples they examined.

Figure 88 shows the El Mimbral profile and samples analyzed by *Longoria and Gamper* (1992). Of the 13 samples they analyzed, 3 are from the Mendez Formation below the clastic deposit and 2 from the Velasco Formation above. Eight samples are from the clastic deposit. Thus, based on only three samples from the Maastrichtian Mendez Formation, it is not surprising that they did not find the relatively rare *A. mayaroensis* index species. In fact, we have found that this species is commonly present based on analysis of 50 samples in the uppermost 3 m of the Mendez Formation (see discussion below). Moreover, at La Lajilla and El Mulato the uppermost Maastrichtian nannofossil index species *Micula prinsii* is present below the clastic deposit, which also indicates that these sediments are of near-KT-boundary age (*Sanchez et al.*, 1993; Pospichal in *Longoria and Grajales*, 1993).

Also in contrast to *Smit et al.* (1992), *Longoria and Gamper* (1992) claim that they found the first appearance of *Parvularugoglobigerina eugubina* (their marker species for the base of the Tertiary) 70 cm above the clastic deposit (sample EM 29A-O in Fig. 88), rather than just above it as reported by *Smit et al.* (1992). Since they analyzed only two samples at 25 cm and 70 cm above the clastic deposit this is a poor test of the age of these sediments. Moreover, we have analyzed 37 samples of the Velasco Formation at 5-cm-intervals and found that *P. eugubina* first occurs at 4–9 cm above the clastic deposit at the edge of the clastic channel-fill deposit and immediately above it (0–1 cm) in the center of the channel fill.

Keller et al. (1994) examined two transects at El Mimbral, one (Mimbral I) across the center of the channel fill at the 28-m mark along the outcrop and the second (Mimbral II) at the right edge of the channel at the 150-m mark. These two transects are discussed below.

El Mimbral I: Channel-fill transect at 28 m: Figure 89 illustrates the planktic foraminiferal biostratigraphy across the channel-fill deposit at 28 m along the outcrop. The uppermost 3.2 m of the Maastrichtian Mendez Formation analyzed at this location indicate the presence of a rich and well-developed fauna with the upper Maastrichtian index taxon *Abathomphalus mayaroensis* commonly present to the base of the channel deposit. Thus, the Mendez marls below are unquestionably of upper Maastrichtian age. Because an erosional surface marks the contact between the Mendez Formation and the base of the channel deposit, it is not possible to determine how much of the uppermost Maastrichtian may be missing.

The 3-m-thick channel-fill clastic deposit is sandwiched between normal pelagic sedimentation of the Mendez and Velasco Formations (Fig. 90). However, the presence of upper Cretaceous planktic foraminifera, including the index taxon *Abathomphalus mayaroensis* throughout the clastic deposit, indicates that deposition of this unit also occurred during the uppermost Maastrichtian *A. mayaroensis* zone. Within the spherule-rich unit 1, both mudclasts and matrix contain diverse *A. mayaroensis*-zone planktic foraminifers similar to the underlying Mendez Formation. However, some mud-clasts in units 1 and 2 also contain lower to middle Turonian age foraminifers (*Marginotruncana sigali, M. pseudolinneiana,* Sliter, personal communication, 1992), indicating erosion and transport of older sediments.

The upper unit 3 of the clastic deposit consists of alternating laminated sandstone, shale, and silt layers topped by a 25-cm-thick sandy rippled limestone. Bioturbation (feeding tubes) by *Chondrites* is apparent in the sandy rippled limestone, indicating a normal long-term rather than a sudden short-term depositional environment. Burrowing occurred prior to deposition of the overlying boundary clay, rather than thereafter, because the burrows are infilled with the same sediment of the rippled sandy limestone. Foraminifers are few, except in a thin marly layer below the rippled limestone that contains abundant *A. mayaroensis*-zone planktic foraminifera (including *Globotruncanita contusa, Racemiguembelina fructicosa,* and *A. mayaroensis*) and only rare benthic foraminifera similar to the Mendez Formation. This thin marly layer also has a similar mineralogical composition as the Mendez marls below. This marly layer, like the bioturbated interval, suggests that intervals of normal hemipelagic sedimentation occurred during deposition of unit 3.

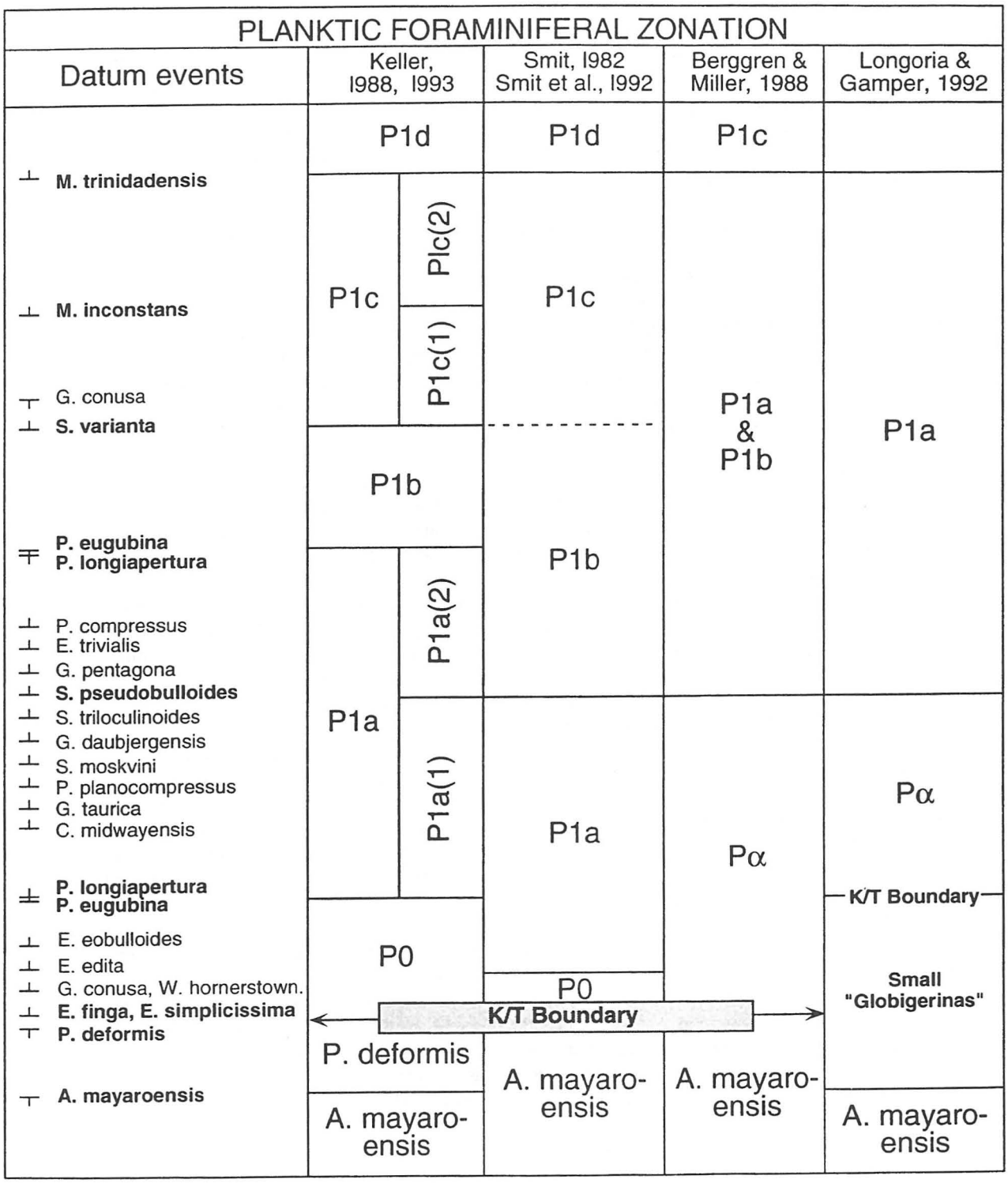

Fig. 87. Correlation of commonly used planktic foraminiferal zonal schemes for the KT transition.

Above the clastic channel deposit, thin layers of shale, sand, and bentonite mark the first 8 cm of the Tertiary Velasco Formation. No bioturbation is apparent. The first Tertiary planktic foraminifera are present in the basal shale layer along with many Cretaceous taxa (Fig. 90). The abundant presence of *P. eugubina, P. longiapertura,* and *Globoconusa daubjergensis* in this basal shale layer indicates that the earliest Tertiary Zone P0 and probably the lower part of the succeeding Zone P1a are missing in this channel transect. This is also apparent in the absence of the KT boundary clay and thin red layer that is present outside the channel deposit.

Cretaceous taxa are also abundant in these basal Tertiary sediments. These appear to be Cretaceous survivor taxa as indicated by the presence of only cosmopolitan forms (hedbergellids, heterohelicids, pseudoguembelinids, guembelitrids) and the apparent extinction of more complex tropical taxa by KT boundary time (Fig. 89). A similar pattern of cosmopolitan species survivorship has been observed worldwide (*Keller*, 1993; *Keller et al.*, 1993; *MacLeod and Keller*, 1994; MacLeod and Keller, in preparation).

El Mimbral II: Edge of channel transect at 150 m: An estimate of the biostratigraphy, age, and depositional environment of the Mimbral region can be obtained from a transect at the right edge of the channel at 150 m along the outcrop. At this location, the clastic deposit is represented only by the 20-cm sandy rippled limestone at the top of unit 3 and a thin discontinuous lens (1 cm) of the spherule layer of unit 1 (the latter is absent at 152 m). Figure 91 illustrates the species ranges of planktic foraminifera observed in the >63-mm size fraction. This figure shows that a nearly continuous KT boundary transition is present at Mimbral with a comparable biostratigraphic record to that of Agost and Caravaca in Spain (*Canudo et al.*, 1991).

In the 25 cm of exposed uppermost Mendez Formation at this transect, a diverse upper Maastrichtian assemblage of the *A. mayaroensis* zone, including the index taxon *A. mayaroensis*, is present to just below the sandy rippled limestone (Fig. 91). Without analysis of additional sections in Mexico that lack the clastic deposit of Mimbral, however, it is not presently possible to determine how much, if any, of the latest Maastrichtian is missing.

The KT boundary is marked by a 4-cm-thick clay layer containing a 3-mm-thick red layer 1 cm above the sandy rippled limestone bed. No planktic foraminifera are present in the clay layer in the >63-mm size fraction. Stratigraphically, this clay layer (including the red layer) is equivalent to Zone P0 in similar KT boundary lithologies in Spain, Tunisia, and Denmark. It is therefore possible that the Mimbral clay layer also represents Zone P0. This interpretation is supported by the disappearance of all large subtropical and tropical taxa at the top or below the sandy rippled limestone, and the first appearance of *Parvularugoglobigerina eugubina* and *P. longiapertura,* the index taxa for Zone P1a, above the clay layer (Fig. 91). We therefore place the KT boundary at Mimbral at the red layer and base of clay layer immediately above the sandy rippled limestone. It is apparent, however, that the KT boundary interval is very condensed or even discontinuous as suggested by the relatively thin boundary clay (4 cm as compared to 50 cm at El Kef, Tunisia), and bioturbation is present in the sandy rippled limestone, but not in the boundary clay. A disconformity is also suggested by the presence of a very small Ir anomaly (<1 ppb) in this interval, as compared to other KT sections. No elevated levels of Ir are present in the clastic deposit (*Smit et al.*, 1992; *Stinnesbeck et al.*, 1993, see also Fig. 98).

The first Tertiary planktic foraminifera appear in a sample between 4 and 9 cm above the rippled sandy limestone. This sample contains a well-developed early Zone P1a fauna with *P. eugubina, P. longiapertura, W. hornerstownensis, G. fringa, G. edita, Guembelitria cretacea,* and *G. trifolia* (Fig. 91). Zone P1a spans 1.5 m upsection, as indicated by the range of the index taxa *P. eugubina* and *P. longiapertura,* and has a comparable sedimentation rate to Agost and Caravaca in southern Spain (*Canudo et al.*, 1991). The uppermost 70 cm of the Velasco shales and marls exposed at Mimbral are of Zone P1b age. Sediment accumulation appears to have been nearly continuous throughout the P1a and P1b Zone intervals.

Our biostratigraphic analyses of two transects thus indicates that the channel-fill deposit is of Upper Maastrichtian *A. mayaroensis*-zone age. It is likely, however, that sediment deposition occurred over an extended time interval (tens of thousands of years) as suggested by multiple disconformities, some intervals of normal hemipelagic sedimentation and zeolites, and bioturbation at the top. The KT boundary occurs between the top of the channel-fill and the base of the Velasco Formation. Sedimentation during deposition of the boundary clay was reduced similar to KT boundary sections worldwide with the possible exception of shallow water sections (*Donovan et al.*, 1988; *Keller*, 1989; *MacLeod and Keller*, 1991a,b).

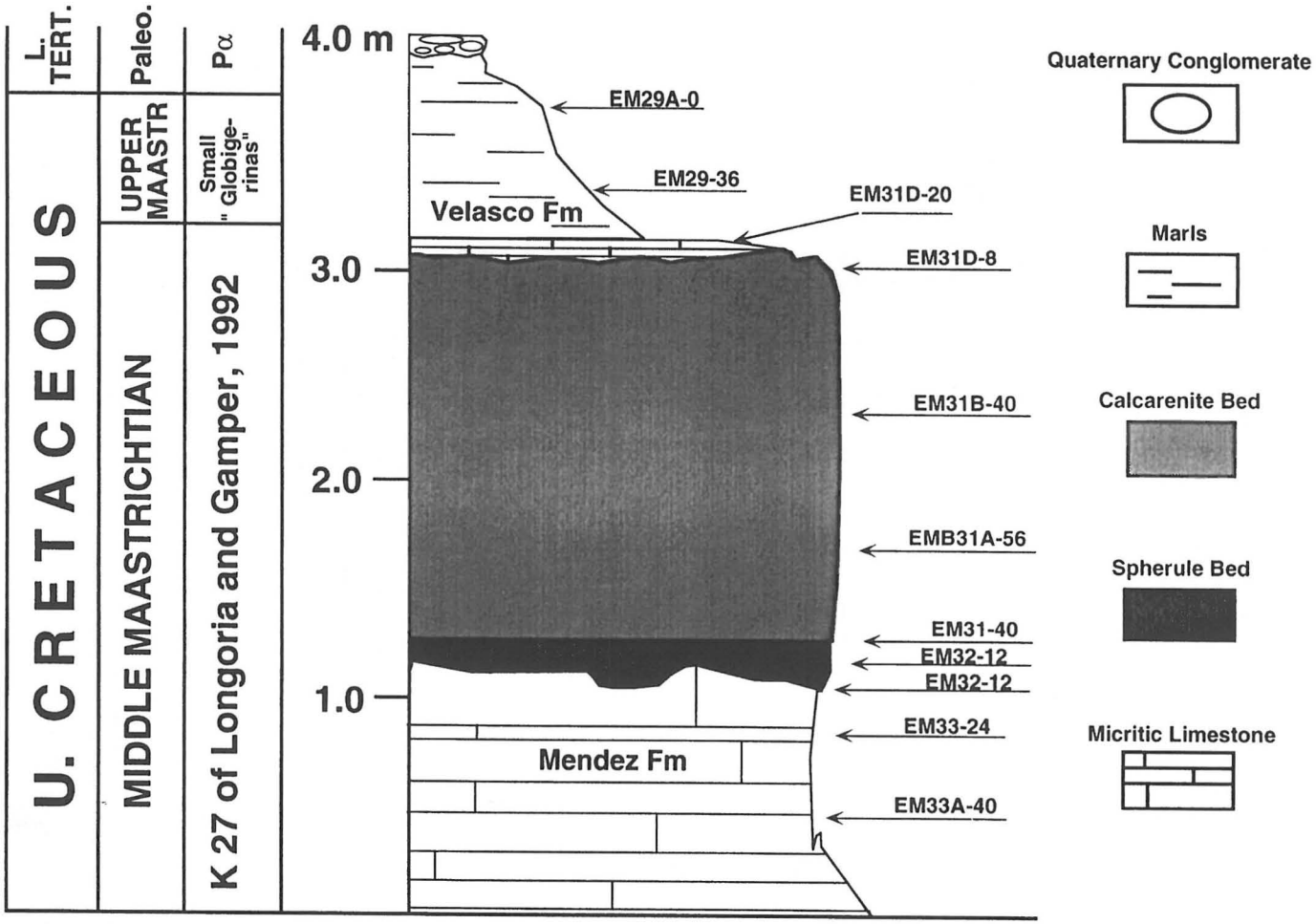

Fig. 88. Lithology and stratigraphy of the El Mimbral section modified from Longoria and Gamper (1992). Note that these authors consider the clastic deposit to be of middle Maastrichtian age and the lower Velasco Formation as of upper Maastrichtian age (see discussion).

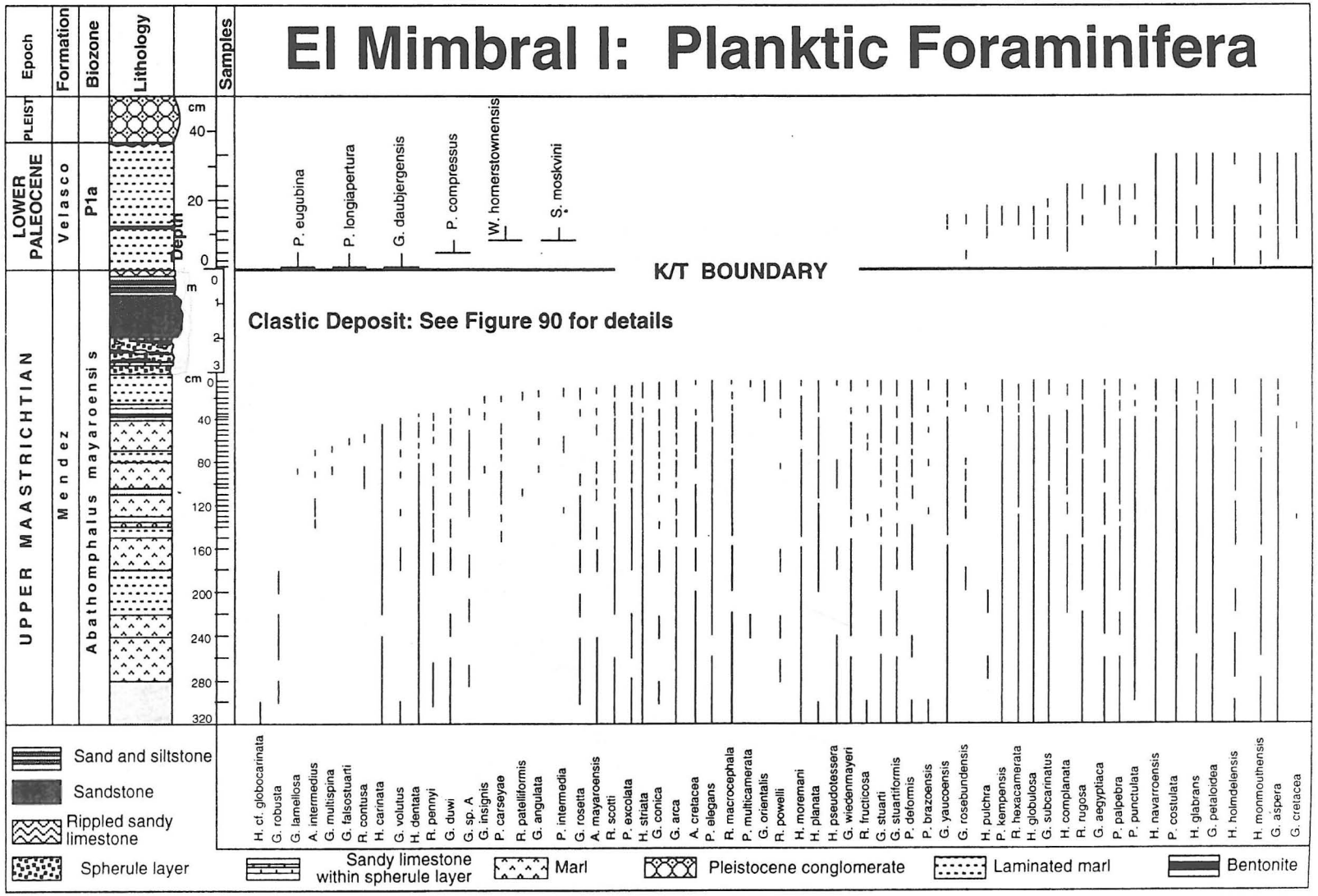

Fig. 89. Stratigraphy and planktic foraminiferal species ranges of the El Mimbral I section at 28 m along the outcrop.

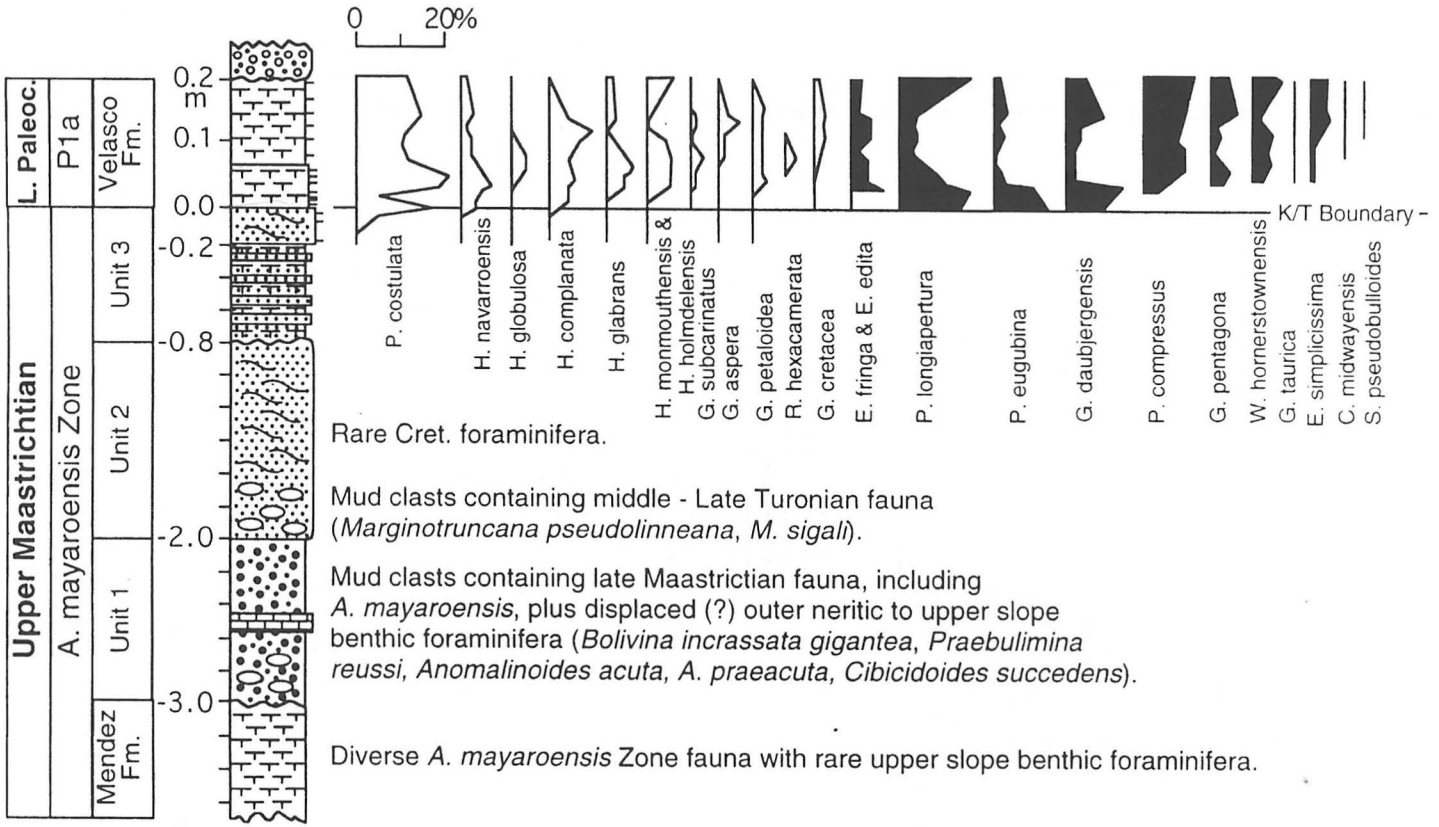

Fig. 90. *Faunal and biostratigraphic information of the channel-fill clastic deposit and overlying Velasco Formation at 28 m along the outcrop at Mimbral. Note the presence of a short hiatus as indicated by the absence of Zone P0. The first occurrence and high abundance of P. eugubina, P. longiapertura, and G. daubjergensis at the base of the Velasco Formation also suggests that the lowermost part of Zone P1a is missing in this channel transect. From Keller et al. (1994).*

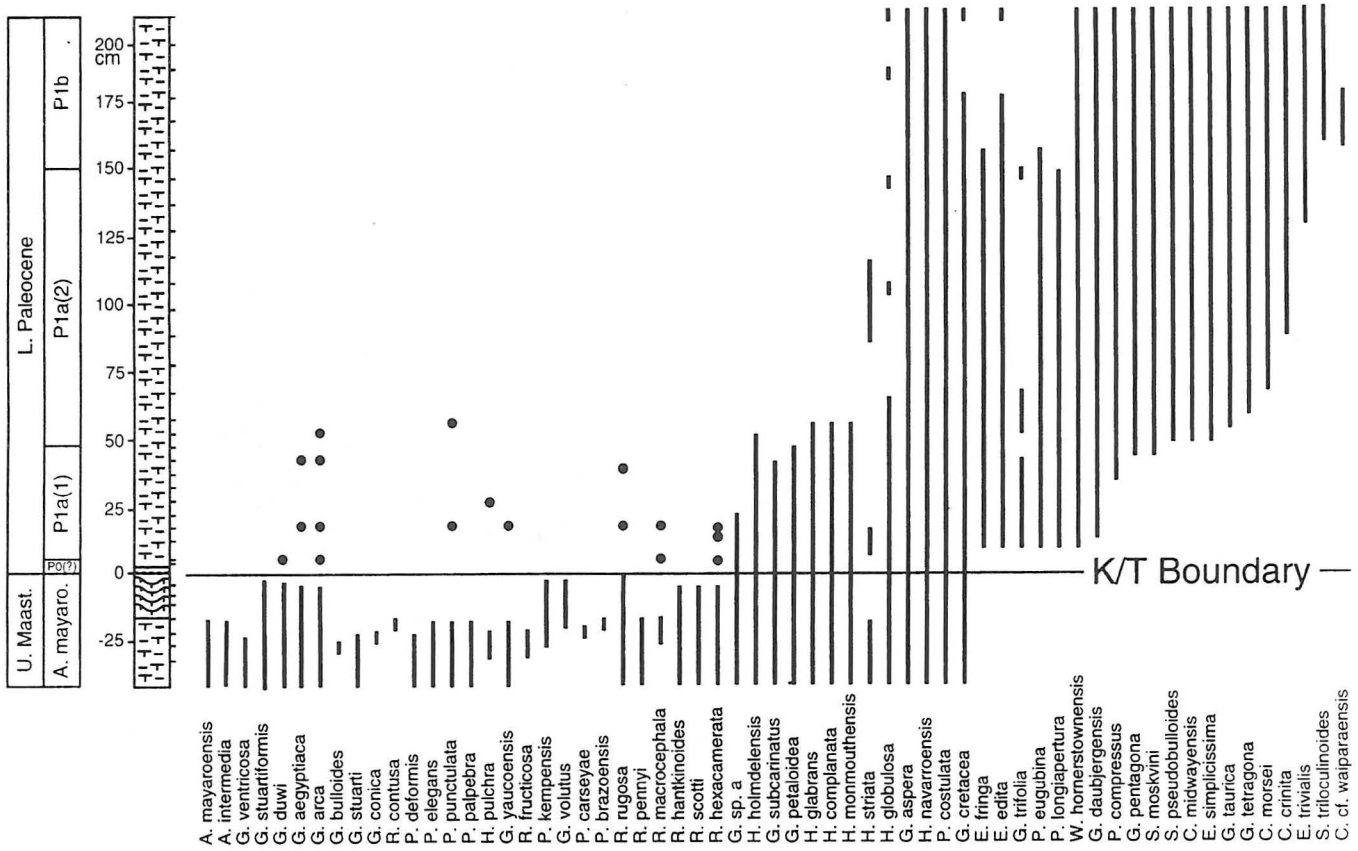

Fig. 91. *Biostratigraphy and ranges of planktic foraminifera across the KT boundary in a nearly continuous sedimentary sequence (at 150 m along the outcrop) outside the clastic channel deposit at Mimbral, northeastern Mexico. Note that all large, complex, tropical, and subtropical Cretaceous taxa disappear at or below the KT boundary. (Isolated dots above the KT boundary indicate the presence of reworked specimens.) Cosmopolitan Cretaceous taxa survive well into the Tertiary. From Keller et al. (1994).*

La Lajilla

The KT boundary transition was studied at 5-cm intervals in a 3.6-m transect at La Lajilla I. This faunal and biostratigraphic sequence is very similar to that of the Mimbral I section. A rich (43 species) and well-developed planktic foraminiferal fauna is present in the Mendez marls below the clastic channel fill, which includes the upper Maastrichtian index species *A. mayaroensis* (Fig. 92) as well as the uppermost Maastrichtian nannofossil index taxon *Micula prinsii* [see Pospichal in *Longoria and Grajales* (1993)]. Within the clastic deposit, which consists of the spherule-rich unit 1 and the alternating sand-silt beds of unit 3, planktic foraminifera are abundant in some silt interlayers, but are otherwise poorly represented. This suggests short intervals of normal hemipelagic sedimentation alternated with increased detrital influx during deposition of unit 3, similar to unit 3 at Mimbral I.

Similar to Mimbral, the sandy limestone layer at the top of the channel deposit is bioturbated and burrows are infilled with the same sediment of the sandy limestone layer. Above the rippled sandy limestone that caps the channel deposit is a thin (~5 cm) Mendez marl with a Maastrichtian *A. mayaroensis*-zone foraminiferal assemblage, including the index taxon, and no evidence of Tertiary planktic foraminifera. This marly layer indicates that normal Maastrichtian sedimentation resumed after deposition of the clastic channel deposit. Thus, the channel deposit must predate the KT boundary. Immediately above the marly layer, a well-developed Zone P1a fauna is present including *Parvularugoglobigerina eugubina, P. longiapertura, Eoglobigerina fringa, E. edita, Planorotalites compressus, Chiloguembelina waiparaensis, Woodringina hornerstownensis,* and *Globanomalina pentagona* (Fig. 92). This assemblage is characteristic of the upper part of Zone P1a [Subzone P1a(2), Fig. 87] and indicates that the lowermost Danian Zone P0 and the lower part of Zone P1a are missing. This is also implied by the absence of a boundary clay.

The faunal record of the La Lajilla KT boundary transition is thus nearly identical to that at Mimbral 50 km to the south. The similarities are also evident in outcrop lithologies. The main difference between the two sections is in the lithologic sequence of the channel fill and the presence of a thin marly limestone of Maastrichtian age above the channel deposit at La Lajilla. For instance, at Mimbral all three lithological units are present, whereas at La Lajilla the massive sandstone of unit 2 is missing. This is presumably because the La Lajilla outcrop represents the near edge of the channel deposit where unit 2 pinches out. The most important difference, however, is the presence of the marly limestone of Maastrichtian age above the channel deposit that indicates that deposition of this clastic deposit preceded the KT boundary event. A similar Mendez marl layer is present above the clastic deposit at the El Mulato section.

Other KT Boundary Sections

No detailed biostratigraphic studies have been published to date of any other KT boundary sections. However, high-resolution biostratigraphic analyses have been completed of all the sections discussed in this field guide (Lopez-Oliva and Keller, in preparation), and brief summaries are given below.

El Peñon: Mendez marls below the clastic deposit contain a diverse upper Maastrichtian fauna of the *A. mayaroensis* zone. Within the clastic deposits of units 1, 2, and 3, foraminifera are rare and invariably of late Maastrichtian age.

La Sierrita: Mendez marls above and below the spherule-rich layer of unit 1 at La Sierrita I contain a diverse Upper Maastrichtian fauna of the *A. mayaroensis* zone. Mendez marls have not been observed above the spherule-rich unit 1 in any of the other clastic deposits. Foraminifers are rare within the clastic deposits of units 2 and 3.

El Mulato: Mendez marls below the clastic deposit contain a diverse upper Maastrichtian fauna of the *A. mayaroensis* zone including the uppermost Maastrichtian nannofossil index taxon *Micula prinsii* (see *Sanchez et al.*, 1993). Foraminifers are rare within the clastic deposit. Above the sandy rippled limestone is a thin marly limestone layer with abundant planktic foraminifera of the *A. mayaroensis* zone similar to La Lajilla. This indicates that deposition of the clastic deposit preceded the KT boundary by a short time interval. Immediately above the marly limestone, a well-developed Danian fauna of Zone P1a is present. Zone P1a spans the lowermost 70 cm of the Velasco Formation followed by 50 cm of Zone P1b

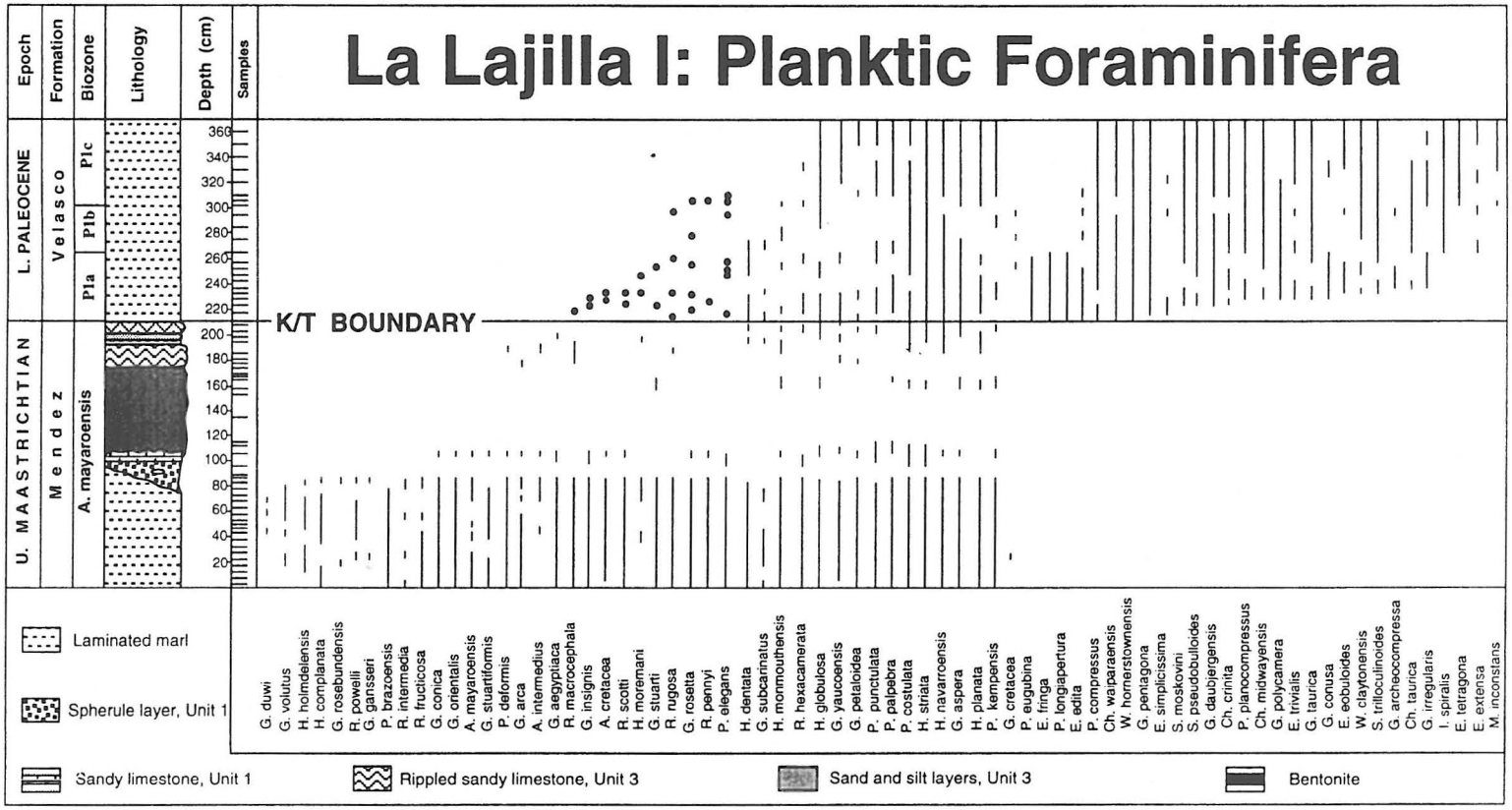

Fig. 92. *Stratigraphy and planktic foraminiferal species ranges across the KT transition at the La Lajilla I section. Note the consistent occurrence of cosmopolitan Cretaceous taxa in the Velasco Formation that indicate survivorship of these taxa. Isolated occurrences of larger tropical taxa are marked by dots and may represent reworked specimens. Data from Lopez-Oliva and Keller, in preparation.*

and 1.5 m of Zone P1c. The basal Tertiary Zone P0 and the boundary clay are absent in the Mulato section, indicating a disconformity between the Cretaceous and Tertiary deposits.

Los Ramones: Mendez marls of the Los Ramones section are of upper Maastrichtian age. The overlying clastic deposit consists largely of well-rounded sand grains with few silicified shallow-water Cretaceous foraminifers. This clastic deposit at the top of the Mendez Formation is thus also of near KT boundary age.

BIOTIC EFFECTS OF THE KT BOUNDARY EVENT IN NORTHEASTERN MEXICO

Although the evidence for a large KT boundary bolide impact near Chicxulub on the the Yucatan Peninsula (*Hildebrand et al.*, 1991; *Pope et al.*, 1991; *Swisher et al.*, 1992) is still in dispute (*Officer et al.*, 1992; *Lyons and Officer*, 1992; *Jéhanno et al.*, 1992), such a catastrophe would have produced biotic effects in nearby areas, including northeastern Mexico. *Keller et al.* (1994) have examined the biotic effects of the KT boundary event at El Mimbral based on species diversity, extinctions, and relative abundance changes of dominant planktic foraminifera (Fig. 93) and found them to be comparable to the biotic effects observed at El Kef, Tunisia, Agost, and Caravaca, Spain, and the eastern Tethys (*Keller*, 1988; *Canudo et al.*, 1991; *Keller and Benjamini*, 1991).

Biotic effects of the KT boundary event were not instantaneously catastrophic, nor were they restricted to the boundary event in planktic foraminiferal faunas at El Mimbral. Although two-thirds of the Cretaceous species (28 taxa) disappeared at or below the KT boundary (Fig. 91), the effect on the overall foraminiferal population was small (<17%, Fig. 93) because only rare, apparently endangered taxa disappeared. These taxa were specialized tropical and subtropical forms intolerant of environmental changes. The dominant taxa (>83%, Fig. 93) consisted by cosmopolitan forms tolerant of wide-ranging environmental conditions. These species survived the KT boundary event without any sudden changes in their relative abundances (see Fig. 94). Their terminal decline about 100 k.y. after the KT boundary is related to competition from the evolving Tertiary fauna, as illustrated in Fig. 94. The limited biotic effects observed across the KT boundary at El Mimbral, as well as at La Lajilla (Lopez-Oliva and Keller, in preparation), are consistent with other low-latitude sections. These data indicate that if a bolide impact occurred in the Caribbean, the biologic consequences were not as catastrophic as generally assumed, even within a radius of 2000 miles.

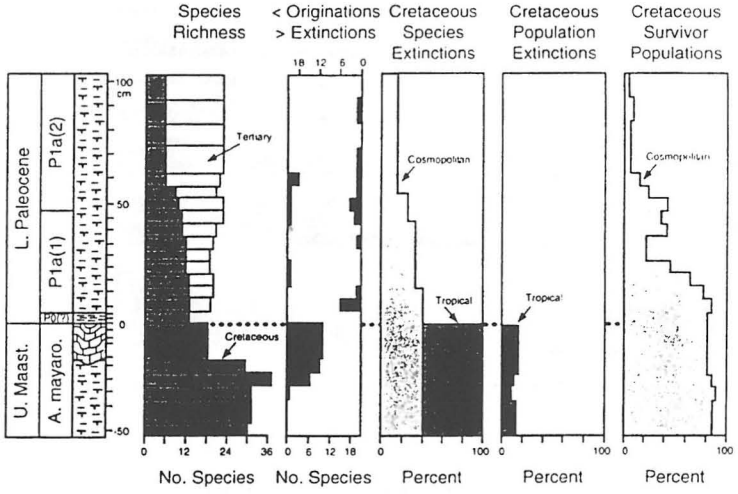

Fig. 93. *Summary of biotic effects of planktic foraminifera across the KT boundary at El Mimbral II (see discussion for explanation.) From Keller et al. (1994).*

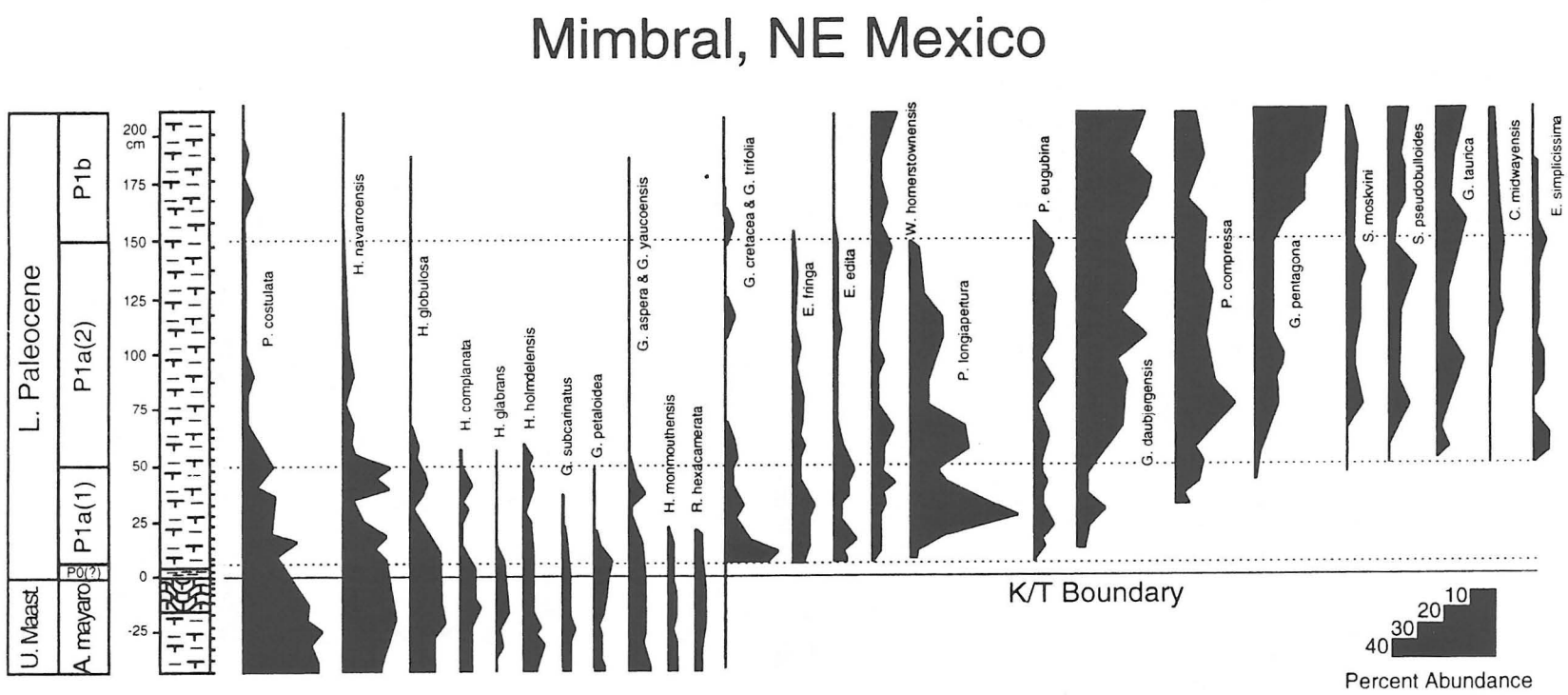

Fig. 94. *Stratigraphic ranges and relative abundances of dominant (87%) planktic foraminifera across the KT boundary at El Mimbral II. Note the absence of catastrophic changes at the KT boundary in the relative abundances of dominant taxa. This suggests that the effect of the KT boundary event was not instantaneous or catastrophic. From Keller et al. (1994).*

LITHOSTRATIGRAPHIC CORRELATIONS

Near-KT boundary channel-fill clastic deposits of northeastern Mexico consist primarily of transported terrigenous and shallow-water neritic debris from multiple sources (e.g., terrestrial, shallow neritic, neritic, upper bathyal) and ages (e.g., Maastrichtian, Campanian, Turonian). Nevertheless, the depositional sequence of this varied transported debris is surprisingly constant. It allows recognition of three well-defined units based on lithologic and sedimentologic characteristics (see description in Part I) that can be traced over a distance of over 300 km. Even mineralogic variations are correlatable as discussed in the Mineralogy section. Because of the relatively constant characteristics of these units, and even subunits (e.g., sandy limestone of unit 1, rippled sandy limestone of unit 3), all sections can be correlated with confidence.

Figure 95 shows the stratigraphic correlation of all six sections examined in nine outcrops. The horizontal correlation line A marks the KT boundary at the top of the sandy rippled limestone of unit 3, which is present in all sections except Los Ramones. This sandy rippled limestone generally contains two or more distinct layers of *Chondrites, Zoophycos,* and Y-shaped *Thalassinoides*-like burrows and feeding tracks. In the El Mulato and La Lajilla sections, the sandy rippled limestone is capped by marly limestone with abundant planktic foraminifera of the upper *A. mayaroensis* zone. This indicates deposition of the clastic deposit occurred during the uppermost Cretaceous preceding the KT boundary and that normal pelagic sedimentation of the uppermost Maastrichtian succeeded deposition of the clastic deposit. Absence of this marly limestone above the channel deposits in most other sections appears to be due to erosion, as also indicated by the absence of the lower part of Zone P1a, Zone P0, and the boundary clay in most sections.

Correlation line B marks the base of unit 3 (alternating sand, silt, and shale layers) and top of unit 2 (massive sandstone). Unit 3 is of variable thickness; it is thickest at the center of the channel and thinning toward the edges as seen at Mimbral II where only the sandy rippled limestone is present. In the very shallow depositional environment of Los Ramones, units 2 and 3 cannot be distinguished.

Correlation line C marks the base of the massive sandstone of unit 2 and the top of the spherule-rich layer of unit 1. Unit 2 is thickest at the center of the channel and frequently absent toward the edges as observed at Mimbral II, La Lajilla I, and El Peñon II (Fig. 95a).

Correlation line D marks the top of the Mendez Formation and base of the spherule-rich unit 1. Within unit 1 there is a distinct subunit consisting of a resistant 10–20-cm-thick sandy limestone layer (well-cemented packstone of *Smit et al.*, 1992) that is present at El Mimbral, El Peñon, and La Lajilla (Fig. 95a). The presence of this sandy limestone layer is thus correlatable over a distance of over 200 km.

Not all KT boundary outcrops in the region appear to have clastic sediment deposition, as noted by *Gamper* (1977) and *Longoria and Gamper* (1993) in outcrops near Aldama (Arroyo Pedregoso) and Magiscatzin in the State of Tamaulipas (Fig. 3).

Near-KT-boundary clastic deposits in northeastern Mexico appear to be channel fills that partially erode the Maastrichtian Mendez Formation. An excellent example of a typical channel cross-section is exposed at Mimbral, where thick clastic beds crop out over more than 150 m, marking the center and edge of the channel. At the edge of the channel only the topmost 20-cm-thick rippled sandy limestone of the channel fill is present. This sandy limestone layer lies conformably between the Upper Maastrichtian Mendez and Lower Paleocene Velasco marls.

An idealized cross section of a channel and its clastic deposits (characterized by the three units discussed above) is illustrated in Fig. 95b. Most outcrops examined represent only a part of the channelized deposit, as illustrated by arrows for El Mimbral, La Lajilla, El Peñon, El Mulato, and La Sierrita. Depending on which part of the channel is exposed, all three or only one or two lithological units are present. For example, in the center of the channel, all three units are present. But near the edges of the channel, unit 2 first disappears, followed by unit 1 and finally unit 3 (Fig. 95b).

The thickness of each of the three units (and subunits) varies depending on their relative position within the channel. Various deposits range from 0 to 1 m for the spherule-rich unit 1, 0 to 4 m for the massive sandstone of unit 2, and 20 cm to about 3 m for the interlayered sand, shale, and siltstone beds of unit 3. Deposition is always most expanded near the channel centers. Toward the edges the units thin out and disappear (Fig. 95b). We observed that unit 2 thins out first away from the channel center. Unit 1

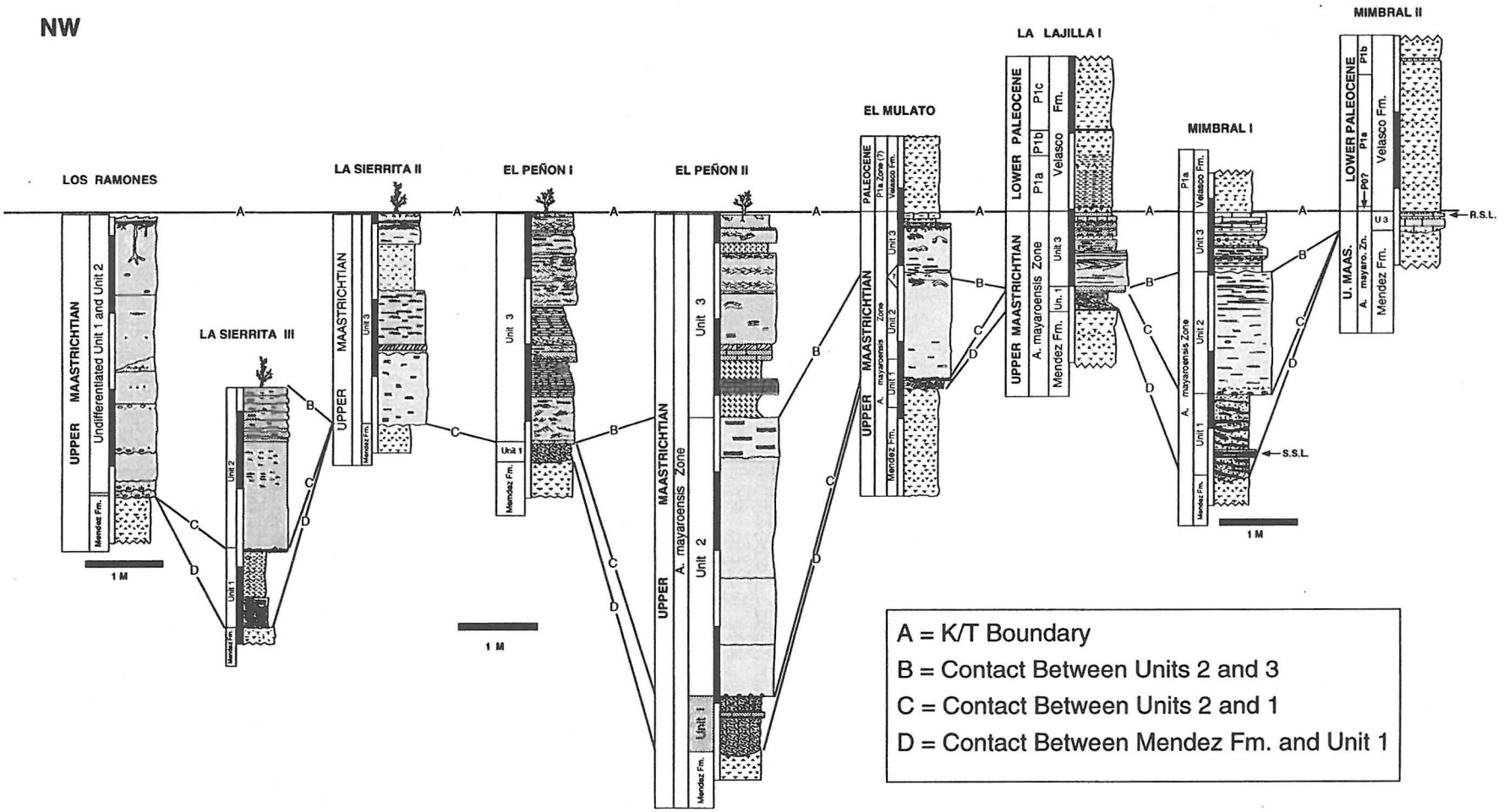

Fig. 95a. *Lithostratigraphic correlation of units 1, 2, and 3 of the channel deposits in the KT boundary sections of northeastern Mexico.*

thins out and disappears near the channel edge, whereas at least the upper part of unit 3 (rippled sandy limestone) seems to reach beyond the channel edge (Fig. 95b).

The height and length of channel cross sections is variable, ranging from less than 200 m to several kilometers. For instance, at El Mimbral the channel is more than 150 m wide. In the La Sierrita region the clastic deposit is exposed along several hills, spanning 3–4 km and suggests a north-northwest/south-southeast flow direction. At El Peñon, clastic beds can also be followed for at least one kilometer. All outcrops are aligned in a north-northwest/south-southeast direction.

MINERALOGICAL CORRELATIONS

Whole rock and clay mineral analyses for El Mimbral I and II, La Lajilla I, El Mulato, El Peñon I, and La Sierrita sections indicate that each lithological unit, units 1, 2, and 3 of the clastic channel deposits and the Mendez Formation, have distinct and correlatable compositions as illustrated in Figs. 96 and 97 as discussed below. Whole-rock compositions were determined by XRD (SCINTAG XRD 2000 diffractometer) based on methods by *Ferrero* (1966) and *Kübler* (1983), and clay mineral analyses were based on methods by *Kübler* (1987). Clay minerals are given in percent abundance without correction factors; content in swelling (% smectite) is estimated by using *Reynolds'* (1989) method. All analyses were done in the Mineralogy, Petrography, and Geochemistry Laboratory of the University of Neuchâtel.

Mendez Formation

Analyses indicate that the Mendez Formation is characterized by marl composition containing an average of 50% calcite, 30% phyllosilicates, 15–20% quartz, and 5–10% plagioclase (Fig. 97). The content in clay minerals, such as mica (illite), chlorite, irregular mixed layer chlorite-smectite, and irregular mixed layer mica-smectite, is variable. This is especially the case for in chlorite content, which varies from >60% (>2-μm size fraction) in the La Lajilla I and Mulato sections to <20% in the La Sierrita and Peñon I sections. This difference in chlorite content indicates that the Mendez marls, below the disconformity that separates the channel deposits above, are not coeval in all sections and that differential amounts of erosion occurred.

Unit 1

The loosely cemented spherule-rich unit 1 that disconformably overlies the Mendez Formation is characterized by high calcite (60–70%) and low phyllosilicates (20%), quartz (10–15%), and plagioclase (albite 5%). The clay mineral fraction is primarily composed of illite-smectite (>25%) and chlorite-smectite (40–60%) with very low amounts of chlorite and mica (illite, Figs. 96 and 97). However, the composition in the 10–20-cm-thick sandy limestone layer (SLL) that is present within unit 1 is significantly different with lower calcite and higher quartz, plagioclase, chlorite, and mica (illite). This difference in whole-rock and clay-mineral compositions indicates that the detrital influx varied between deposition of the sandy limestone layer and the loosely cemented spherule-rich sediments above and below. Deposition of unit 1 could thus not be the result of a single event, but reflects multiple events with differing detrital influx.

Unit 2

The massive laminated sandstone of unit 2 is characterized by low calcite (20–40%) and phyllosilicates (10–15%) and high quartz (up to 40%) and plagioclase (albite 15–25%, Fig. 97). Clay minerals show an increase in mica (illite) and chlorite relative to unit 1 (Fig. 96). These mineralogical data indicate an increase in detrital influx relative to units 1 and 3 and probably more rapid deposition.

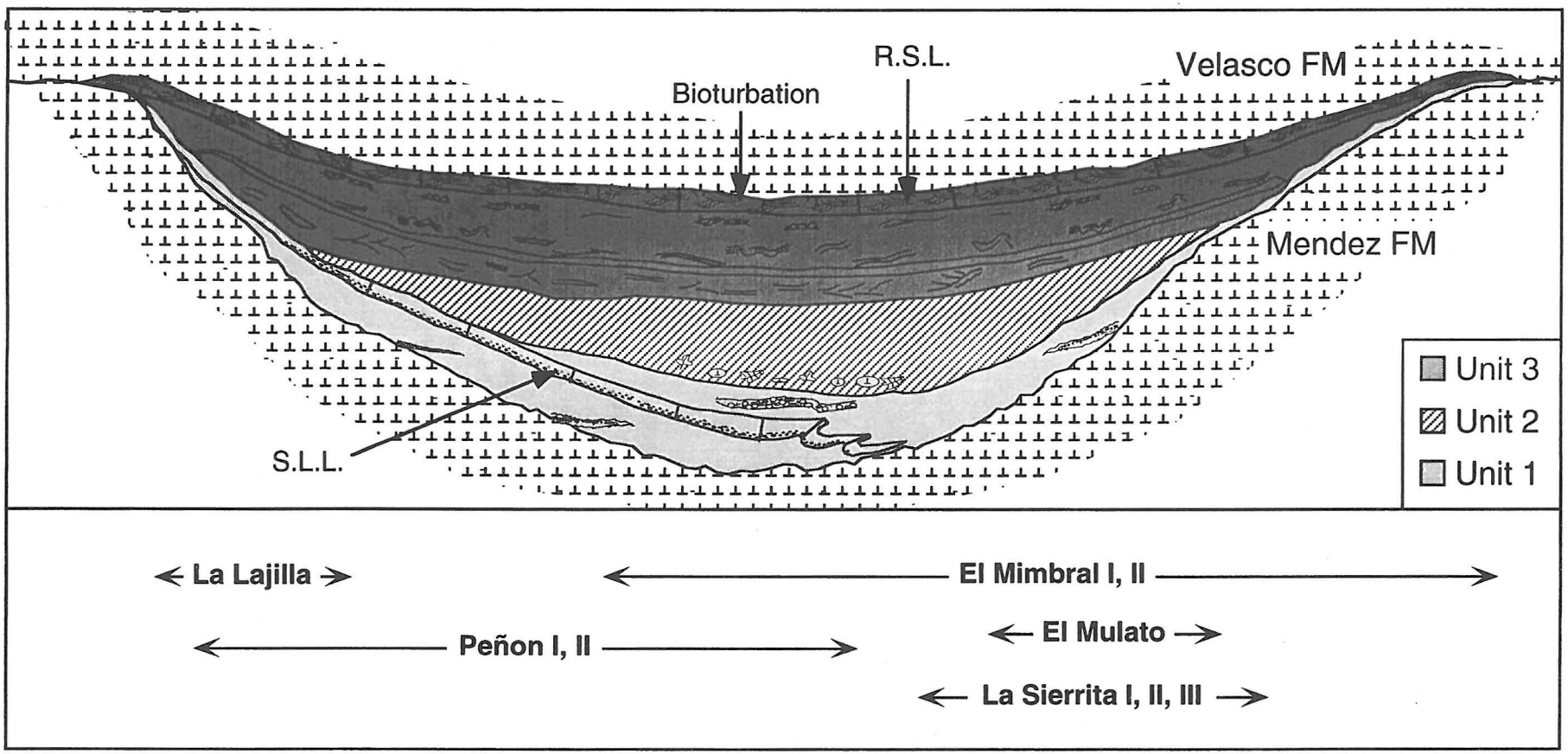

Fig. 95b. *Sketch of idealized channel deposit showing thinning out of units 1, 2, and 3 toward the edge of the channel. SLL refers to the sandy limestone layer within unit 1. RSL refers to the rippled sandy limestone layer that caps unit 3. Bioturbation is ubiquitous in the RSL layer in two or more intervals.*

Unit 3

The sand, silt, and shale layers of unit 3, which are topped by a rippled sandy limestone (RSL), are highly variable in calcite (but generally higher than in unit 2), phyllosilicates, quartz, and plagioclase (Fig. 97). Two distinct clay mineral associations can be identified: One, characterized by the rippled sandy limestone and sandy layers, is high in chlorite (40–70%) and mica (illite, 40–50%), which suggests increased detrital influx and probably more rapid deposition similar to unit 2 (Figs. 96 and 97). The second clay mineral association is characterized by shale layers rich in mixed layers chlorite-smectite and some layers also rich in illite-smectite (30–70%, <2-μm fraction) that are similar to the Mendez Formation and represent periods of normal hemipelagic sedimentation. Thus, unit 3 represents depositional environments alternating between increased detrital influx and rapid deposition (sand and silt layers) and normal hemipelagic deposition (shale layers).

Two distinct layers rich in zeolites (clinoptilolite-heulandite) have also been recognized near the base and near the top of unit 3, below the rippled sandy limestone (Figs. 96 and 98). Significant enrichment in zeolites is also observed in the basal Tertiary clay layer at El Mimbral II (Fig. 98). The presence of distinct intervals enriched in zeolites in units 1 and 3 and the boundary clay indicates significant volcanoclastic influx during these times. The zeolite-enriched layers of unit 3 are correlatable in all sections examined (Fig. 98).

Whole-rock and clay mineral compositions thus indicate the presence of distinct and correlatable units spanning over 300 km. Such systematic variation in detrital influx alternating with periods of normal hemipelagic sedimentation over such a large region is incompatible with an impact-generated tsunami megawave and deposition within hours to a few days. We conclude that deposition of units 1, 2, and 3 of the channel deposit occurred over a long time period (tens of thousands of years?) with periods of normal hemipelagic sedimentation alternating with times of increased detrital influx and more rapid sedimentation that may have coincided with sea-level lowstands and/or regional tectonic activity.

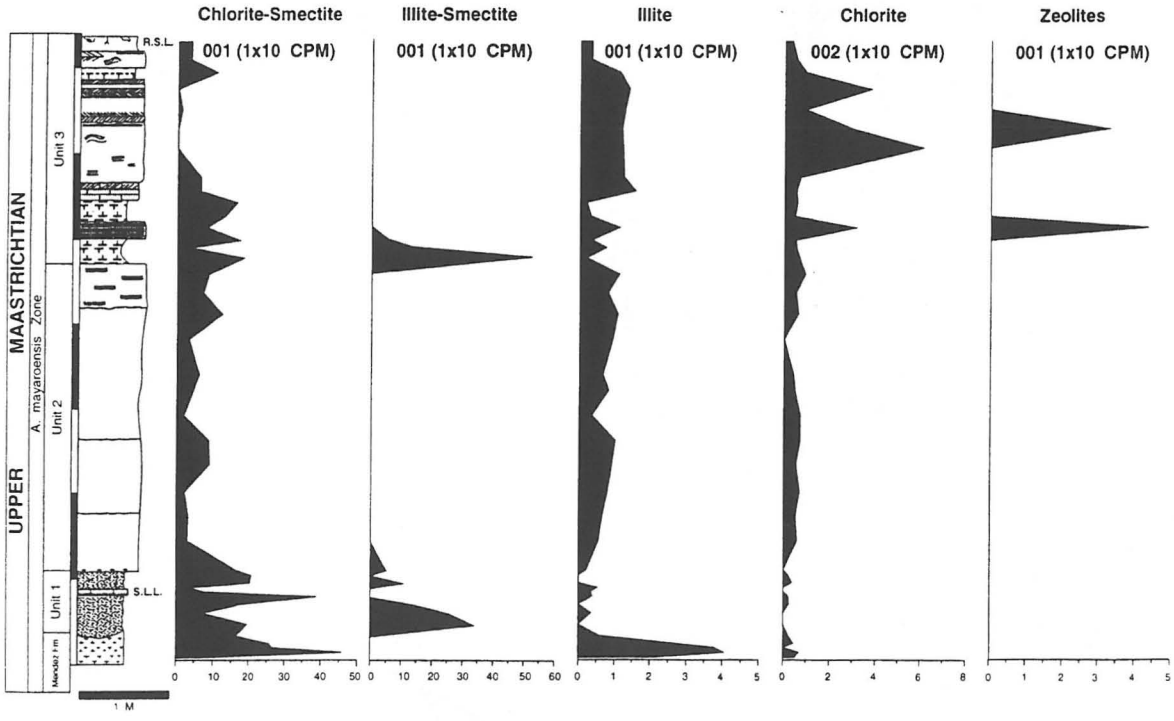

Fig. 96. *Phyllosilicate distribution in the El Peñon KT clastic deposit. Note the two distinct layers enriched in zeolites in unit 3, as well as layers enriched in illite-smectite or chlorite. See discussion for interpretation. From Adatte et al. (in preparation)..*

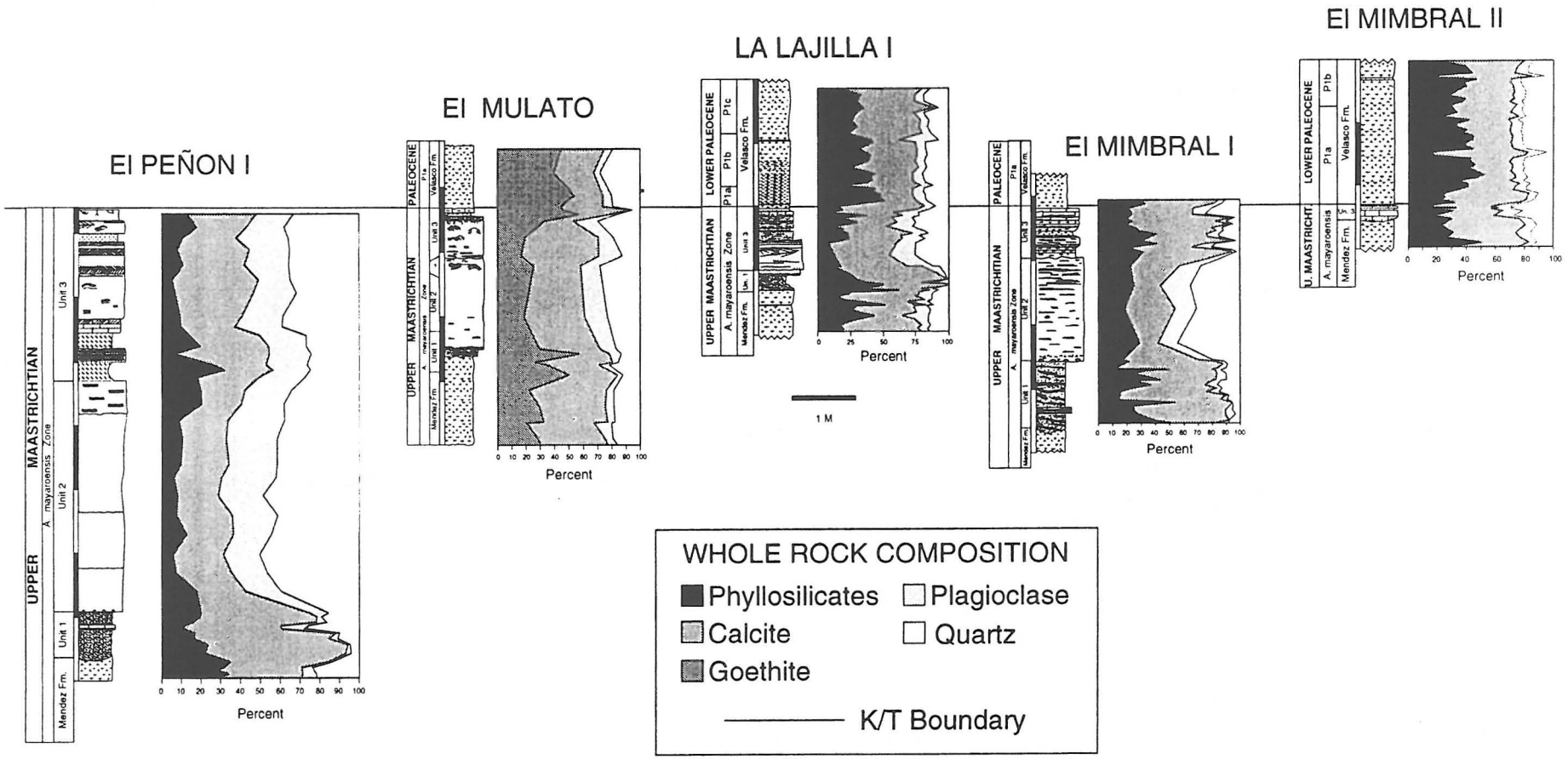

Fig. 97. Mineralogical correlations of KT boundary outcrops in northeastern Mexico.

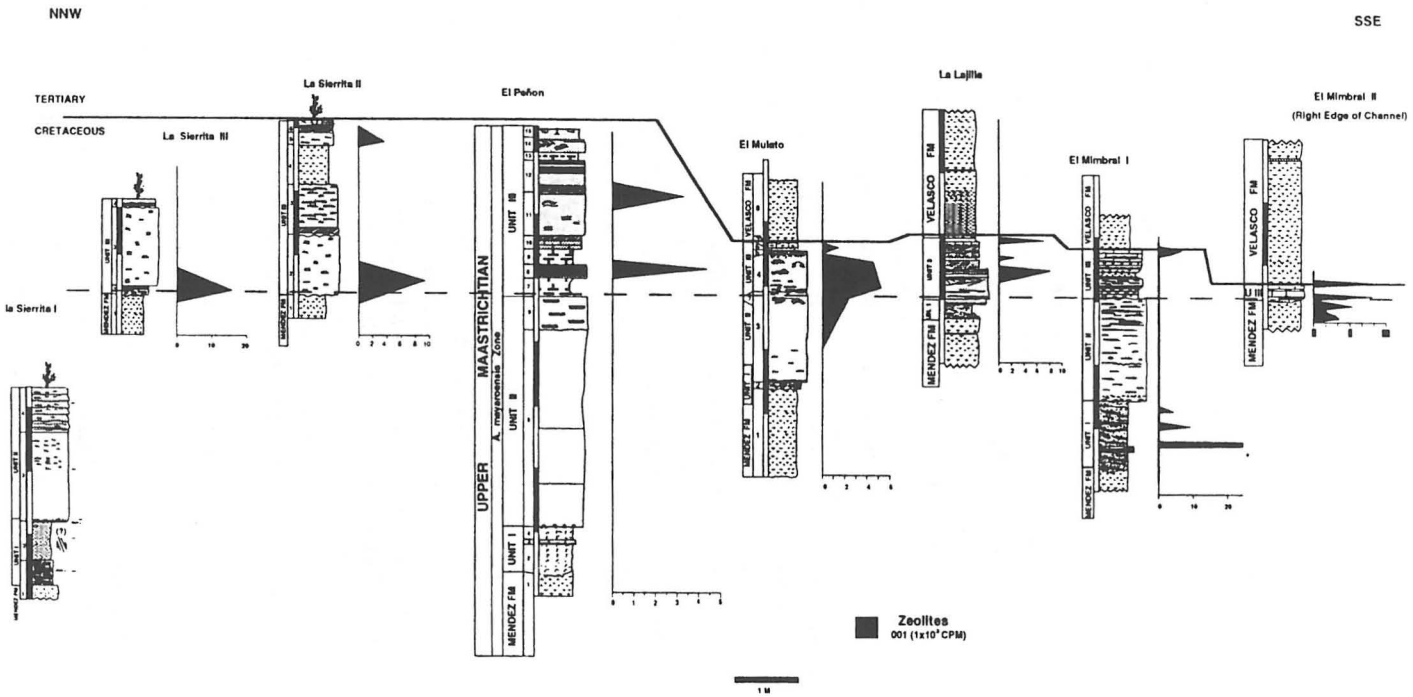

Fig. 98. *Correlation of zeolite-enriched layers in KT boundary outcrops of northeastern Mexico (from Adatte et al., in preparation).*

OTHER CHARACTERISTICS OF KT DEPOSITS IN NORTHEASTERN MEXICO

Spherules

Spherules in unit 1 of the channel-fill deposit are generally 1–5 mm in diameter, commonly filled with blocky calcite and surrounded or partly filled by mixed layers (illite/smectite, chlorite, or mica, *Stinnesbeck et al.*, 1993). According to *Margolis et al.* (1992), spherules are altered to kaolinite and calcite at La Lajilla. Replacement is by smectite, pyrite, and other Fe-rich minerals at El Porvenir, El Mulato, and El Peñon and by glauconite and smectite at the Rancho Nuevo and La Sierrita localities. Many large spherules contain smaller spherules (Fig. 17). Some spherules contain apatite concretions, rounded clasts of limestone, rutile crystals (Fig. 18), or foraminiferal tests filled with glauconite (Figs. 19 and 20). No glassy spherules were observed similar to those found at Beloc, Haiti, either by us, Hildebrand (personal communication) or Smit (personal communication). All glass shards found (a total of over 500) are angular and vesicular fragments and provide no evidence of a former existence as a glass sphere. Glass fragments are occasionally found enclosed within calcite.

Commonly, spherules infilled with blocky calcite have a brown coating that after acid treatment remains as a thin tan-colored hollow sphere. These hollow spheres are probably algal resting cysts that have also been observed by *Hansen et al.* (1986) at Stevns Klint, Denmark. Moreover, there is a significant organic content in the spherule-rich unit 1 (0.34%, *Stinnesbeck et al.*, 1993), relative to units 2 and 3, that also suggests an organic or authigenic origin for at least some spherules.

Acid-treated residue commonly contains green chlorite spherules with radiating spherule structure and brown palagonite subspherules of radiating smectite (Lyons, personal communication, 1993). These two minerals and structures suggest a volcanic affinity. Additional evidence of a volcanic input is found in the presence of aluminum chromite with almost no Ni in all three units at Mimbral as well as above and below the channel deposit (*Stinnesbeck et al.*, 1993).

Thus, the spherules of unit 1 are of multiple origins including organic, authigenic, volcanic, and accretionary oolites that probably formed at neritic depths and were subsequently transported. The absence of glassy spherules and extreme rarity of glass fragments (see discussion later) does not support a large airborne component (e.g., bolide impact-fallout) for this spherule-rich deposit.

Glass

Glass shards are extremely rare and restricted to the spherule-rich unit 1 (about 1 glass particle per 200-g sediment) (*Smit et al.*, 1992; *Stinnesbeck et al.*, 1993). Standard thin section or washed residue analyses generally yield no evidence of glass. To concentrate glass particles, about 1 kg bulk sediment should be acid (HCL) reduced over several weeks with repeated applications of HCL. Glass shards vary in size from <100 mm to >400 mm. They are irregular in outline and commonly vesicular. Colors vary from yellow-amber, green, brown, and red to rarely black (only two black grains were found in over 300 grains, Fig. 23). Black and opaque glass shards have total oxides close to 100%. Green, red, and amber glasses have similar compositions to the dark glasses but with total oxides averaging 87%; these hydrated glasses are probably weathered.

Preliminary analyses of three Mimbral glasses indicate that the black glass composition is similar to black glass from Beloc, Haiti, and that the hydrated glasses are probably of the same origin, but weathered (*Stinnesbeck et al.*, 1993, Table 1, *Bohor and Betterton*, 1993, Table 2). Subsequent analyses of over 30 glasses by Lyons (personal communication, 1993) also reveal average compositions similar to Beloc, Haiti. Beloc glass was earlier interpreted by *Jéhanno et al.* (1992) and *Lyons and Officer* (1992) as possibly of local volcanic origin and probably not of tektite origin because of its high Fe oxidation state and the absence of lechatelierite. *Izett et al.* (1990), *Sigurdsson et al.* (1991), and *Blum and Chamberlain* (1992) interpret Beloc glass as of impact origin.

TABLE 1. Chemical composition of three Mimbral (me) glasses and comparison with Beloc black glass (Bbg.), Haiti.

	BBG[10]	ME4[7]	ME2[3]	ME3[4]
Na_2O	4.1	3.8	1.8	3.4
MgO	3.0	3.6	3.1	1.3
Al_2O_3	15.5	15.7	13.9	14.5
SiO_2	61.6	59.8	55.2	58.1
SO_3	<0.1	<0.1	0.2	<0.1
K_2O	1.5	1.5	0.6	1.1
CaO	8.4	6.2	5.5	4.0
TiO_2	0.7	0.8	0.7	0.7
MnO	<0.1	0.3	<0.1	<0.1
Fe_2O_3*	6.2	7.0	6.3	3.9
Total (%)	101.2	98.8	87.4	87.2

*Total Fe as Fe_2O_3. Number in brackets corresponds to the number of analyses. Beloc glass analysis from *Jéhanno et al.* (1992). From *Stinnesbeck et al.* (1993).

TABLE 2. Comparison of Mimbral and Beloc relict glass analyses.

	Mimbral, Mexico Relict Glasses					Beloc, Haiti Glasses	
	Dk. Brn.	Yellow	Dk. Grn.	Lt. Grn.	K-rich[2]	Dk. Brn.[5]	Yellow[7]
SiO_2	60.43	50.38	60.68	60.68	66.20	63.09	49.06
Al_2O_3	15.75	13.78	15.41	14.88	18.73	15.21	13.19
FeO	6.42	5.15	3.63	4.35	5.67	5.44	5.14
MgO	3.79	4.64	1.16	2.46	2.64	2.74	4.09
CaO	7.21	23.66	3.76	5.21	0.84	7.26	24.54
K_2O	1.27	0.61	1.11	0.91	3.68	1.59	0.63
Na_2O	2.65	2.15	1.46	0.99	0.84	3.63	2.10
TiO_2	0.78	0.64	0.83	0.70	0.02	0.67	0.64
MnO	—	—	—	—	0.00	0.14	0.16
Total	98.34	101.2	88.10	90.38	98.83	99.76	99.56

[2] From *Smit et al.* (1992); [5] from *Sigurdsson et al.* (1991); [7] from *Maurasse and Sen* (1991). Table 2 from *Bohor and Betterton* (1993).

Shocked Quartz

Quartz grains with multiple sets of lamellae are very rare (<1%, not common as reported by *Smit et al.*, 1992). The grains are often subrounded and occur within as well as above and below units 1, 2, and 3 (*Stinnesbeck et al.*, 1993). The lamellae are often curved and irregularly spaced, a characteristic of tectonic origin (*Carter and Friedman*, 1965). Some lamellae are decorated with trains of fluid inclusions. The orientation of 12 quartz grains observed show a broad distribution (one between 15° and 20°, three between 25° and 30°, one between 50° and 55°, two between 60° and 65°, three between 65° and 70°, and two between 85° and 90°) that is characteristic of lamellae of tectonic or strain rate origin, rather than impact origin (*Carter and Friedman*, 1965).

Lamellar features in subrounded quartz grains were also observed in a sample 2–3 m below the spherule layer and in the red layer at the base of the KT boundary clay. These subrounded grains suggest an origin prior to the KT boundary event, followed by subsequent erosion and transport to their current resting place.

Thus, shocked quartz grains are very rare and found in clastic units 1, 2, and 3 as well as in the Maastrichtian Mendez marls below and Tertiary Velasco shales above. Subrounded outlines of some of these grains and lamellae decorated with trains of fluid inclusions in others suggest transport and a tectonic origin for at least some of them. If the spherule-rich unit 1 represents tektite concentrations due to impact fallout as suggested by *Smit et al.* (1992), it is difficult to understand why pristine quartz is so abundant and shocked quartz so rare.

Iridium

Iridium analysis of the clastic deposit at Mimbral by *Smit et al.* (1992) and Rocchia and Robin (in *Stinnesbeck et al.*, 1993, and personal communication, 1992) revealed no anomalous concentrations in the spherule layer of unit 1, or the massive sandstone of unit 2, and only very low concentrations of 0.2–0.4 ng/g (200–400 pg/g) in the uppermost 10 cm of the rippled sandy limestone layer at the top of unit 3 (Figs. 99a,b). Rocchia and Robin analyzed the Ir concentration at Mimbral outside the channel deposit between meter marks 150–152. The maximum Ir concentration of 0.8 ng/g (800 pg/g) was measured 10 cm above the thin rust-colored layer that is located just above unit 3 and marks the base of the Tertiary Velasco Formation. This rust-colored layer and overlying 4-cm-thick clayey layer represent biozone P0, which has only been observed at this location at the edge of the channel deposit. Biostratigraphically, the maximum increase in Ir coincides with the base of Zone P1a *(P. eugubina)*, whereas the preceding Zone P0 has lower Ir values (~500 pg/g, Fig. 99b). *Smit et al.* (1992) measured a similar maximum Ir concentration in the marls just above the rippled sandy limestone at a location between meter mark 21–25 within the channel (Fig. 99b). They interpreted this Ir enhancement to occur in Zone P0 marking the KT boundary. However, our biostratigraphic restudy of this section shows that biozone P0 and probably the lower part of Zone P1a are not present within the channel, since Zone P1a index taxa *Parvularugoglobigerina eugubina* and *P. longiapertura* are abundant immediately above the sandy rippled limestone at the top of unit 3 (see Fig. 90). This is also indicated by the differing Ir profiles (Figs. 99a,b). The maximum Ir concentration in *Smit et al.*'s (1992) analysis coincides with the base of Zone P1a, whereas in Rocchia and Robin's analysis in the more complete KT boundary transect at the edge of the channel, Ir values increase in Zone P0 and reach maximum values near the base of Zone P1a (Fig. 99b).

Compared with other KT boundary sections such as Gubio, Caravaca, or El Kef, where Ir concentrations reach 10,000 pg/g, the maximum concentration at El Mimbral of <1000 pg/g is very low. This is probably because the basal Danian and KT boundary is incomplete with possibly part of Zone P0 missing due to erosion and/or nondeposition as discussed in the Biostratigraphy section.

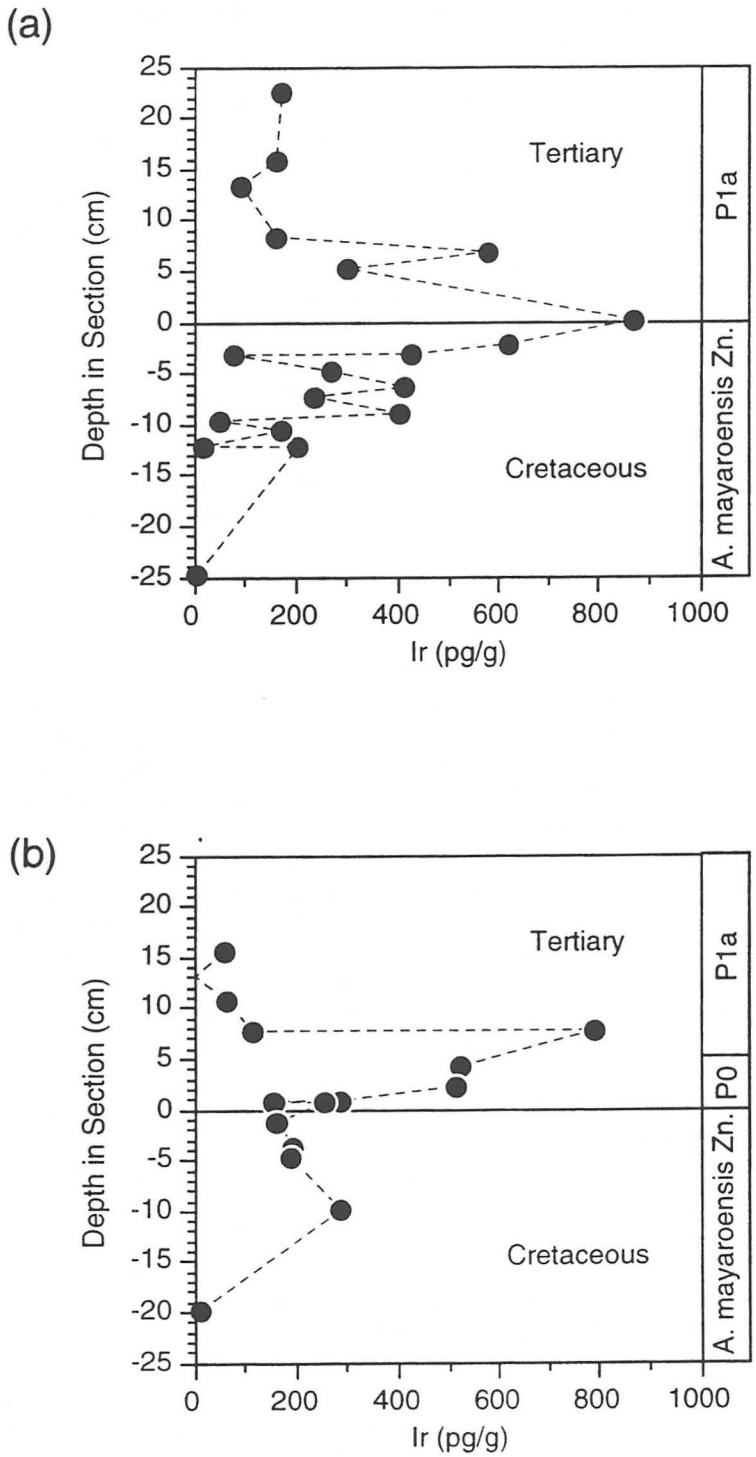

Fig. 99. *Iridium concentrations at (**a**) El Mimbral I in the center of channel (from Smit et al., 1992), and (**b**) at El Mimbral II outside the channel (from Rocchia and Robin, in Stinnesbeck et al., 1993).*

Ni-rich Spinels

Robin and Rocchia (in *Stinnesbeck et al.*, 1993, and personal communication, 1992) searched for Ni-rich spinels in the Mimbral section, including the Mendez marls clastic deposit and Velasco marls, but found none. *Smit et al.*(1992) reported the presence of "Ni, Ti and Cr-rich magnetite and spinel-like crystals (. . .) from Mimbral tektite glass." Our investigation of several samples from the spherule layer at Mimbral revealed only the presence of aluminian chromite, but with no Ni (<0.1%). These chromites have morphologies that resemble those of KT and cosmic spinels, but they are easily distinguishable from the latter by their low Ni content (<0.1% as compared with 1–5% in cosmic and KT spinels (*Robin et al.*, 1991, 1992), and their low Fe^{3+}/Fe_{tot} ratio (~40–50% as compared with >65% in cosmic and KT spinels). Aluminian chromite with similar composition to those found in spherule layer of unit 1 at Mimbral exist in terrestrial basalt. Moreover, these chromites are observed in sediments far below (Mendez marls) and above (Velasco marls) the spherule layer at Mimbral. Magnetite and titanomagnetite are also abundant, but show a marked decrease in their concentration above the spherule layer.

The absence of Ni-rich spinels in KT boundary sediments at El Mimbral could be due to uneven geographical distribution. These minerals are less uniformly distributed on the surface of the Earth than Ir and some sections known to be complete (e.g., Nye Kløv, Denmark) do not have Ni-rich spinels. At Mimbral, however, the basal Tertiary layer ("cosmic fallout layer") is probably missing similar to the Brazos sections (*Beeson et al.*, 1994). The low concentration and integrated flux of Ir (<0.8 ng/g) at El Mimbral as compared with typical KT boundary values of 4–18 ng/g support the hypothesis of an incomplete record of the KT event at El Mimbral.

Bioturbation: Trace Fossils

Bioturbation marks, including feeding tracks and burrows of *Chondrites*, *Zoophycos*, and Y-shaped *Thalassinoides*-like structures, are commonly present in the rippled sandy limestone at the top of unit 3. The burrows and feeding tracks are found in at least two distinct layers at the top and within the rippled sandy limestone. They are infilled with the same tan-colored sediment of the host sandy limestone, and show no traces of the overlying grey shale of the Tertiary Velasco Formation or of Tertiary planktic foraminifera. Furthermore, in two sections at La Lajilla and El Mulatto a marly calcareous layer of the Mendez Formation with abundant Maastrichtian planktic foraminifera of the *A. mayaroensis* zone (including the index taxon) is present. This indicates that normal Maastrichtian sedimentation resumed for a short time after deposition of the clastic deposit and after bioturbation of the sandy limestone layer at the top of unit 3 of the clastic deposit. Thus, burrowing is not postdepositional and of Tertiary origin as suggested by *Smit et al.* (this volume). Moreover, no similar burrows are present in the Tertiary Velasco Formation. The burrowing in the rippled sandy limestone layers thus indicates the presence of living benthic communities at the time of deposition and excludes the possibility that deposition occurred by means of a tsunami wave during a period of hours or days.

Burrows of *Chondrites* are most common in all sections. They are easily recognized by their plantlike dentritic patterns of small cylindrical ramifying tunnels. These structures are generally regarded as feeding tracks of detritus-feeding organisms that preferred oxygen-depleted sediments that are inhospitable to most other burrowers (Figs. 57, 58, and 69).

Zoophycos burrows are also common at La Sierrita, El Mulato, and El Peñon. These organisms produced complex spreiten structures by reworking the sediments into a series of closely spaced lunate to Y-shaped patterns (Figs. 59 and 71). The outline varies considerably, but is often lobate or tonguelike. Like *Chondrites*, *Zoophycos* are considered opportunists that usually thrive in organic-rich and oxygen-poor sediments of outer neritic to upper bathyal environments.

Horizontal networks of *Thalassinoides*-like burrows are found at El Peñon, El Mulato, La Sierrita, and La Lajilla. The tubelike structures are smooth-walled, about 1 cm in diameter and show the Y-shaped bifurcations characteristic of *Thalassinoides* (Figs. 57 and 70). These Y-shaped bifurcations distinguish *Thalassinoides* burrows from otherwise similar burrows by *Planolites*. *Thalassinoides* burrows are generally regarded as dwelling structures of callianassid crustaceans (crabs).

Horizontal *Ophiomorpha* networks and unknown vertical burrows with diagonal sidebranches (Figs. 84 and 85) were recognized only near the top of the Los Ramones section underlying a thin

microconglomerate. The *Ophiomorpha* burrows form horizontal Y-shaped branching systems of cylindrical tubes 1.0–1.5 cm in diameter. Characteristic of this genus are the distinctly mammilated exterior surfaces of the burrows due to the presence of pelleted grains. *Ophiomorpha* is regarded as an indicator of littoral to inner neritic environments. Like *Thalassinoides*, they are callianassid crustaceans.

NEAR-KT-BOUNDARY CLASTIC DEPOSITS IN NORTHEASTERN MEXICO: NORMAL NOT CATASTROPHIC SEDIMENTARY PROCESSES

Cretaceous-Tertiary (KT) boundary sections in northeastern Mexico are characterized by thick clastic deposits of uppermost Maastrichtian age. In some sections, the clastic deposit directly underlies lowermost Tertiary sediments of the Velasco Formation, as for instance at El Mimbral. But in other sections a thin layer of Maastrichtian marls of the Mendez Formation tops the clastic deposit and underlies the basal Tertiary Velasco Formation, such as at La Lajilla and El Mulato (Lopez-Oliva and Keller, in preparation). Moreover, bioturbation in the topmost clastic sediment (rippled sandy limestone) is of Maastrichtian, not Tertiary, origin. This is indicated by the consistent absence of burrowing across the KT boundary and the absence of Tertiary gray shale and Tertiary foraminifera within the tan-colored burrows of the Maastrichtian clastic deposit. For these reasons, the age of the clastic deposit predates the KT boundary by at least several thousand years.

Of the more than a dozen outcrops discovered so far over a distance of >300 km, all trend in a north-northwest/south-southeast direction and are located 40–70 km east of the Sierra Madre Oriental mountain ranges (Fig. 3). This alignment of outcrops and constant distance from mountain ranges is not accidental, but is determined by the availability of terrigenous and near-shore sediments to the west and north and the distance of travel. There is no source of shallow-water clastic sediments eastward toward the Gulf of Mexico (Figs. 1 and 2).

All clastic deposits, spanning a distance over 300 km, are similar in their lithology, mineralogy, petrology, and microfossils. Similarities are such that not only individual lithological units and subunits can be correlated, but even thin layers of zeolites (indicating volcanogenic influx) and hemipelagic sedimentation (*Stinnesbeck et al.*, 1993; see also Mineralogical Correlations section). Such systematic similarity and correlatability of clastic deposits, down to the presence of zeolite-enriched layers, cannot be explained by an impact-generated tsunami wave deposit or a turbidite deposit. We propose that these sediments were deposited by normal, rather than catastrophic, sedimentary processes over an interval of many thousands of years.

Unit 1

The clastic deposit can be subdivided into three units. Basal unit 1 consists of a poorly-cemented glauconite and spherule-rich layer that disconformably overlies the Mendez Formation (Fig. 10). Within this layer is a highly resistant 20–25-cm-thick sandy limestone that is present in outcrops spanning over 200 km. This sandy limestone contains relatively few but graded spherules and convolute bedding that is draped by the overlying spherule-rich sediments (Figs. 13, 15, and 16). At Mimbral near meter mark 36, the sandy limestone is in contact with the overlying massive sandstone of unit 2 that also drapes around it (Fig. 15). This indicates that the sandy limestone layer was at least semilithified prior to deposition of the spherule-rich sediments above it, and also prior to deposition of the sandstone of unit 2. Thus, deposition of unit 1 occurred over a long time and not in a matter of hours as suggested by *Smit et al.* (1992, this volume) or *Bohor and Betterton* (1993) and *Bohor* (this volume). Moreover, the sandy limestone is not the result of local fusion of soft Mendez marl clasts as suggested by *Smit et al.* (this volume), since it is lithologically very different from Mendez marls, which contain no glauconite, whereas unit 1 and the sandy limestone layer are rich in glauconite and can be traced over 200 km (Fig. 95a).

Spherules: Within the spherule-rich unit 1, as well as at the base of unit 2, are numerous mudclasts of varying sizes, some of which are of upper Maastrichtian age (*A. mayaroensis* zone) and others of which are of Turonian to Campanian age (*Stinnesbeck et al.*, 1993; *Keller et al.*, 1994). These indicate transport from various distant sources to the north and west. The spherules of unit 1 are of multiple origins, including abundant organic spherules, which have thin organic coatings and calcite infillings. These

appear to be agal resting cysts (*Tasmanites* ?) that are commonly found in near-KT-boundary deposits (*Hansen et al.*, 1986). They are generally considered "disaster" species able to thrive under adverse conditions (*Tappan*, 1980). Many spherules formed around small limestone clasts or foraminiferal tests that are often infilled with glauconite (Figs. 19 and 20); these (oolites) generally form in shallow glauconite-rich environments. Commonly, spherules are large (up to 5 mm in size). These usually consist of a composite of smaller spherules (Fig. 17) and are surrounded or partly filled by mixed layers (illite/smectite, chlorite, or mica, *Stinnesbeck et al.*, 1993). They probably also formed in a shallow high-energy environment. Some spherules contain opaque crystals (rutile?, Fig. 18) and apatite concretions. No glassy spherules or glassy interiors of spherules were observed in acid residues of several kilograms of spherule-rich sediment. The multiple origins and their most common formation in a shallow neritic environment contradicts a tektite origin for these spherules and deposition via airborne impact ejecta as suggested by *Smit et al.* (1992, this volume), or a subsequent gravity flow of predominantly impact ejecta as suggested by *Bohor and Betterton* (1993) and *Bohor* (this volume). We propose that sediment transport from shallow water occurred over a significantly long time (long enough for sandy limestone to form) via channel systems during a sea-level lowstand and intensified currents. Disconformities and sediment scour occurred within the channels at the base of unit 1, in the upper part of unit 1 (absence of spherule-rich sediments above sandy limestone at Lajilla and Peñon II) and at the contact with unit 2.

Impact evidence: It is unclear at this time whether any impact evidence is present in unit 1. Glass shards are extremely rare (~1 particle per 200-g sediment). They are vesicular, yellow-amber, brown, green, red, and very rarely black (Fig. 23). Their compositions are very similar to Haiti glasses although many are hydrated (weathered?) (*Bohor and Betterton*, 1993; *Stinnesbeck et al.*, 1993; this volume). Haiti glasses have been variously interpreted as of impact origin (*Izett*, 1991; *Sigurdsson et al.*, 1991; *Blum and Chamberlain*, 1992) and of volcanic origin (*Jéhanno et al.*, 1992; *Lyons and Officer*, 1992). These disagreements in interpretation seem to stem largely from the lack of a broad database that could statistically define impact and volcanic origins. If the Mimbral glass is determined to be of impact origin, it will predate the KT boundary, perhaps necessitating a multiple-impact scenario.

Unit 2

The massive laminated sandstone of unit 2 is mineralogically distinct from units 1 and 3 and indicates an increase in the detrital influx and probably more rapid deposition. The most interesting feature of unit 2 at El Mimbral is the presence of distinct layers of leaf and wood debris at the base. Very small fragments of wood debris can be found throughout the sandstone of unit 2 and occasionally in sandy layers of unit 3. However, the abundance and large size of plant debris at the base of unit 2 is unique and has not been observed in any of the other sections. *Smit et al.* (1992, this volume) interpret the large plant debris as transported from coastal region by the tsunami wave and the small fragments as evidence of combustion by a gigantic wildfire. These interpretations are not supported by the available evidence. Small wood fragments are commonly present in any predominantly detrital sediments and are not restricted to KT boundary deposits. The abundance of large plant debris at the base of unit 2 at El Mimbral suggests a major detrital influx from the coastal region. However, it does not support deposition of unit 2 by a tsunami wave or a single turbidite deposit (*Bohor and Betterton*, 1993; *Bohor*, this volume), because wood and leaves, being lighter than sand, should settle out at the top and not at the bottom of unit 2. Since the plant debris (including leaves) is at the bottom, we suggest that deposition of unit 2 did not occur in a single event, and that the first detrital influx with plant debris was separated from the subsequent detrital influx by sufficient time to allow plant debris to settle.

Unit 3

Unit 3 disconformably overlies unit 2 and consists of alternating sand, silt, and shale layers topped by a rippled sandy limestone. Ripple marks, flaser bedding, convolute bedding, climbing ripples, and small-scale cross bedding are commonly found. Unit 3 is lithologically, mineralogically, and petrographically most variable and contains two distinct thin layers rich in zeolites (Figs. 96 and 97) and various layers rich in planktic foraminiferal assemblages that indicate periods of normal hemipelagic sedimentation and volcanogenic influx. The two zeolite-enriched layers have been found at Mimbral, Lajilla, Mulato, and

Peñon and thus represent widespread and correlatable volcanic events (Fig. 97; Adatte et al., in preparation).

The rippled sandy limestone at the top of unit 3 is bioturbated in all outcrops. Burrows of *Chondrites*, *Zoophycos*, and *Thalassinoides*-like structures are commonly found in at least two discrete levels and burrowing is restricted to the clastic deposit with no evidence of burrowing downward from the basal Tertiary shale or clay. If postdepositional burrowing occurred, as suggested by *Smit et al.* (this volume), then there should be downward mixing of the gray Tertiary sediments and Tertiary foraminifera into the tan-colored clastic deposit. This is not the case at any of the outcrops. Moreover, in two sections (Lajilla and Mulato) a thin layer of Maastrichtian marl overlies the burrowed top of the clastic deposit, indicating that normal hemipelagic sedimentation resumed after deposition of the bioturbated sandy rippled limestone prior to the KT boundary. Contrary to *Smit et al.* (1992, this volume) and *Bohor* (this volume), we found no evidence of glass, Ni-rich spinels, or Ir enrichment in unit 3 (*Stinnesbeck et al.*, 1993). (See also discussion on Ir and Ni-rich spinels, and Fig. 99.)

Deposition of unit 3 probably occurred over tens of thousands of years with times of high detrital influx (sands) alternating with times of more normal hemipelagic deposition. Two enriched layers of zeolites in unit 3 and in the boundary clay indicate a significant volcanogenic influx during these times. Deposition of the rippled sandy limestone at the top of the clastic deposit occurred slowly enough to permit a thriving benthic community to exist.

DISCUSSION

The channelized near-KT-boundary clastic deposits of northeastern Mexico are deposited over a geologically extended time period, rather than hours or days, and by normal sedimentary processes that include debris flows, gravity flows, and turbidity currents, rather than by impact-generated tsunami wave. Major lines of evidence for this interpretation are: (1) lithologically and mineralogically distinct units and subunits that can be correlated over 200–300 km (Figs. 95 and 97)—such similarity and correlatability are not characteristics of tsunami deposits; (2) semilithification of sandy limestone within the spherule-rich unit 1 prior to deposition of the upper spherule-rich sediments and deposition of sandstone of unit 2 (Figs. 13 and 16a); (3) multiple origins of spherules, predominantly volcanic, organic, and oolitic, that formed in a shallow neritic and glauconite-rich environment (Figs. 19 and 20) with no evidence of glassy tektite spherules; (4) presence of plant debris in discrete horizons at the base of the sandstone of unit 2 that could not have settled within hours or days and would not have settled prior to coarse sand grains or in discrete layers, if deposition was due to tsunami wave(s); (5) two or more discrete thin layers enriched in zeolites correlatable over 200 km indicate at least two new volcanogenic sources during deposition of unit 3 (Figs. 96 and 98). (6) discrete thin layers of hemipelagic sedimentation in unit 3 with rich, unwinnowed foraminiferal assemblages; and (7) bioturbation that is of Maastrichtian, not Tertiary, origin, within at least two horizons in the rippled sandy limestone at the top of the clastic deposit. A Maastrichtian origin for bioturbation is also indicated by the presence of Mendez-type marls containing the *A. mayaroensis*-zone fauna overlying the burrowed sandy limestone layers at La Lajilla and El Mulatto.

Deposition of the clastic deposit occurred in a series of channel systems spreading south and east from the Sierra Madre Oriental (Fig. 3) as also indicated by the north-northwest/south-southeast alignment of all sections parallel to this mountain range. The sediment source area is to the north, west, or south where emergent areas of thick terrigenous and shallow water deposits of Maastrichtian age are found. For example, to the south-southeast is the Cardenas Formation on the Cd. Valles-San Luis Potosi platform that consists of 200–1100 m of shale, silt, sand, and bioclastic limestone (*Myers*, 1968). To the north-northwest is the Difunta Group in the Monterey-Saltillo area that consists of several thousand meters of deltaic and prodeltaic sands and silts (*Weidie et al.*, 1972). The latter appears to be the principle source area for at least the northernmost Los Ramones section and probably also for the other sections to the south. East and southeast, toward the Gulf of Mexico and Yucatan, only condensed pelagic carbonate sequences and calcareous platform sediments are present.

Clastic deposits in northeastern Mexico are related to the major eustatic sea-level lowstand near the end of the Maastrichtian (*Haq et al.*, 1987). At that time erosion, sediment bypass, and incised valleys formed on the shelf, canyons were cut into the slope, and submarine fan deposition occurred in the basins

(*Haq et al.*, 1987; *Donovan et al.*, 1988). The near-KT-boundary channelized clastic deposition of northeastern Mexico appears to be related to this sea-level lowstand. The top of the clastic deposit marks the end of the regressive cycle, which is followed by transgression and sediment starvation as also indicated by the bioturbation in the rippled sandy limestone of unit 3. The age of the northeastern Mexico clastic deposits indicates that the sea-level transgression began a few thousand years below the KT boundary as indicated by deposition of uppermost Maastrichtian marls above the top of the clastic deposit at La Lajilla and El Mulato. A similar latest Maastrichtian sea-level lowstand and clastic deposit followed by rising sea-levels across the KT boundary is found at Brazos, Texas (*Keller*, 1989; Beeson et al., in preparation). In the Danish KT boundary sections, sea-levels began to rise a few thousand years before the KT boundary and continued to rise into the earliest Tertiary (*Schmitz et al.*, 1992; *Keller et al.*, 1993b).

Our scenario for the clastic deposits in northeastern Mexico thus calls for normal depositional processes characteristic of fluvial transport, erosion, incised valleys, and canyons during times of sea-level lowstands. In northeastern Mexico, the clastic deposits coincide with the latest Maastrichtian sea-level lowstand and the sediment source area(s) appears to be primarily to the north-northwest (Difunta group). The different lithological units probably reflect successive stages in the regressive cycle beginning with erosion of sediments (unit 1) on the shelf. As the sea-level continues to drop, erosion of sandy sediments leads to the formation of incised valleys on the shelf and canyons on the slope (deposition of unit 2). The alternating sand and silt layers of unit 3 probably represent a prolonged period of low sea levels, which culminated in deposition of the rippled sandy limestone at the top of unit 3. Subsequently, sea levels transgressed in the latest Maastrichtian leading to sediment starvation and deposition of hemipelagic marls (at Lajilla and El Mulato). Continued transgression across the KT boundary led to deposition of the sediment-starved but organic-rich boundary clay observed worldwide. The KT boundary event coincides with this transgressive phase. Ir enrichment, shocked quartz, and Ni-rich spinels are frequently present at the base of the boundary clay. At Mimbral, only a small Ir-enrichment of 0.9 ppb is present, which suggests that the KT boundary is incomplete as also indicated by biostratigraphy.

Clastic channelized deposits such as those found in northeastern Mexico are not unique; they typically form at times of sea-level lowstands and are commonly found within the Maastrichtian Mendez Formation (good outcrops can be seen near the Linares cemetery).

TSUNAMI-GENERATED BEDS AT THE KT BOUNDARY IN NORTHEASTERN MEXICO

J. Smit, A. Montanari, and W. Alvarez

The KT boundary is marked worldwide by a (dispersed) few-millimeters-thick layer of clay, characterized by enrichment of siderophile elements, shocked minerals, microkrystite remains, and spherules with Ni-rich spinels. The clay is interpreted as the distal ejecta of the Chicxulub impact. However, the KT boundary around the Chicxulub structure itself is associated with unusual coarse-grained deposits (*Smit et al.*, 1992). These clastic deposits are the chronostratigraphic equivalent of the few millimeters of distal ejecta clay. Because of the complicated structure of the KT clastic deposits, we will group them together as the KT clastic complex.

Coarse-grained KT deposits were noticed already in the 1930s, but interpreted as shallow-water deposits, marking an unconformity between the Maastrichtian Mendez and Paleocene Velasco Formations (*Hay*, 1960; *Muir*, 1936). *Ganapathy et al.* (1981) noticed the clastic layer just below the KT Ir anomaly at Brazos River, but believed it was of upper Cretaceous age and did not further interpret it. *Smit and Romein* (1985) interpreted the Brazos clastic layer as a KT boundary turbidite or tsunami-generated deposit, indicating a nearby impact. *Bourgeois et al.* (1988) elaborated on the tsunami interpretation, and calculated high current velocities, at an estimated water depth where even hurricane storm waves cannot transport fine sand (50–100 m). Since then, the KT clastic complex has been studied in the classical Borrega Canyon-Arroyo de Mimbral section (*Smit et al.*, 1992) and many other KT outcrops in eastern Mexico (*Alvarez et al.*, 1992). Although the details may differ, the basic depositional sequence of the clastic complex is the same in all outcrops.

The clastic complex can be subdivided into three units (*Smit et al.*, 1992): (1) The basal unit 1 contains ejecta and local rip-up clasts, but little quartz sand; (2) unit 2 is a stack of channels of sands derived from near-shore areas displaying a great variety of sedimentary structures providing evidence for strong, periodic, bidirectional currents; and (3) the top unit III consists of thinning upward, fine sandstone current ripples alternating with silt drapes, containing anomalous Ir and Ni-rich spinels. The top ripples are burrowed, but the burrows postdate the deposition of the clastic complex. The deposition of the entire clastic complex probably took place in a few days at most.

ARROYO DE MIMBRAL

The KT clastic complex crops out in the southbank of the Arroyo de Mimbral, some 4.5 km east of the electric power lines 35 m of well bedded upper Maastrichtian, *A. mayaroensis*-zone Mendez marls are exposed below the clastic complex. The entire outcrop is depicted in Fig. 100. Unit 1 is deposited in four shallow channels along the outcrop, maximum 1.2 m thick. The axis of the deepest, best-exposed, middle channel strikes north-south, and is laterally infilled from the west. The lateral aggradational layers are composed of a variable mixture of reworked bubbly spherules, some with impact glass interiors, small limestone clast ejecta, winnowed foraminifera, and very soft plastically deformed Mendez rip-up clasts, derived from local seafloor oozes. The aggradational layers are included to up to 15° with respect to the overlying layers, giving the false impression of an angular unconformity at the west side of the channel (*Hay*, 1960). In the layers where the soft Mendez clasts dominate they are fused together and those layers seemingly form "continuous" layers leading to the wrong impression of moral hemipelagic sedimentation alternating with coarse-grained layers. This impression has led to estimates of sedimentation of the clastic complex of tens of thousands of years (*Lyons et al.*, 1992). The soft oozes of the local seafloor could not bear the weight of the rapidly accumulating unit 1 channel fill, and were squeezed away, creating diapirlike structures between the channels. The sand layers near the channel walls were dragged along and are oversteepened, even overturned by this diapiric movement. The best example of this "loading diapirism" can be observed at Rancho Nuevo. Current velocities involved in deposition of unit 1 are obviously very high, based on the upper flow-regime parallel beds, antidune and low-angle mega cross stratification. Unit 1 shows few adequate current direction indicators, but the direction of lateral aggradation suggest infill by both backwash and upwash sages of the first tsunami waves.

Unit 2 is made up of at least five fining upward, stacked, thinning upward channels. Often the higher channels erode into the lower ones. Unit 2 differs petrographically and texturally from unit 1. In unit 1 detrital quartz grains are rare, and the sand fraction is made up of foraminifers and small ejecta. The amount of detrital sand increases suddenly at the base of unit 2 and further increases upward. The impact spherule remains are found almost exclusively in unit 1, although a few are reworked into the base of unit 2. The sediment of unit 2 is dominantly detrital sand and winnowed planktic foraminifera, with some shallow-water benthic foraminifer and sponges. If the clastic complex represented a set of debris flows or turbidites, the sand fraction in all sublayers should have the same composition, and that is not the case here. The axial part of the basal unit 2 channels contains large pieces of wood. Many of these wood fragments were bored, and were probably lying as water saturated bottom material in coastal "bayous," before they were transported onto the deeper shelf. Small charred plant fragments in the higher channels were transformed to "coke," indicating they might have been combusted at low O supply such as happens in really gigantic wildfires.

Unit 2 overlies unit 1 and the Mendez diapirs with a sharp contact. However, in the middle of the unit 1 channels, the transition is rapid, but gradual and nonerosive. The uppermost layers in unit 1 channels show changes leading up to unit 2. Detrital sand content increases, and the Mendez rip-up clasts are rounded and often armoured with a peppering of impact spherules. These armoured mudballs are eroded from deeper, more compacted Mendez beds. At meter level 29 in the outcrop an 80-cm armoured mudball occurs. Unit 2 is dominantly semiparallel bedded with primary current lineations in different orientations at different levels (75°–180°), low angle mega cross bedding, and flute-casts showing 120° and 350° current directions.

Unit 3 conformably overlies unit 2, where the first silt layer between thin current ripples appears. The first silt layer is also the first to be enriched in Ir. The ripples are current ripples, falsely resembling hummocky cross-stratification (*Lyons et al.*, 1992), but only on the rock face cut at right angles to the current direction. However, at a rock face parallel to the current, it is clear that the ripples are current ripples. The resemblance to hummocky cross stratification has led to erroneous storm-wave interpretations (*Lyons et al.*, 1992). The highest ripples underlie the basal Danian (P0) Velasco shales, still enriched in Ir as elsewhere. The topmost ripples are burrowed. Current directions are bidirectional, both upwash and backwash directions, but in between the arrival of individual waves, capable of transporting sand on the seafloor, silt was able to settle, and thus the time of deposition of unit 3 is longer than units 1 and 2 combined, but still cannot be longer than a few days.

LA LAJILLA

At La Lajilla the KT clastic complex outcrops at both sides of the overflow channel of the reservoir. The upper Mendez is fluidized due to loading of unit 1 channels, although not as extensive as at Mimbral. Impact spherules are "injected" into the fluidized Mendez. The beds of unit 2 are more continuous than at Mimbral, and units 2 and 3 show a wide variety of current ripple structures, which allow over 80 individual paleocurrent measurements (Fig. 101). The paleocurrent directions are clearly bidirectional, with the dominant directions away from and toward the Chicxulub Crater. These opposite current directions demonstrate that the sandstone layers are deposited from periodic bidirectional currents with a high suspension load (climbing ripples). The bidirectional currents are easiest to explain by landward-breaking wave surges alternating with the seaward return flow of successive large tsunami waves, not by debris-flows or turbidity currents. Gravity flows may have helped to transport clastic material from the coast, >70 km to the west, to the deeper basin, but are not directly involved in the deposition of the clastic complex. The general thinning and fining upward trend shows the decreasing energy of tsunami waves, and in the final stages current velocity decreases in between individual wave arrivals allowing the settling of fine silt and clay of unit 3.

EL PEÑON

El Peñon is the hilltop where the "flagstones" covering the dam of the Porvenir reservoir were quarried, mainly from the units 2 and 3 of the clastic complex. These units are therefore exposed over several acres, allowing investigation of the sedimentary structures at the surface of the clastic complex layers (Figs. 102 and 103).

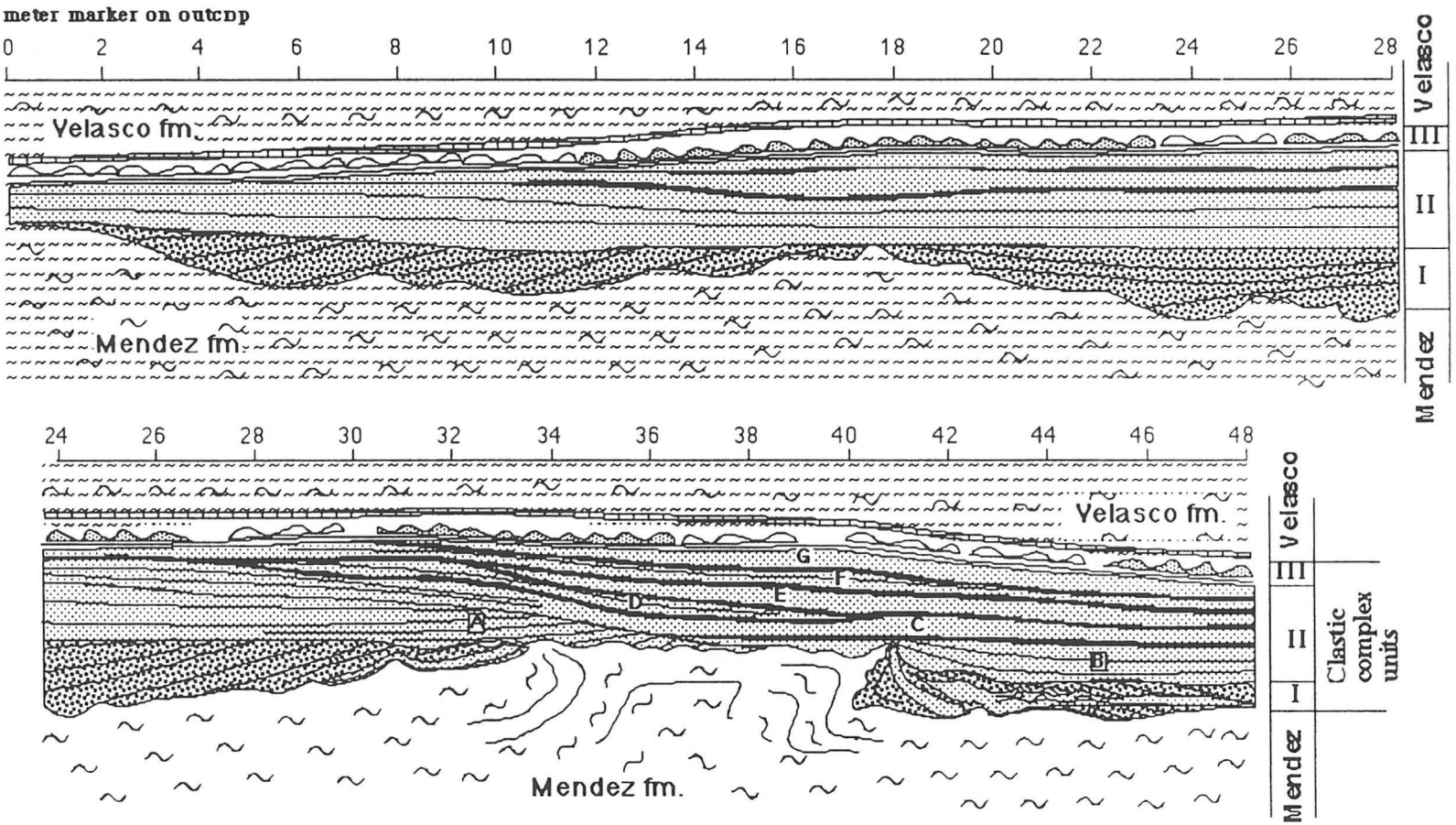

Fig. 100. *Simplified cross section through the Mimbral clastic complex outcrop. Numbers are meter markings painted along the outcrop. Subchannels of unit II are numbered A–G in stratigraphic sequence.*

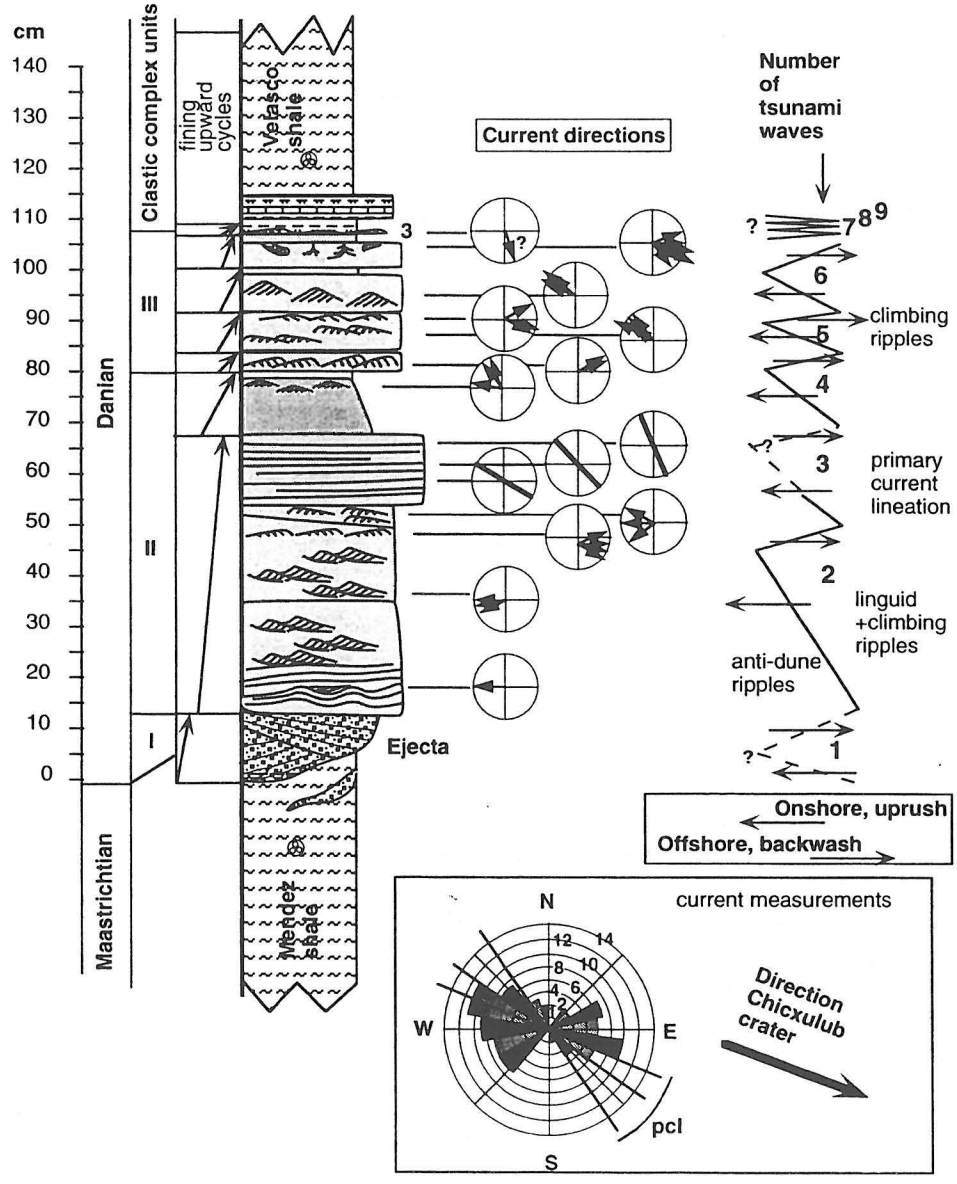

Fig. 101. *La Lajilla. Stratigraphic column and paleocurrents of the KT clastic complex. Current directions change 180° at least six times, indicating passage of six tsunami waves. The isolated ripple-layers in the top of unit III indicate three more tsunami waves, or the effects of the developing seiche. All paleocurrent directions are plotted in the pie diagram at the bottom. Arrow indicates the gradual change of the primary current lineations (=pcl) in the top of unit II.*

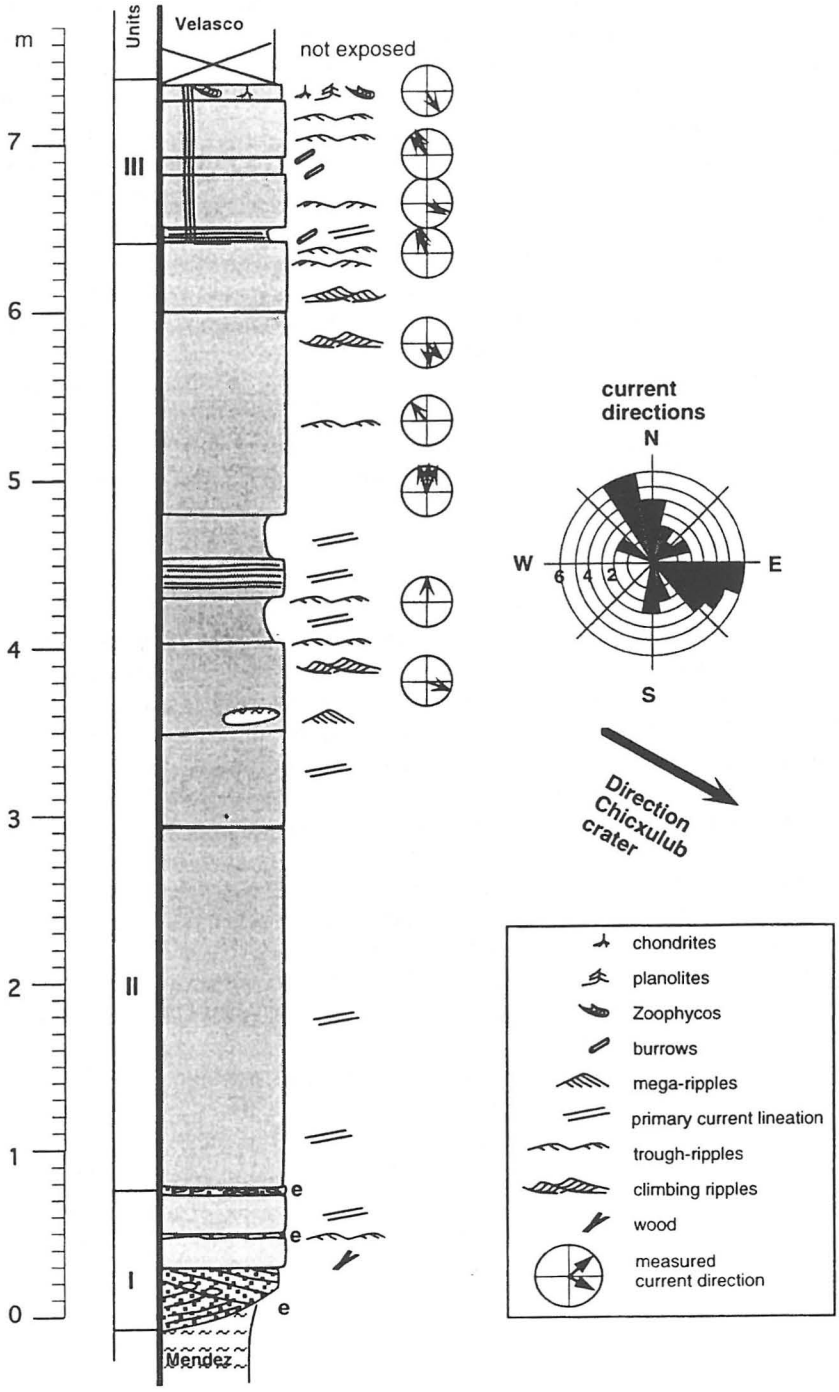

Fig. 102. *El Peñon, stratigraphic column through the clastic complex. Paleocurrent directions (n = ~75) are plotted on the righthand side. The top and contact with overlying Velasco shale is not exposed here. e = ejecta-rich layers.*

Like at Mimbral and Lajilla, current measurements demonstrate periodic bidirectional currents, indicative of breading tsunami-wave deposits.

El Peñon is important for the correct interpretation of the many burrow structures that occur on and in top of the KT clastic complex in almost every outcrop of the Gulf coast. Most burrows *(Zoophycos, Chondrites)* occur in the topmost sand layer only, and clearly penetrate from above *after* deposition of the clastic complex. However, an unknown type of burrow occurs up to 50 cm below the top of the clastic complex (Fig. 101). These burrows consist of 1-cm-diameter, up to 3-m-long, often branching, usually straight horizontal compressed tubes, and follow the thin silt layers in between unit 3 ripples. The horizontal tubes radiate from a central bundle of vertical burrows, with a greenish, calcite lining penetrating through sandstone layers. The burrowing animal is apparently capable of penetrating 50 cm down through sand layers, before spreading out horizontally in silt layers. Presumably these burrows also *postdate* the deposition of the clastic complex. We assume that similar burrows at the same position in the Brazos River KT clastic layer originate the same way, though we did not see the vertical central tubes. The basal 2.75 m of unit 2 at El Peñon are characterized by massive bedding, without any clear sedimentary structures except frequent water escape structures. A similar lack of sedimentary structures is also common in unit 2 of nearby KT outcrops Las Bruselas, Porvenir, Rancho Nuevo, La Sierrita, Loma las Rusias, and Los Ramones, showing that some characteristics are shared by KT outcrops in the same area, but are absent further south. The water escape structures indicate rapid deposition of the massive sand.

DISCUSSION

The KT clastic complex forms a coherent, amalgamated set of channelized beds, unique in the geological record. The consistent sequence of three different units, a basal unit with ejecta and local rip-up, followed by sands backwashed from coastal areas and deposited by bidirectional currents, topped by an alternation of thin silts and rippled sand layers enriched in Ir, are easiest to explain by a series of tsunami waves, originating from the Chicxulub impact. Estimates of deposition of the entire clastic complex are a few days, not tens of thousands of years as suggested by others (*Lyons et al.*, 1992; *Adatte et al.*, 1993).

However, this proposed origin has been questioned. *Bohor and Betterton* (1993) hypothesized an origin as debris flow/turbidite. Several observations are in conflict with this interpretation: The basal unit 1 is different in composition from the upper units 2 and 3 in the same size fraction. In turbidites this is not the case. Both turbidite and debris flow should display unidirectional paleocurrent directions, by necessity downslope, at most deviating by a few tens of degrees. Repeated 180° current direction changes, thus also in an upslope direction, are inconsistent with a turbidite origin.

Aggradational layers filling the basal channel have been interpreted as a normal sandy limestone (*Adatte et al.*, 1993) or as hemipelagic limestone layer (*Lyons et al.*, 1992). The sandy limestone would be lithified prior to deposition of unit 2, but the "sculpted" wave ripples supposedly in relief before deposition of the next layer are actually deformed convolute structures, as seen by internal laminations. The "hemipelagic layers" are actually layers of accumulated soft Mendez clasts fused together.

Erosional unconformities within the clastic complex, supposedly representing considerable time, are easily explained by erosion of the top of the lower deposits by currents generated by the next wave.

The burrows in (the top of) unit 3 have also been raised to support the hypothesis of more time in between deposition of the individual sandstone layers than just a few days, as suggested by a tsunami origin. At El Peñon, however, it can be shown that all the burrowing activity *postdates* the deposition of the clastic complex.

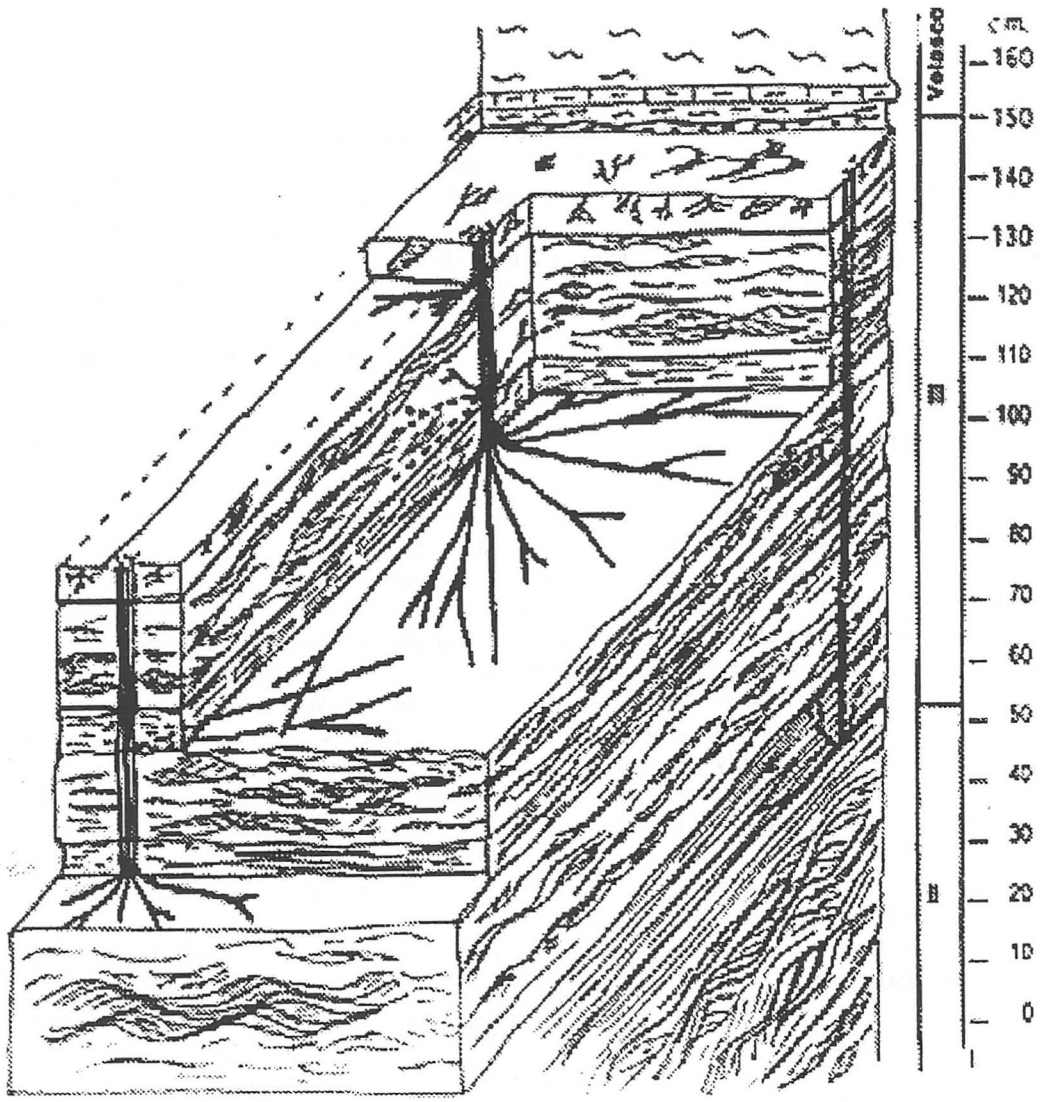

Fig. 103. Sketch of burrowing structures.

KT CLASTIC DEPOSITS, NORTHEASTERN MEXICO: SINGLE-PULSE DEBRIS FLOW/TURBIDITE UNITS ASSOCIATED WITH IMPACT

Bruce F. Bohor

Smit et al. (1992) reported that an outcrop of the KT boundary along the Arroyo el Mimbral, on the southwest flank of the Sierra de Tamaulipas, Mexico, contains a clastic unit containing impact ejecta (spherules). Later, *Alvarez et al.* (1992) discovered nine other outcrops at the KT boundary with similar clastic units in adjacent areas of northeastern Mexico. I visited the Arroyo el Mimbral (northwest of Tampico) and La Lajilla (east of Ciudad Victoria) sites in the state of Tamaulipas, Mexico, in late June 1992 in the company of W. Betterton, from U.S.G.S.-Denver, and H. Montgomery, E. Pessagno, J. Carter, and two graduate students, all from the University of Texas at Dallas. Because of limited time available, we spent only several hours at each site. These field observations are therefore somewhat generalized impressions; an in-depth study probably would have required more time per outcrop.

FIELD EXAMINATION

My first impression of the coarse clastic deposits in the Mimbral outcrop was that of a channelized unit intercalated within fine-grained, deepwater carbonates (marls). *Smit et al.* (1992) interpreted this clastic unit as being deposited by an impact megawave or tsunami at the ocean floor, but such a deposit almost certainly would not be channelized with an erosional base. Closer examination of both sites by our group revealed two separate clastic units: a calcite-cemented bed containing poorly sorted and graded spherules altered to clay, overlain by a massive, well-graded, laminated to rippled, siliceous sandstone unit. These two clastic units are well described and illustrated in both *Smit et al.* (1992) and *Stinnesbeck et al.* (1993), as well as in this guidebook. Both of these sets of authors designate the basal spherule-bearing bed as unit 1, and variably subdivide the overlying sandstone into units 2 and 3. However, I interpret the entire upper sandstone as a single sedimentation unit, and the inability of other workers to agree upon where to place supposed discontinuities for the purposes of subdivision tends to support my interpretation.

The lithology of the lower spherule-bearing bed (unit 1 of *Smit et al.*, 1992, and *Stinnesbeck et al.*, 1993) is quite different from that of the overlying sandstone bed. The spherule bed (up to 1 m in thickness near the center of the channel at Mimbral) is composed of poorly sorted, poorly graded, obliquely stratified, clay-rich (diagenetically altered) spherules up to 3 mm in diameter in a clay and carbonate matrix. Some of the altered spherules contain rare relict glass fragments similar in composition to the relict impact glass cores in the Haitian spherule beds (*Smit et al.*, 1992; *Bohor and Betterton*, 1993). Calcite is the cementing agent, and layers rich in clay (altered glass) spherules alternate with calcite-rich layers poor in spherules. Millimeter- to centimeter-sized clasts of Mendez marl are incorporated throughout this bed, as are upper Maastrichtian benthic foraminifers derived from sediments deposited in shallow neritic environments (*Keller et al.*, 1992; *Stinnesbeck et al.*, 1993). The base of the spherule bed is erosionally scoured into the underlying marl of the Mendez Formation, forming a low-relief submarine channel profile.

The overlying quartz-rich, normally graded sandstone (~3 m at Mimbral) appears massive near its lower contact with the spherule bed, becoming thinly laminated upward. Both *Smit et al.* (1992) and *Stinnesbeck et al.* (1993) described organic fragments (including wood and leaves) and mud clasts from near the base of this unit (their unit 2). *Smit et al.* (1992) called this unit a calcarenite, but it is really a quartzose sandstone cemented with calcite and containing foraminifers similar in age and type to those in the spherule bed. The massive to laminated sandstone slightly overlaps the channel scoured out by the underlying spherules. Above the massive sandstone, wavy-bedded and rippled laminae of sandstone and siltstone grade upward into alternating thin siltstone and clay layers, and finally to hemipelagic marlstone at the top of the unit.

These other two sets of investigators divided the sandstone bed into two separate units. *Smit et al.* (1992) placed the division at the base of the uppermost "ripple beds"; *Stinnesbeck et al.* (1993) marked the unit boundary somewhat lower, at a supposed disconformity between the underlying massive (lami-

nated) sandstone of their unit 2 and the laminated and wavy cross-bedded sandstone alternating with thin siltstone and claystone layers of their unit 3. Neither of these other authors' subdivisions of this sandstone unit seems justified sedimentologically. Both sets of previous authors also found an Ir anomaly (~0.8–0.9 ppb) in a clay-rich zone at the top of or just above their unit 3.

DISCUSSION OF PROPOSED ORIGINS

Smit et al. (1992) stated that this clastic unit was deposited by a tsunami or impact megawave operating at a depth of more than 400 m, even though they admit that the KT bolide could not have generated such an enormous wave by impacting a shallow carbonate shelf in northern Yucatan. These authors considered the possibility of a turbidity current origin for this clastic body, but rejected it in part because (1) it is unique in the exposed Mendez strata, (2) they didn't find any Bouma sequences in it, (3) there is a strong contrast in lithologies between the locally derived intraclasts and ejecta products of the spherule bed, and (4) the far-transported sands and wood fragments with borings in the sandstone unit indicate a shallower-water origin. I would answer these objections to a turbidite origin thus:

1. This clastic lithology is unique in the underlying exposed Mendez strata at Mimbral because it is a single-pulse channelized event caused by the KT impact, and not part of a series of sheet-flow pulses normally encountered in deep marine fan turbidite sequences.

2. The upper sandstone bed strongly resembles a modified Bouma turbidite sequence. This can be shown by comparison of units 2 and 3 with an idealized Bouma sequence (Ta-e) from *Howell and Normark* (1982) shown in Fig. 105. Almost every division in this idealized sequence has a corresponding textural and lithological component in the sandstone unit at Mimbral. Thus, it would be difficult to consider the sandstone unit anything but a modified single-pulse turbidite.

3. The spherule bed also contains foraminiferal evidence of derivation from a far-removed neritic shelf environment (*Keller et al.*, 1992); the Mendez marl intraclasts may be locally derived, but this is common during channelization by debris flows.

4. Wood fragments with borings indicate that the wood debris was waterlogged prior to redeposition in the sandstone unit. Tsunami waves would backwash new wood off the shoreline and therefore should not provide waterlogged and bored (Teredolites?) wood to these deep basinal clastic deposits; new wood recently swept off of coastal land surfaces would float. Turbidites commonly contain bored wood debris and other organic fragments that were derived from estuaries.

Smit et al. (1992) recognized that the spherules in the basal bed are impact ejecta, but proposed that they represent primary deposition of this ejecta in place without any significant redeposition, except for local reworking of seafloor sediment into the spherule bed by a megawave. Left unexplained by these authors is why no spherules exist on the coeval Mendez seafloor surface outside of these channelized units, and why this supposed locally derived spherule bed in this deep basinal setting also contains benthic fossils from a shallow neritic environment.

Conversely, *Stinnesbeck et al.* (1993) rejected any influence of impact waves and postulated deposition of these clastics, derived from distant shallow shelf environments, in incised valleys occurring at relatively shallow depths over an extended period of time. Unaccountably, no modes of transport or deposition were proposed by these authors, and the term turbidite was never once mentioned in their paper. The reader is left to wonder what process incised these valleys out in the basin and how these shelf sediments were transported to their final resting place among the deep-water Mendez marls. *Stinnesbeck et al.* (1993) found no Ni-rich spinels (magnesioferrite), shocked quartz, glassy spherules, or any other impact signatures anywhere in these clastic units, although they don't attempt to explain the origin of the Ir anomaly at the top of their unit 3. The rare glass shards that they did find in the spherule bed were explained as volcanic glass derived from an event preceding the KT boundary event. I would make these comments on their study:

1. A flaw in their argument is the failure to propose a mechanism for emplacement of this clastic unit into this otherwise deepwater, fine-grained carbonate sediment (Mendez marl). There seem to be only two ways to accomplish this: turbiditic/debris flows or tsunamis. They had already rejected tsunamis as a causal agent, they did not mentioned turbid flow as a possible mechanism.

2. The spherule bed definitely contains impact ejecta in the form of altered impact glass spherules, some with relict glass cores. The clay layer above their unit 3 not only contains an Ir anomaly, but we

have also found rare Ni-rich spinels characteristic of impact occurring there. I interpret this layer above the sandstone unit as representing a partial fireball layer deposited in place, while the spherule bed represents allochthonous melt ejecta layer (*Bohor and Betterton*, 1992). *Smit et al.* (1992) found shocked quartz grains in the spherule bed as well.

3. These authors only briefly mention a two-step mechanism similar to that proposed earlier for the Haiti KT boundary sequence, but these Mexican KT boundary clastic units differ significantly from those in Haiti both sedimentologically and lithologically. No explanation is given for these obvious differences, nor are they assessed in assigning a similar origin to both sequences.

4. An important finding of these authors is that of the shallow shelf neritic origin of both units of these clastic deposits, based on included benthic foraminifers. This means that these units are allochthonous, and have not been accumulated in place in a deep basinal setting by an impact wave.

TURBIDITE/DEBRIS FLOW ORIGIN

The Mimbral outcrop displays the cross section of a low-relief channel (or channels) scoured into upper Maastrichtian Mendez Formation marls by a single pulse of coarse clastics, transported by a combination of debris flow and turbidity flow regimes (*Bohor and Betterton*, 1993). At the La Lajilla outcrop northwest of Arroyo el Mimbral, these two clastic units are somewhat thinner and not as well displayed, but most of the sedimentary features described from Mimbral can be found on a slightly smaller scale at La Lajilla as well (see *Stinnesbeck et al.*, 1993, Fig. 106).

My interpretation of this clastic unit's origin differs significantly from those of both *Smit et al.* (1992) and *Stinnesbeck et al.* (1993) discussed above. I believe that the field evidence shows a turbidity current/debris flow genesis for these units, based on the following:

1. The sandstone unit at Mimbral almost matches an idealized Bouma turbidite sequence (Fig. 105), except for the basal portion of Ta; this subdivision is replaced by coarse spherules that were transported as a debris-flow unit. The quartzose sands making up the sandstone unit were derived from the continental shelf, based on included benthic forams, and were transported down the slope and into the basin in turbulent suspension. Depending on the distance of the channelized deposit from the shelf-slope environment (proximal, middle, or distal), local modifications due to channel avulsion, etc., the idealized complete Bouma sequence may be truncated or otherwise modified at any particular outcrop. The trend of channel axes of the 10 clastic deposits at the KT boundary discovered so far is north-northwest/south-southeast, away from the known Late Cretaceous shelf and into the Mendez basin (*Stinnesbeck et al.*, 1993). Current directional indicators should predominantly reflect this direction of transport, with occasional anomalies due to the influence of bottom currents.

2. The basal spherule-bearing bed at Mimbral is composed of altered impact ejecta (spherules) that was deposited originally on the continental shelf, based on included forams. Restriction of deposition to the shelf locale implies possible raylike distribution of ejecta from the impact crater. Like the sands composing the upper sandstone unit, the spherules were also mobilized and transported down slope and out across the basin. The spherules now occupy the basal position because, although they were originally deposited on top of the sands on the shelf, they assumed a basal position during mobilization and transport. These large spherules were solid glass at time of deposition, so they rapidly migrated via a sieve mechanism to the bottom of the flow unit because of size and density differences with co-mobilized sands and silts. The larger spherules moved down the slope canyons in the form of a debris flow, changing to a laminar slurry flow regime further out into the basin (*Howell and Normark*, 1982). This debris flow generated turbidity currents that suspended the less-dense shelf sands and silts above and behind it, as has been shown to occur experimentally by *Hampton* (1972).

3. The basal debris flow unit scoured into the soft Mendez marls out in the basin, forming shallow channels now filled with altered spherules and rip-up clasts of Mendez marl. The presence of relatively soft marl clasts within the spherule bed suggests that this unit was emplaced by a nonturbulent, debris flow regime (cf. *Nelson et al.*, 1992), rather than a turbulent current.

4. The quartzose sandstones, siltstones, and claystones forming the upper unit rest disconformably on the spherule bed. The entire normally graded sandstone unit fines upward. A disconformity occurs between the spherule bed and the sandstone unit because of differences in flow regimes and sediment

densities. The shelf sands in turbulent suspension followed along the same courses scoured out by the spherule-bearing debris flow unit, overlapping the channel boundaries slightly on both sides.

5. This model is somewhat similar to observed chaotic silt and sand lobes transported as channelized flows (both debris flows and turbidity currents) more than 600 km across the floor of the Gulf of Mexico during the Pleistocene (*Nelson et al.*, 1992), except for the grain size of the basal unit. Figure 106, from *Nelson et al.* (1992), shows a generalized diagram of these channelized flow units. The spherule bed at Mimbral would be equivalent in position to the chaotic silt unit in this Pleistocene example, and both this more recent example and the Mimbral section show a turbidite-like sand unit overlying and overspreading the channel previously scoured by a basal debris flow unit. However, due to the unique nature of the KT event that instantly loaded a substantial thickness of glass spherules onto preexisting shelf sands and silts and then mobilized the whole unstable mass into debris/turbidity flows because of some impact-related event, the resulting clastic units will not exactly resemble any other deposits resulting from normal flow mechanisms down submarine slopes and canyons.

6. The triggering mechanism initiating the debris and turbidity flows up on the shelf could be either tsunami(s), Earth tremors, or storm waves, all closely associated with formation of the KT impact crater on the Yucatan peninsula to the south.

7. Overlying the uppermost layer of the sandstone turbidite-like unit is a clayey layer containing an Ir anomaly and Ni-rich magnesioferrite spinel crystals, identifying it as the KT fireball layer (or at least a part of this layer). Thus, these flow units were emplaced after the impact distributed the spherules of the melt ejecta layer via an ejecta curtain, and before the fireball layer finished settling through the atmosphere and water column. This scenario conforms with the single-impact, dual-dispersion-mode model of *Bohor and Betterton* (1992), and suggests that this entire clastic unit was deposited in a matter of hours to days after impact of the KT bolide.

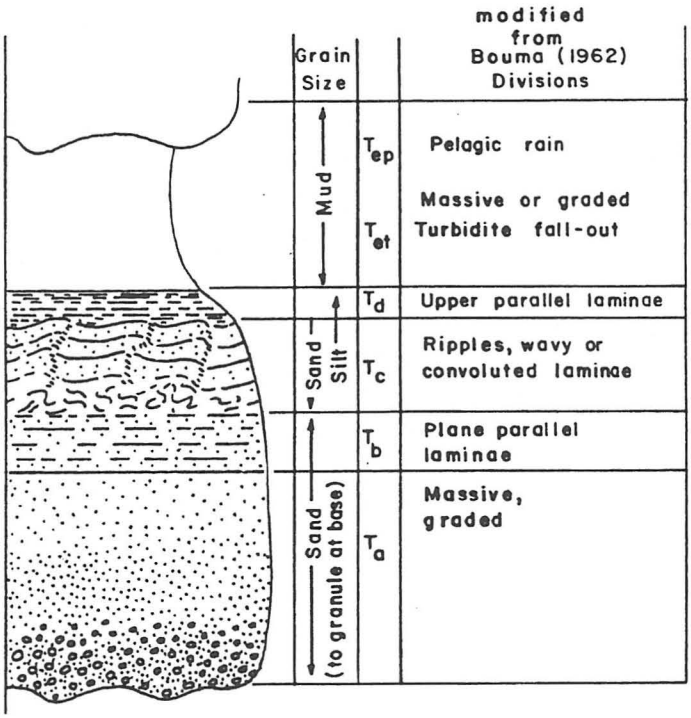

Fig. 104. *Idealized complete Ta-Te Bouma sequence, showing turbidite and hemipelagic subdivisions for the Te unit. From Howell and Normark (1982). Compare with sections through the clastic sandstone unit at Arroyo el Mimbral shown in Smit et al. (1992).*

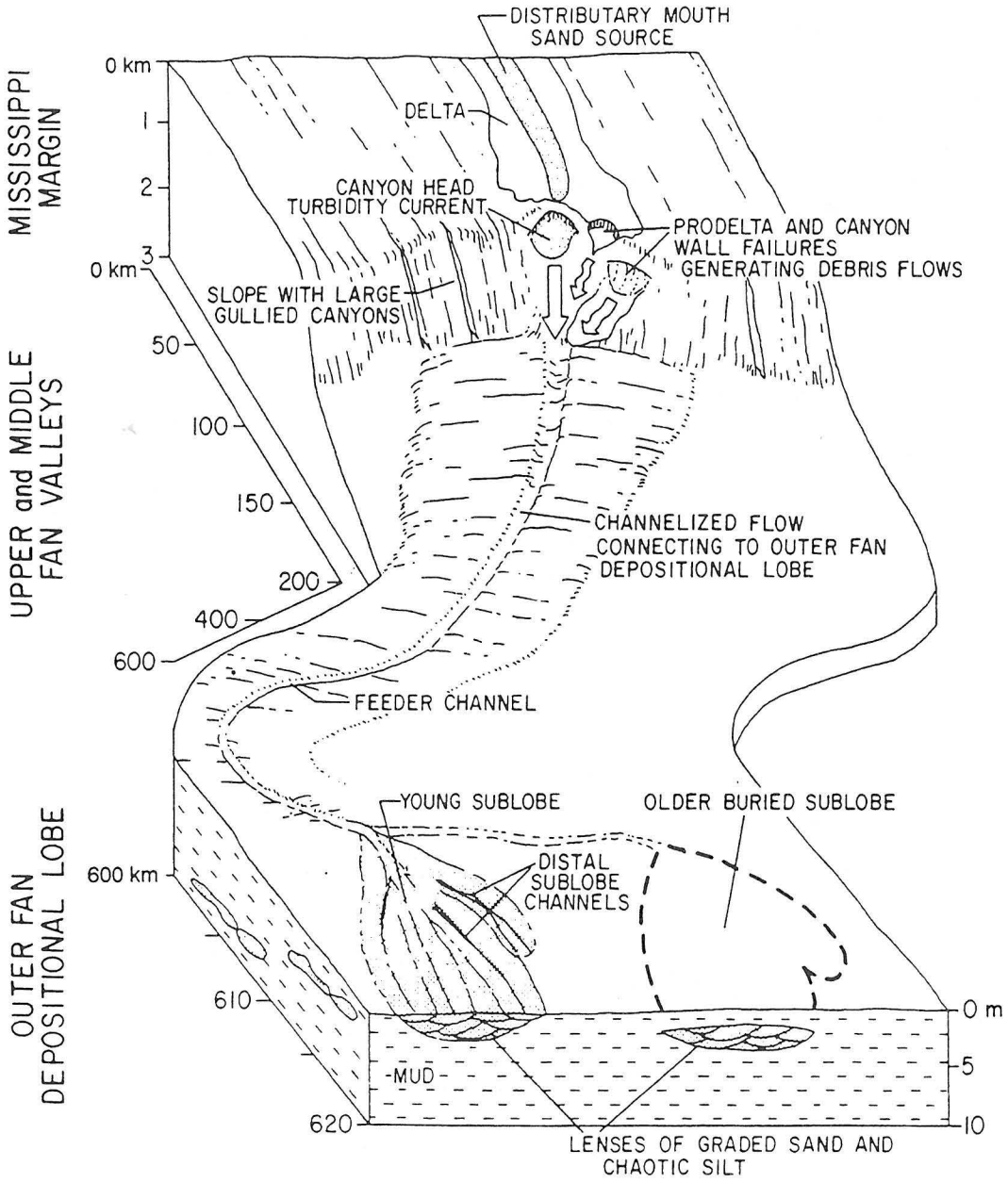

Fig. 105. *Conceptual diagram of feeder channel morphology and lithology of Pleistocene chaotic silt flows and accompanying turbidites on distal lobes of the Mississippi fan (from Nelson et al., 1992). Somewhat similar model is proposed here for origin of the KT boundary clastic units at Arroyo el Mimbral and La Lajilla, northeastern Mexico.*

REFERENCES

Adatte T., Keller G., and Stinnesbeck W. (1993) No evidence for KT boundary impact tsunami deposits and mass extinction in NE Mexico. *EUG VII*, Strasbourg.

Alvarez L. W., Alvarez W., Asaro F., and Michel H. (1980) Extraterrestrial cause for the Cretaceous-Tertiary extinction. *Science, 208*, 1095-1108.

Alvarez W., Smit J., Lowrie W., Asaro F., Margolis S. V., Claeys P., Kastner M., and Hildebrand A. (1992) The Cretaceous-Tertiary boundary impact-tsunami deposit in NE Mexico. *Geol. Soc. Am. Abstr. with Progr., 24*, A331.

Alvarez W., Smit J., Lowrie W., Asaro F., Margolis S. V., Claeys P., Kastner M., and Hildebrand A. R. (1992) Proximal impact deposits at the Cretaceous-Tertiary boundary in the Gulf of Mexico: A restudy of DSDP Leg 77 Sites 536 and 540. *Geology, 20*, 697-700.

Beeson D., Gartner S., Keller G., MacLeod N., Médus J., Rocchia R., and Robin E. (1994) Multidisciplinary stratigraphy and depositional environment across the Cretaceous-Tertiary Boundary at the Brazos River, Falls County, Texas. *Palaios*, in press.

Ben Abdelkader O. B. (1992) Planktonic foraminifera content of El Kef Cretaceous-Tertiary (KT) boundary type section (Tunisia). *International Workshop on Cretaceous-Tertiary Transitions (El Kef Section) Part I Abstracts*, p. 9. Geological Survey of Tunisia, Tunis.

Berggren W. A. and Miller K. G. (1988) Paleogene tropical planktic foraminiferal biostratigraphy and magnetobiochronology. *Micropaleontology, 34*, 362-380.

Blum J. D. and Chamberlain C. P. (1992) Oxygen isotope constraints on the origin of impact glasses from the Cretaceous-Tertiary boundary. *Science, 257*, 1104-1107.

Bohor B. F. and Betterton W. J. (1992) Ejection and dispersal mechanisms of the KT impact (abstract). In *Lunar and Planetary Science XXIII*, pp. 136-136. Lunar and Planetary Institute, Houston.

Bohor B. F. and Betterton W. J. (1993) Arroyo el Mimbral, Mexico, KT unit: Origin as debris flow/ turbidite, not a tsunami deposit (abstract). In *Lunar and Planetary Science XXIV*, pp. 143-144. Lunar and Planetary Institute, Houston.

Bouma A. H. (1962) *Sedimentology of Some Flysch Deposits.* Elsevier, Amsterdam. 168 pp.

Bourgeois J., Hansen T. A., Wiberg P. L., and Kauffman E. G. (1988) A tsunami deposit at the Cretaceous-Tertiary boundary in Texas. *Science, 241*, 567-570.

Canudo J. I., Keller G., and Molina E. (1991) Cretaceous/Tertiary boundary extinction pattern and faunal turnover at Agost and Caravaca, SE Spain. *Marine Micropaleontol.*, 17, 319-341.

Carter N. L. and Friedman M. (1965) Dynamic analysis of deformed quartz and calcite from the Dry Creek Ridge anticline, Montana. *Am. J. Sci., 263*, 747–785.

Donovan A. D., Baum G. R., Blechschmidt G. L., Loutit T. S., Pflum C. E., and Vail P. R. (1988) Sequence stratigraphic setting of the Cretaceous-Tertiary boundary in Central Alabama. In *Sea-Level Changes: An Integrated Approach* (C. K. Wilgus et al., eds.), pp. 300-307. SEPM Spec. Publ. No. 42.

Ferrero J. (1966) *Nouvelle méthode empirique pour le dosage des minéraux par diffraction.* R. X.-Rapport C. F. P., Bordeaux, France (inédit).

Galloway W. E., Bebout D. G., Fisher W. L., Dunlap J. B. Jr., Cabrera-Castro R., Lugo-Rivera J. E., and Scott T. M. (1991) Cenozoic. In *The Gulf of Mexico Basin: The Geology of North America, Vol. J* (A. Salvador, ed.), Geological Society of America, Boulder.

Gamper M. A. (1977) Acerca del limite Cretácico-Terciario en México. *Revista, 1*, 23-27. Universidad Nacional Autónoma de México, Instituto de Geologia.

Ganapathy R., Gartner S., and Jiang M.-J. (1981) Iridium anomaly at the Cretaceous-Tertiary boundary in Texas. *Earth Planet. Sci. Lett., 54*, 393-396.

Hampton M. A. (1972) The role of subaqueous debris flow in generating turbidity currents. *J. Sediment. Petrol., 42*, 775-793.

Hansen H. J., Gwozdz R., Bromley R. G., Rasmusseu K. L., Vogensen E. W., and Pedersen K. R. (1986) Cretaceous-Tertiary boundary spherules from Denmark, New Zealand, and Spain: Geological Society of Denmark, New Zealand, and Spain. *Geol. Soc. Denmark Bull., 35*, 75-82.

Haq B. U., Hardenbol J., and Vail P. R. (1987) Chronology of fluctuating sea levels since the Triassic. *Science, 235*, 1156-1166.

Hay W. W. (1960) The Cretaceous-Tertiary boundary in the Tampico Embayment, Mexico. *Proceedings of the Twenty-First International Geological Congress, Copenhagen, Part 5*, pp. 70-77.

Hildebrand A. R., Penfield G. T., Kring D. A., Pilkington M., Camargo Z. A., Jacobsen S. B., and Boynton W. V. (1991) Chicxulub crater: A possible Cretaceous-Tertiary boundary impact crater on the Yucatán Peninsula, Mexico. *Geology, 19*, 867-871.

Howell D. G. and Normark W. R. (1982) Sedimentology of submarine fans. In *Sandstone Depositional Environments* (P. A. Scholle and D. Spearing, eds.), pp. 365-404. American Association of Petroleum Geologists, Tulsa.

Izett G. A. (1991) Tektites in Cretaceous-Tertiary boundary rocks on Haiti and their bearing on the Alvarez impact extinction hypothesis. *J. Geophys. Res., 94*, 20879–20905.

Izett G. A., Maurrasse F. J. M. R., Lichte F. E., Meeker G. P., and Bates R. (1990) Tektites in Cretaceous-Tertiary boundary rocks on Haiti. *U. S. Geol. Surv. Open-File Rept. 90-635*, pp. 1-31.

Jéhanno C., Boclet D., Froget L., Lambert B., Robin E., Rocchia R., and Turpin L. (1992) The Cretaceous-Tertiary boundary at Beloc, Haiti: No evidence for an impact in the Caribbean area. *Earth Planet. Sci. Lett., 109*, 229-241.

Jiang M. J. and Gartner S. (1986) Calcareous nannofossil succession across the Cretaceous/Tertiary boundary in east-central Texas. *Micropaleontol., 32*, 232-255.

Keller G. (1988) Extinction, survivorship and evolution of planktic foraminifera across the Cretaceous/Tertiary boundary at El Kef, Tunisia. *Marine Micropaleontol., 13*, 239-263.

Keller G. (1989a) Extended period of extinctions across the Cretaceous/Tertiary boundary in planktic foraminifera of continental shelf sections: Implications for impact and volcanism theories. *Geol. Soc. Am. Bull., 101*, 1408-1419.

Keller G. (1989b) Extended Cretaceous-Tertiary boundary extinctions and delayed populational change in planktic Foraminifera from Brazos River, Texas. *Paleoceanogr., 4*, 287-332.

Keller G. (1993) The Cretaceous-Tertiary boundary transition in the Antarctic Ocean and its global implications. *Marine Micropaleontol., 21*, 1-45.

Keller G. and Lindinger M. (1989) Stable isotope, TOC and $CaCO_3$ records across the Cretaceous/Tertiary boundary at El Kef, Tunisia. *Paleogeogr., Paleoclimatol., Paleoecol., 73*, 243-265.

Keller G. and Benjamini C. (1991) Paleoenvironment of the eastern Tethys in the Early Paleocene. *Palaios, 6*, 439-464.

Keller G., Stinnesbeck W., and Lopez J. G. (1992) The Cretaceous/Tertiary boundary at Arroyo el Mimbral, NE Mexico: One or two events? *Geol. Soc. Am. Abstr. with Progr., 24*, A332.

Keller G., MacLeod N., Lyons J. B., and Officer C. B. (1993a) Is there evidence for Cretaceous-Tertiary boundary-age deep water deposits in the Caribbean and Gulf of Mexico? *Geology, 21*, 776-780.

Keller G., Barrera E., Schmitz B., and Mattson E. (1993b) Gradual mass extinction, species survivorship and long-term environmental changes across the Cretaceous-Tertiary Boundary in high latitudes. *Geol. Soc. Am. Bull., 105*, 979-997.

Keller G., Stinnesbeck W., and Lopez-Oliva J. G. (1994) Age, deposition and biotic effects of the Cretaceous/Tertiary boundary event at Mimbral, NE Mexico. *Palaios*, in press.

Kübler B. (1983) Dosage quantitatif des minéraux majeurs des roches sédimentaires par diffraction X. *Cahiers Inst. Géol. Neuchâtel, Suisse, série ADX*, 1.

Kübler B. (1987) Cristallinité de l'illite, méthodes normalisées de préparations, méthodes normalisées de mesures. *Cahiers Inst. Géol. Neuchâtel, Suisse, série ADX*.

Kuslys M. and Krähenbühl U. (1983) Noble metals in Cretaceous/Tertiary sediments from El Kef. *Radiochim. Acta, 34*, 139-141.

Liu G. and Olsson R. K. (1992) Evolutionary radiation of microperforate planktonic foraminifera following the KT mass extinction event. *J. Foram. Res., 22*, 328-346.

Longoria J. F. (1977) Bioestratigrafía del Cretácio Superior basada en foraminíferos planctónicos. *Revista, 1*, 10-22. Universidad Nacional Autónoma de México, Instituto de Geología.

Longoria J. F. (1984) Cretaceous biochronology from the Gulf of Mexico region based on planktonic microfossils. *Micropaleontol., 30*, 225-242.

Longoria J. F. and Gamper M. A. (1992) Planktonic foraminiferal biochronology across the KT boundary

from the Gulf coastal plain of Mexico: Implications for timing the extraterrestrial bolide impact in Yucatan. *Boletin Ass. Mexicana Petrol. Geol., XLII (2)*, 19-40.

Longoria J. F. and Grajales Nishimura J. M. (1993) *The Cretaceous/Tertiary Event in Mexico, Field Trip Guide to Selected KT Boundary Localities in Tamaulipas and Nuevo León, Northeast Mexico.* Sociedad Mexicana de Paleontologia.

Lyons J. B. and Officer C. B. (1992) Mineralogy and petrology of the Haiti Cretaceous/Tertiary section. *Earth Planet. Sci. Lett., 109*, 205-224.

Lyons J. B., Pivnik D. A., and Officer C. B. (1992) Sedimentology and petrology of KT boundary deposits at Arroyo Mimbral, Mexico and DSDP core 540, offshore Yucatan. *Geol. Soc. Am. Abstr. with Progr., 24*, A331.

MacLeod N. and Keller G. (1991a) Hiatus distribution and mass extinctions at the Cretaceous/Tertiary boundary. *Geology, 19*, 497-501.

MacLeod N. and Keller G. (1991b) How complete are Cretaceous/Tertiary boundary sections? A chronostratigraphic estimate based on graphic correlation. *Geol. Soc. Am. Bull., 113*, 1439-1457.

MacLeod N. and Keller G. (1994) Comparative biogeographic analysis of planktic foraminiferal survivorship across the Cretaceous/Tertiary boundary: a biogeographic test. *Paleobiology, 20*, in press.

Margolis S. V. et al. (1992) Impact spherules from the Cretaceous-Tertiary Boundary, NE Mexico. *Geol. Soc. Am. Abstr. with Progr., 24*, A331.

Maurasse F. J. M. R. and Sen G. (1991) Impacts, tsunamis, and the Haitian Cretaceous-Tertiary boundary layer. *Science, 252*, 1690-1693.

Montanari A., Claeys P., Asaro F., Bermudez J., and Smit J. (1994) Preliminary stratigraphy and iridium and other geochemical anomalies across the KT boundary in the Bochil Section (Chiapas, SE Mexico) (abstract). In *Lunar and Planetary Science XXIII*, in press.

Myers R. L. (1968) *Biostratigraphy of the Cardenas Formation (Upper Cretaceous), San Luis Potosi, Mexico.* Universidad Nacional Autónoma de Mexico, Paleontologia Mexicana 24, 89 pp.

Muir J. M. (1936) *Geology of the Tampico region, Mexico.* American Association of Petroleum Geologists, Tulsa. 280 pp.

Nelson C. H., Twichell D.C., Schwab W. C., Lee H. J., and Kenyen N. H. (1992) Upper Pleistocene turbidite sand beds and chaotic silt beds in the channelized, distal, outer-fan lobes of the Mississippi fan. *Geology, 20*, 693-696.

Officer C. B., Drake C. L., Pindell J. L., and Meyerhoff A. A. (1992) Cretaceous/Tertiary events and the Caribbean caper. *Geol. Soc. Am. Today*, 69-70.

Olsson R. K. and Liu G. (1993) Controversies on the placement of the Cretaceous-Tertiary boundary and the KT mass extinction of planktonic foraminifera. *Palaios, 8*, 127-139.

Pessagno E. A. Jr. (1969) *Upper Cretaceous stratigraphy of the western Gulf Coast area of México, Texas, and Arkansas.* Geological Society of America Memoir 111. 139 pp.

Pope K. O., Ocampo A. C., and Duller C. E. (1991) Mexican site for KT impact crater. *Nature, 351*, 105.

Reynolds R. C. (1989) Principles and techniques of quantitative analysis of clay minerals by X-ray powder diffraction. In *Quantitative Mineral Analysis of Clays* (D. R. Pevear and F. A. Mumpton, eds.), *CMS Workshop Lectures, 1*, 4–36. Exxon Production Research Co.

Robin E., Boclet D., Bonté Ph., Froget L., Jéhanno C., and Rocchia R. (1991) The stratigraphic distribution of Ni-rich spinels in Cretaceous-Tertiary boundary rocks at El Kef (Tunisia), Caravaca (Spain) and Hole 761C (Leg 122). *Earth Planet. Sci. Lett., 107*, 715-721.

Robin E., Bonté Ph., Froget L., Jéhanno C., and Rocchia R. (1992) Formation of spinels in cosmic objects during atmospheric entry: a clue to the Cretaceous-Tertiary boundary event. *Earth Planet. Sci. Lett., 108*, 181-190.

Sanchez M. A., Padilla P. A., Jiménez T., and Martinez R. (1993) El nannoplankton caleáreo y los foraminiferos planctónicos del limite KT de la seccion El Mulato, Estado de Tamaulipas. In *The Cretaceous/Tertiary Event in Mexico: Field Trip Guide to Selected KT Boundary Localities in Tamaulipas and Nuevo León, Northeast Mexico* (J. Longoria and J. M. Grajales Nishimura, eds.). Sociedad Mexicana de Paleontologia.

Schmitz B., Keller G., and Stenval O. (1992) Stable isotope and foraminiferal changes across the Creta ceous-Tertiary boundary at Stevns Klint, Denmark: Arguments for longterm oceanic instability

before and after bolide impact event. *Paleogeogr., Paleoclimatol., Paleoecol., 96*, 233–260.

Sharpton V. L., Dalrymple L. E., Ryder G., Schuraytz C., and Urrutia-Fucugauchi J. (1992) New links between the Chicxulub impact structure and the Cretaceous/Tertiary boundary. *Nature, 359*, 819–820.

Sigurdsson H., D'Hondt S., Arthur M. A., Bralower T. J., Zachos J. C., Van Fossen M., and Channell J. E. T. (1991) Glass from the Cretaceous-Tertiary boundary in Haiti. *Nature, 349*, 482-487.

Smit J. (1982) Extinction and evolution of planktonic foraminifera after a major impact at the Cretaceous/Tertiary boundary. *Geol. Soc. Am. Spec. Paper 190*, 329-352.

Smit J. (1990) Meteorite impact, extinctions and the Cretaceous/Tertiary boundary. *Geol. Mijnbouw, 69*, 187-204.

Smit J. and ten Kate W. G. H. Z. (1982) Trace element patterns at the Cretaceous/Tertiary boundary—consequence of a large impact. *Cretaceous Res., 3*, 307-332.

Smit J. and Romein A. J. T. (1985) A sequence of events across the Cretaceous-Tertiary boundary. *Earth Planet. Sci. Lett., 74*, 155-170.

Smit J., Nederbragt A. J., Alvarez W., Montanari A., and Alvarez W. (1992) The Cretaceous-Tertiary (K/Pg) boundary type section of El Kef, Tunisia, compared with proximal (K/Pg) transition sections from the Gulf of Mexico (abstract). In *Global Sedimentary Geological Program and Ass. Tunisienne des études internationales de Géologies*, 48.

Smit J., Montanari A., Swinburne N. H. M., Alvarez W., Hildebrand A., Margolis S. V., Claeys P., Lowrie W., and Asaro F. (1992) Tektite-bearing deep-water clastic unit at the Cretaceous-Tertiary boundary in northeastern Mexico. *Geology, 20*, 99-103.

Sohl N. F., Martinez R. E., Salmerón-Ureña P., and Soto-Jaramillo F. (1991) Upper Cretaceous. In *The Gulf of Mexico Basin: The Geology of North America, Vol. J* (A. Salvador, ed.). Geological Society of America, Boulder.

Stinnesbeck W., Barbarin J. M., Keller G., Lopez-Oliva J. G., Pivnik D. A., Lyons J. B., Officer C. B., Adatte T., Graup G., Rocchia R., and Robin E. (1993) Deposition of channel deposits near the Cretaceous-Tertiary boundary in northeastern Mexico: Catastrophic or "normal" sedimentary deposits? *Geology, 21*, 797-800.

Stinnesbeck W., Adatte T., and Keller G. (1994) KT boundary sections in southern Mexico (Chiapas): Implications for the proposed Chicxulub impact site (abstract). In *Lunar and Planetary Science XXV*, in press.

Swisher C. C. III et al. (1992) Coeval $^{40}Ar/^{39}Ar$ ages of 65.0 million years ago from Chicxulub crater melt rock and Cretaceous-Tertiary boundary tektites. *Science, 257*, 954-958.

Tappan H. N. (1980) *The Paleobiology of Plant Protists*. Freeman, San Francisco.

Weidie A. E., Wolleben J. A., and McBride E. F. (1972) Late Cretaceous depositional systems in northeastern Mexico. *Gulf Coast Assoc. Geol. Soc. Trans., 22*, 323-329.

FIELD NOTES